We thank the referees for the helpful comments. We have revised the manuscript according to the suggestions and responded to their concerns below. And we carefully edited the language and expression.

**Rerfee # 1**

**Comments from referee (1)** Seemly, the authors have some wrong citation in this paper. For example, L61 Tang et al., (2016), In the reference, there are two Tang et al, (2016). I don't know which one should be cited here. L75-77, SIA mixed with BC. Not just revealed by Wang et al., (2018). There are different methods revealing it. You should point out it. Such as Wang et al., ESTL, (2017) 4 (11), 487-493; Peng et al., PNAS, 113(16), 4266-4271;

**Response:** We will label a and b to distinguish the two references in the manuscript and corresponding modifications will be made in references.

As mentioned by the refree, there are different methods revealing mixing state of BC and SIA. Transmission electron microscopy (TEM) was used to calculate variation of fractal dimension (Df) to reflect soot aging process (Wang et al., 2017a). Also, change in the mass equivalent diameter ($\Delta D_{me}$) and coating fraction (ratio of variation in BC mass equivalent diameter to initial BC diameter, $\Delta D_{me}/D_{me,0}$) were also used to depict morphology variation and aging process (Peng et al., 2016). We will point out it and add these references to the manuscript.

**Changes in the manuscript:**

References have been corrected. Please refer to Page 3 line 60, Page 20 line 544.

Black carbon (BC) is usually more thickly coated by SIA and organic aerosols in transported and aged air masses than in fresh particles, as indicated by higher fractal dimension (Wang et al., 2017a), larger coating fraction (ratio of variation in BC mass equivalent diameter to initial BC diameter, $\Delta D_{me}/D_{me,0}$) (Peng et al., 2016) and higher mass ratio of coating to BC ($R_{BC}$) (Wang et al., 2018a). Please refer to Page 3 line 77-79.

**Comments from referee (2)** The study mostly considered the model could not reproduce the sulfate concentration although they did good nitrate and ammonium. Seemly, the authors think that the heterogeneous reactions should be dominant and missed very much in the model. I don't deny the claim. ALSO, the author should consider the primary sulfate emissions from the sources. As the recent study indicate the primary sulfate particles can be emitted from the household coal emissions. As I

knew, the inventory from the household in rural areas still not good enough in the model. The authors should not miss the point in this study. For example, Zhang et al., JGR, 123 (22), 12,964-12,979. They found the coal burning in household can emit certain amounts of sulfates.

**Response:** We agree with the point that primary sulfate particles emitted from the household coal emissions should be considered. Researchers found that high-maturity coals emitted sulfate (Zhang et al., 2018). Traditionally, model takes 5% of $SO_2$ emissions as primary sulfate emission according to convention. For another, residential sector lack reliable statistics and local emission factor measurements (Zhang et al., 2009), let alone the property of coals.

In the study, we take the primary sulfate emission into consideration. We took 40%, 6% and 15% of primary $PM_{2.5}$ from industrial, power and residential emissions, respectively, as primary sulfate emissions. And the percentages are taken according to observed source profiles from industrial, power and household coal-fired boiler (Wang et al., 2009; Zheng et al., 2013; Cao et al., 2014; Ma et al., 2015).

**Changes in the manuscript:**

We will add "household emission" and references in the manuscript. Please refer to Page 20 line 550-552 and Page 9 line 239-246.

**Comments from referee (3)** L24 Discovered, should change to revealed

**Response:** We will change "discovered" to "revealed" in the manuscript.

**Changes in the manuscript:** Changed.

**Comments from referee (4)** L92-97. Introduction part, the description of participant should be avoided here. Probably, you can cite this paper. Shi et al, acp-2018-922, in ACPD.

**Response:** The description of participants will be deleted. We will cite "(Shi et al., 2018)" to introduce the field campaign

**Changes in the manuscript:** "Details can be seen in Shi et al. (2018)" has been added here. Please refer to Page 4 line100.

**Comments from referee (5) L99, Sources of? Deleted of**

**Response:** Accepted. We will delete "of" in the manuscript.

**Changes in the manuscript:** Deleted. Please refer to Page 4 Line 105.

**Comments from referee (6)** L177 miss space before data. You mentioned several times mixing states. I think that you should explain the mixing state in the model. Is this mixing state similar to Li et al, 2016, JGR, 121 (22), 13,784-13,798 or similar to Riemer et al., ACP, 13(22), 11,423–11,439. Seemly, they have different understanding on mixing state. How is your model you think?

**Response:** Agree. Thanks for your suggestion.

There are different understandings about mixing state. Transmission electron microscopy (TEM) was used to investigate the mixing structures of individual particles (Li et al., 2016). And a particle that contains two or more components can be regarded as internally mixed. Otherwise, it is considered to be externally mixed. An affine ratio of the average per-particle species diversity and the bulk population species diversity were used to quantitatively present aerosol population mixing state, namely degree to which population is externally mixed versus internally mixed (Riemer and West, 2013).

In this study, mixing state is a description of aerosol population, taking microphysics process into consideration. Mixing state is assumed to be semi-external (Yu and Luo, 2009;Chen et al., 2014), includes internal mixing, external mixing and core-shell mixing. Seeding particles, including BC, OC, dust, sea salt are generated by emission and secondary aerosols formed by nucleation. Then seeding particles are coated by secondary particles including sulfate, nitrate, ammonia and secondary organic aerosols through condensation, coagulation, chemistry reactions, equilibrium uptake and hygroscopic growth process. Nucleated secondary particle is internally mixed while primary particles coated with SIA or SOA are considered as core-shell mixing. And these coated particles are external mixing with each other. Mixing states in the model are as shown below.

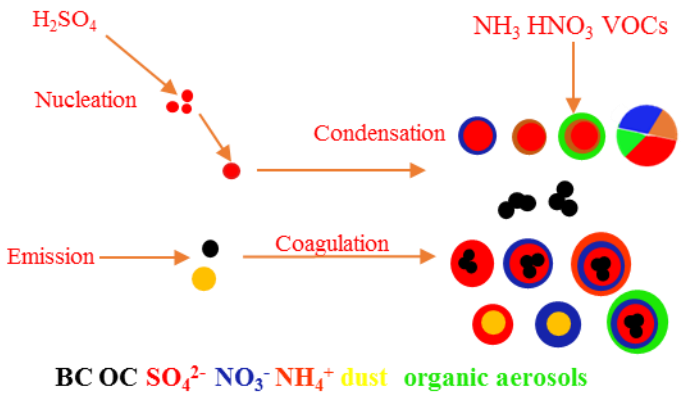

Figure 1 Microphysical process and mixing state in the model

**Changes in the manuscript:** We will add description of mixing state in the manuscript. Please refer to Page 6 line 156-158.

**Comments from referee** (7) L269-270. I don't think this is right reference here. The study worked on iron associated with ocean production. They didn't work on any aerosol particle in Beijing.

**Response:** Thanks for your suggestion. We use this paper to show that heterogenous chemistry can happen on mineral dust surface. Wang et al. (2017b; 2018b) confirmed the importance of dust heterogeneous reactions, and we will add these references here.

**Changes in the manuscript:** References have been changed. "As discussed in the last paragraph, Beijing had high mineral loadings for Ep2, which provided a favorable medium for chemical transformation of anthropogenic $SO_2$ into sulfate in the form of CaSO4 or MgSO4 (Wang et al., 2018b;Wang et al., 2017b). " Please refer to Page 11 line 297.

**Comments from referee** (8) L321, along with

**Response:** Thanks for your suggestion. We think about it carefully. We mean pollution accumulates at the foot of the mountain and forms pollution belts along the mountains because of the obstruction of the terrain. "along" is a preposition here, so we think maybe it's better to use "along"

**Changes in the manuscript:** The sentence will stay the same here.

**Comments from referee** (9) L379-389, I STILL want to emphasize the primary emissions of sulphates here., Seemly, you missed household emission in L500-502.

**Response:** Thanks for your suggestion. L379-389 is meant to tell the different understanding and definition of regional transport. And the transport of secondary inorganic aerosols includes transport of both its precursors and secondary aerosols. Household burning was found emits a large amount of sulfate (Zhang et al., 2012;Zhang et al., 2018). And we will add "household emission" after L502.

**Changes in the manuscript:** Household emission will be added. Please refer to Page 20 line 551-552.

**Comments from referee** (10) Section 4.4, the authors tried to understand the heterogeneous reactions. The possible reactions should occur on aqueous layer which is related to the particle phase anymore (Sun et al., JGR, 123 (2), 1234-1243; Kuang et al., GRL, 43, 8744–8750.). Also, in 513-515.

**Response:** Thanks for your suggestion. We agree.

Researchers investigated deliquescent phenomena of aerosols and found ammonium sulfate played significant roles (Sun et al., 2018;Kuang et al., 2016). And their results focused on phase transition of particles, especially haze particles under high RH(60–80%) with aqueous shell. This phase transition process is not also considered in detail by model.

In the model, growth factor and aerosol water are calculated by thermodynamic equilibrium model ISORROPIA. As mechanism of heterogenous chemistry is not fully understood, heterogeneous chemistry is commonly parameterized using a pseudo-first-order rate constant (Jacob, 2000). And reaction rate is as follows:

$$\kappa=\left[\frac{r}{D}+\frac{4}{C\gamma}\right]^{-1}\times A$$

$\gamma$ is the ratio of the number of collisions that result in reaction to the theoretical total number of collisions, and it depends in general on temperature and types of aerosols. A is the surface area. Under high relative humidity, a higher aerosol surface area resulting from hygroscopic growth is favorable for heterogeneous reactions.

**Changes in the manuscript:**

Please refer to Page 20 line 565-566.

**Comments from referee** (11) Here I still confused on the aqueous chemistry and heterogeneous chemistry. What are differences in the model? Could you please list them. Seemly, heterogeneous chemistry happened in aqueous layer of particles.

**Response:** Thanks for your suggestion. Descriptions about heterogeneous chemistry in the paper may not be so clear. We will explain the treatment of aqueous and heterogeneous reactions in the model.

In the model, aqueous chemistry happened only in **cloud water**, which is provided by WRF. But cloud does not occur frequently in winter over Beijing-Tianjin-Hebei area. Aqueous chemistry reactions mainly include the following five reactions:

$$H_2O_2 + SO_2 \rightarrow SO_4^{2-}$$

$$O_3 + SO_2 \rightarrow SO_4^{2-}$$

$$MHP^a + SO_2 \rightarrow SO_4^{2-}$$

$$PAA^b + SO_2 \rightarrow SO_4^{2-}$$

$$O_2 + SO_2 + Fe(III) / Mn(II) \rightarrow SO_4^{2-}$$

[a] MHP: methylhydroperoxide; [b] PAA: peroxyacetic acid.

Heterogeneous chemistry reactions happen on **aerosol surface** and are related with aerosol liquid water which is provided by ISORROPIA. Heterogeneous chemistry is commonly parameterized using a pseudo-first-order rate constant and reaction rate is as follows:

$$k_{ij}=[\frac{r_{ij}}{D_j}+\frac{4}{C_j\gamma_j}]^{-1} \times A_{ij}$$

$k_{ij}$ is the reaction rate of $j^{th}$ reaction in the $i^{th}$ bin. $\gamma$ is the uptake coefficient for reactant j, $A_{ij}$ is the surface area of the $i^{th}$ bin of reactant j, $r_{ij}$ is the radium of the $i^{th}$ bin of reactant j, $D_j$ is the gas phase molecular diffusion coefficient for reactant j. $C_j$ is molecular speed of reactant j in gas phase.

In this study, we also add the heterogeneous chemistry of $SO_2$ to the model, and more details can be seen in (Li et al., 2018).

$$SO_2 + Aerosol \rightarrow SO_4^{2-}$$

Uptake coefficient is calculated as the following equation:

$$\gamma_{SO2} = \begin{cases} 1 \times 10^{-4} & awc \geq C_{up} \\ (awc - C_{low}) \times \dfrac{10^{-4} - 10^{-6}}{C_{up} - C_{low}} & C_{low} < awc < C_{up} \\ 1 \times 10^{-6} & awc \leq C_{low} \end{cases}$$

$\gamma_{SO2}$ is the uptake coefficient of $SO_2$. Assuming that the upper limit of $\gamma_{SO2}$ does not exceed uptake coefficient on dust surface, upper limit of $\gamma_{SO2}$ is $10^{-4}$ and lower limit is $10^{-6}$. $C_{low}$, the lower limit of AWC required by heterogeneous chemistry, is 10 μg $m^{-3}$. When uptake coefficient reaches peak, $C_{up}$, the upper limit of AWC is 300 μg $m^{-3}$.

**Changes in the manuscript:** Differences between aqueous chemistry and heterogeneous chemistry in the model will be added to the manuscipt. Please refer to Page 5 line 131-133.

**Comments from referee** (12) Figure 6, the pie is too small to see clearly them

**Response:** Thanks for your suggestion. We will modify the pies in figure 6.

**Changes in the manuscript:** Please refer to Page 33 line 868.

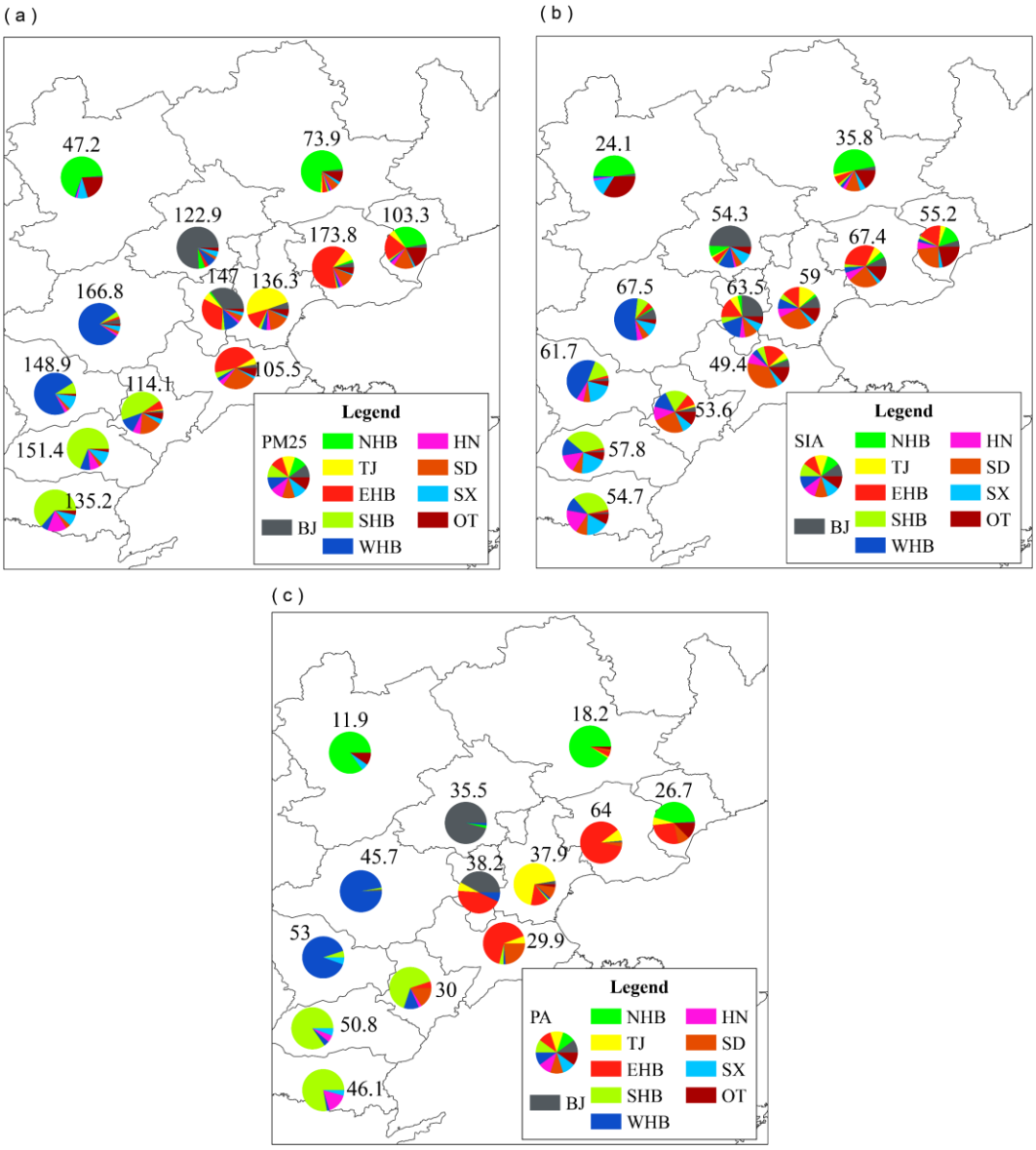


Figure 6. The contribution of regional transport and local emissions to the average (a) total $PM_{2.5}$, (b) secondary inorganic aerosols (SIA), (c) primary aerosols (PA, BC and primary $PM_{2.5}$) over BTH area. The numbers above the pie represent average concentrations (μg $m^{-3}$) of certain species in certain cities.

**Comments from referee** (13) Figure 12. The figure is not clear for me.

**Response:** Thanks for your suggestion. Figure 12. shows variation of aerosol properties

(region sources, aging degree, geometric mean diameter and number concentration) along transport. We will improve the figure and include some of the information in an additional table.

**Changes in the manuscript:** Please refer to Page 40 line 903-914.

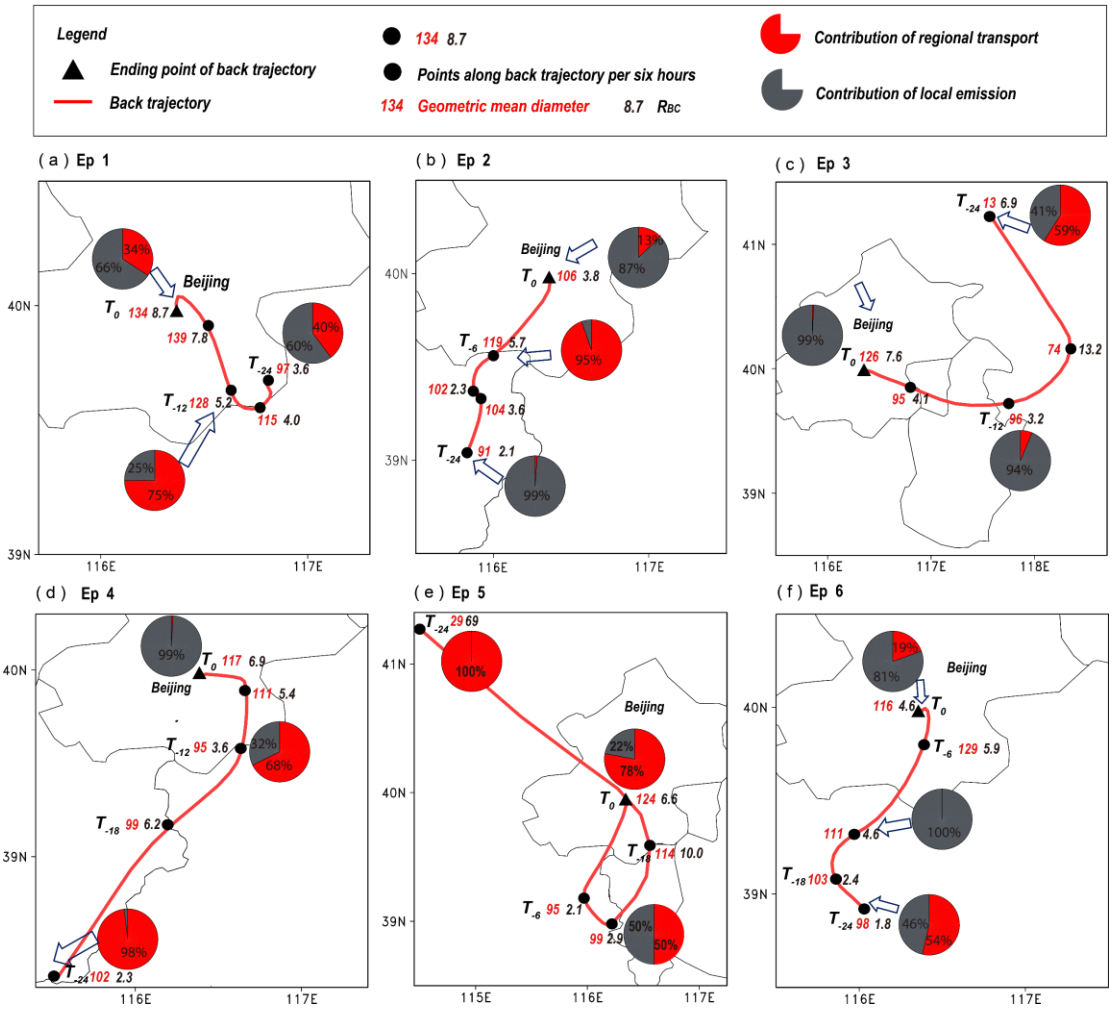


Figure 12. Variation of aerosol properties along transport. Panel a–f refers to episode 1–6. The red lines refer to 24 h backward trajectories. Aerosol properties include geometric mean diameter (GMD [nm], red numbers), mass ratio of coating to BC ($R_{BC}$, the black numbers beside the solid blocks, an indicator of aging degree), region source of BC (pies, the red represents regional transport and the gray is the local contribution). Shaded triangles are ending points of back trajectories and shaded circles are points along trajectories per six hours. T-6, T-12, T-18, T-24 mean 6, 12, 18, 24 hours before arriving at ending site. Ending times of backtrajectories are before pollution peaks at 21:00 on November 18, 22:00 on November 25, 16:00 on November 29, 22:00 on December 03, 0:00 on December 8 and 22:00 on December 11 (LST), respectively.

Table 1. Aerosol properties along transport, including geometric mean diameter (GMD [nm]), mass ratio of coating to BC ($R_{BC}$), number concentration (N) and contribution

of region source to BC (Cr [%]). $T_0$ means ending points of back trajectories and $T_n$ means n hours before arriving at the ending point.

| | | $T_{-24}$ | $T_{-18}$ | $T_{-12}$ | $T_{-6}$ | $T_0$ |
|---|---|---|---|---|---|---|
| **Ep1** | $R_{BC}$ | 3.6 | 4.0 | 5.2 | 7.8 | 8.7 |
| | GMD | 97 | 115 | 128 | 139 | 134 |
| | N | 28994 | 15494 | 15204 | 15592 | 19242 |
| | Cr | 40 | 93 | 75 | 7 | 34 |
| **Ep2** | $R_{BC}$ | 2.1 | 3.6 | 2.3 | 5.7 | 3.8 |
| | GMD | 91 | 104 | 102 | 119 | 106 |
| | N | 23909 | 15189 | 17961 | 10994 | 20121 |
| | Cr | 1.2 | 0.14 | 0.01 | 95 | 13 |
| **Ep3** | $R_{BC}$ | 6.9 | 13.2 | 3.2 | 4.1 | 7.6 |
| | GMD | 13 | 74 | 96 | 95 | 126 |
| | N | 22234 | 11880 | 13481 | 14241 | 12945 |
| | Cr | 59 | 81.4 | 6.2 | 8.8 | 1 |
| **Ep4** | $R_{BC}$ | 2.3 | 6.2 | 3.6 | 5.4 | 6.9 |
| | GMD | 102 | 98 | 95 | 111 | 117 |
| | N | 19754 | 12805 | 21116 | 10536 | 17199 |
| | Cr | 98 | 56 | 68 | 25 | 1 |
| **Ep5** | $R_{BC}$ | 69 | 10.0 | 2.9 | 2.1 | 6.6 |
| | GMD | 29 | 114 | 99 | 95 | 124 |
| | N | 8617 | 8086 | 16494 | 28211 | 13696 |
| | Cr | 100 | 100 | 50 | 4 | 78 |
| **Ep6** | $R_{BC}$ | 1.8 | 2.4 | 4.6 | 5.9 | 4.6 |
| | GMD | 98 | 103 | 111 | 129 | 116 |
| | N | 31691 | 23691 | 17885 | 12897 | 21955 |
| | Cr | 54 | 0.17 | 0.01 | 65 | 19 |

**Comments from referee (14)** Figure 13 what is PSO4? In X-axis

**Response:** Thanks for your suggestion. PSO4 refers to sulfate concentration here. We will change it into sulfate to keep consistent with Figure 13a.

**Changes in the manuscript:** Please refer to Page 43 line 928.

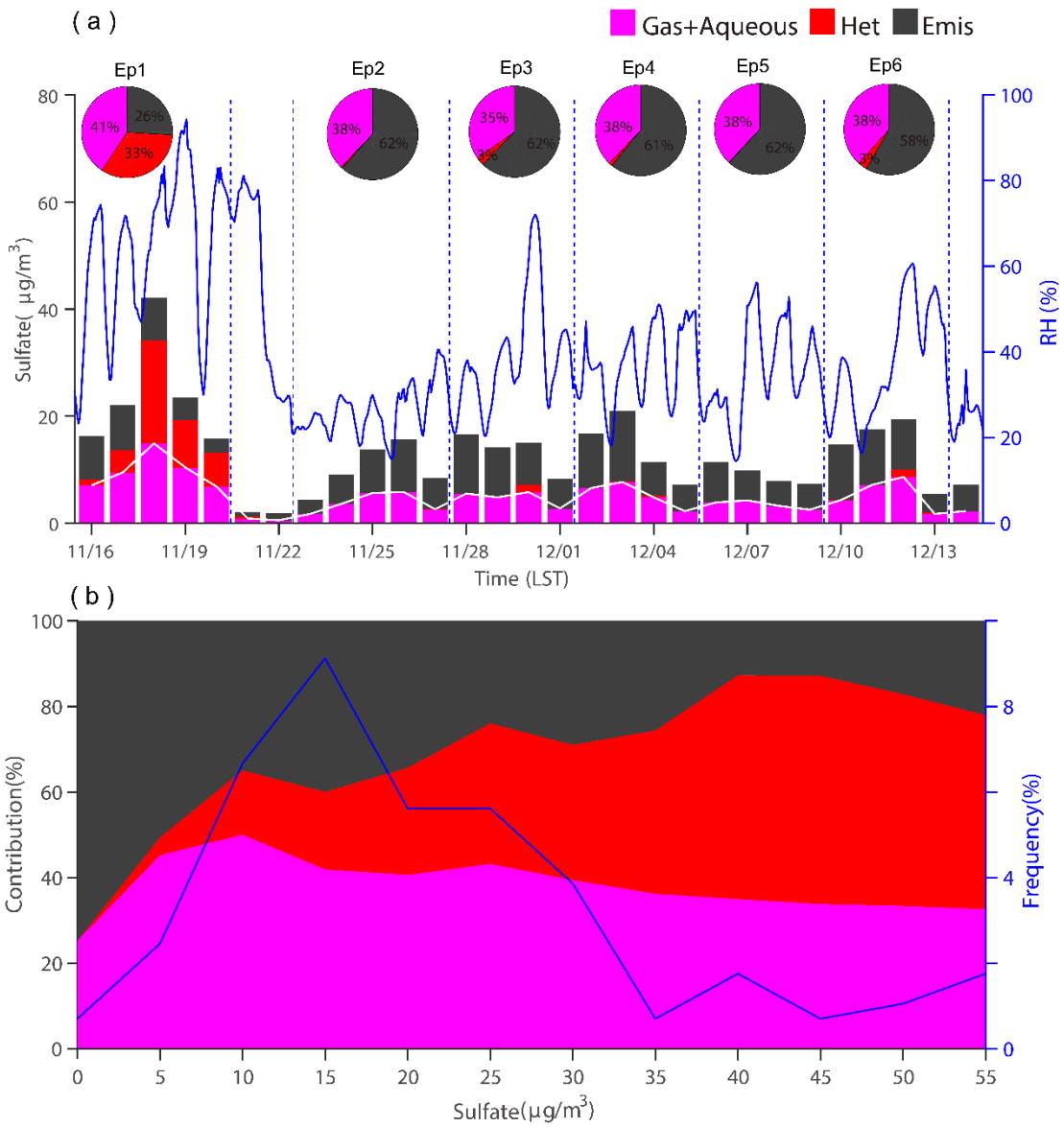


Figure 13. Contribution of different ways of sulfate 830 formation in Beijing. (a) Daily average. Blue line shows relative humidity at Beijing. Pies show average contribution of different ways during each episode. (b) Relationship between sulphate concentration and different pathways of sulphate formation during Ep1.

## References


Cao J.: $PM_{2.5}$ and environment. Science Press, 2014.

Chen, X. S., Wang, Z. F., Li, J., and Yu, F. Q.: Development of a Regional Chemical Transport Model with Size-Resolved Aerosol Microphysics and Its Application on Aerosol Number Concentration Simulation over China, Sola, 10, 83-87, 10.2151/sola.2014-017, 2014.

Jacob, D. J.: Heterogeneous chemistry and tropospheric ozone, Atmospheric

Environment, 34, 2131-2159, Doi 10.1016/S1352-2310(99)00462-8, 2000.

Kuang, Y., Zhao, C. S., Ma, N., Liu, H. J., Bian, Y. X., Tao, J. C., and Hu, M.: Deliquescent phenomena of ambient aerosols on the North China Plain, Geophysical Research Letters, 43, 8744-8750, 10.1002/2016gl070273, 2016.

Li, J., Chen, X., Wang, Z., Du, H., Yang, W., Sun, Y., Hu, B., Li, J., Wang, W., Wang, T., Fu, P., and Huang, H.: Radiative and heterogeneous chemical effects of aerosols on ozone and inorganic aerosols over East Asia, The Science of the total environment, 622-623, 1327-1342, 10.1016/j.scitotenv.2017.12.041, 2018.

Li, W. J., Sun, J. X., Xu, L., Shi, Z. B., Riemer, N., Sun, Y. L., Fu, P. Q., Zhang, J. C., Lin, Y. T., Wang, X. F., Shao, L. Y., Chen, J. M., Zhang, X. Y., Wang, Z. F., and Wang, W. X.: A conceptual framework for mixing structures in individual aerosol particles, Journal of Geophysical Research-Atmospheres, 121, 13784-13798, 10.1002/2016jd025252, 2016.

Ma, Z., Liang YP, Zhang J.: PM2.5 profiles of typical sources in Beijing, Acta Science Circumstantiae, 35(12), 4043-4052, https://doi.org/10.13671/j.hjkxxb.2015.0584, 2015.

Peng, J. F., Hu, M., Guo, S., Du, Z. F., Zheng, J., Shang, D. J., Zamora, M. L., Zeng, L. M., Shao, M., Wu, Y. S., Zheng, J., Wang, Y., Glen, C. R., Collins, D. R., Molina, M. J., and Zhang, R. Y.: Markedly enhanced absorption and direct radiative forcing of black carbon under polluted urban environments, Proceedings of the National Academy of Sciences of the United States of America, 113, 4266-4271, 10.1073/pnas.1602310113, 2016.

Riemer, N., and West, M.: Quantifying aerosol mixing state with entropy and diversity measures, Atmospheric Chemistry and Physics, 13, 11423-11439, 10.5194/acp-13-11423-2013, 2013.

Shi, Z., Vu, T., and Kotthaus, S.: Introduction to Special Issue - In-depth study of air pollution sources and processes within Beijing and its surrounding region(APHH-Beijing), Atmos. Chem. Phys. Discuss., 2018.

Sun, J., Liu, L., Xu, L., Wang, Y., Wu, Z., Hu, M., Shi, Z., Li, Y., Zhang, X., Chen, J., and Li, W.: Key Role of Nitrate in Phase Transitions of Urban Particles: Implications of Important Reactive Surfaces for Secondary Aerosol Formation, Journal of Geophysical Research: Atmospheres, 123, 1234-1243, 10.1002/2017jd027264, 2018.

Wang, J., Liu, D., Ge, X., Wu, Y., Shen, F., Chen, M., Zhao, J., Xie, C., Wang, Q., Xu, W., Zhang, J., Hu, J., Allan, J., Joshi, R., Fu, P., Coe, H., and Sun, Y.: Characterization of black carbon-containing fine particles in Beijing during wintertime, Atmospheric Chemistry and Physics Discussions, 1-25, 10.5194/acp-2018-800, 2018a.

Wang, S., Zhao, X., Li, X., Wei, W., Hao, J.: Study on fine particle emission

characteristics of industrial coal-fired chain furnace. Environmental Science (Chines), 30 (4), 963-968, https://doi.org/10.3321/j.issn:0250-3301.2009.04.004, 2009.

Wang, Y. Y., Liu, F. S., He, C. L., Bi, L., Cheng, T. H., Wang, Z. L., Zhang, H., Zhang, X. Y., Shi, Z. B., and Li, W. J.: Fractal Dimensions and Mixing Structures of Soot Particles during Atmospheric Processing, Environ Sci Tech Let, 4, 487-493, 10.1021/acs.estlett.7b00418, 2017a.

Wang, Z., Pan, X., Uno, I., Li, J., Wang, Z., Chen, X., Fu, P., Yang, T., Kobayashi, H., Shimizu, A., Sugimoto, N., and Yamamoto, S.: Significant impacts of heterogeneous reactions on the chemical composition and mixing state of dust particles: A case study during dust events over northern China, Atmospheric Environment, 159, 83-91, 10.1016/j.atmosenv.2017.03.044, 2017b.

Wang, Z., Pan, X., Uno, I., Chen, X., Yamamoto, S., Zheng, H., Li, J., and Wang, Z.: Importance of mineral dust and anthropogenic pollutants mixing during a long-lasting high PM event over East Asia, Environmental pollution, 234, 368-378, 10.1016/j.envpol.2017.11.068, 2018b.

Yu, F., and Luo, G.: Simulation of particle size distribution with a global aerosol model: contribution of nucleation to aerosol and CCN number concentrations, Atmos. Chem. Phys., 9, 7691–7710, 2009.

Zhang, H. F., Wang, S. X., Hao, J. M., Wan, L., Jiang, J. K., Zhang, M., Mestl, H. E. S., Alnes, L. W. H., Aunan, K., and Mellouki, A. W.: Chemical and size characterization of particles emitted from the burning of coal and wood in rural households in Guizhou, China, Atmospheric Environment, 51, 94-99, 10.1016/j.atmosenv.2012.01.042, 2012.

Zhang, Q., Streets, D. G., Carmichael, G. R., He, K., Huo, H., Kannari, A., Klimont, Z., Park, I., Reddy, S., Fu, J. S., Chen, D., Duan, L., Lei, Y., Wang, L., and Yao, Z.: Asian emissions in 2006 for the NASA INTEX-B mission, Atmospheric Chemistry and Physics Discussions, 9, 4081-4139, 10.5194/acpd-9-4081-2009, 2009.

Zhang, Y., Yuan, Q., Huang, D., and Kong, S.: Direct Observations of Fine Primary Particles From Residential Coal Burning: Insights Into Their Morphology, Composition, and Hygroscopicity, Journal of Geophysical Research, 123, 12964–12979, 2018.

Zheng M., Zhang Y., Yan C., et al.: Establishment of $PM_{2.5}$ industrial source profile in Shanghai, China Environmental Science, 33(8), 1354-1359, https://doi.org/10.3969/j.issn.1000-6923.2013.08.002, 2013.

**Refree # 2**

**Major comments:**

**Major comments 1:** Only the levels and formation of sulfate are discussed whereas aerosol mass is composed of many more inorganic and organic compounds. While a comprehensive analysis of all aerosol constituents might exceed the scope of the paper, the limitation to sulfate should be made clear in the title, abstract and throughout the manuscript.

**Response:** We accepted. The manuscript includes two parts: regional transport and heterogeneous reactions. The chapter of regional transport involved all inorganic and organic species. As recent studies indicated that sulfate is a key driver for severe haze events (Huang et al., 2014;Zheng et al., 2015), the transport of precursors or secondary products, and heterogeneous reactions were mainly focused on sulfate in the manuscript. The title will be changed, and the limitation of sulfate will be described in the abstract and throughout the manuscript.

**Changes in the manuscript:** The title will be changed. "Modeling of aerosol property evolution during winter haze episodes over a megacity cluster in northern China: Roles of regional transport and heterogeneous reactions of $SO_2$"

The limitation of sulfate will be described it in the manuscript. Please refer to Page 4 line 114-116.

**Major comments 2:** Several parts of the paper seem disconnected from each other and/or available information is not sufficiently used in the discussion:

a) The transport of $SO_2$ away from Beijing and its subsequent oxidation followed by transport back to Beijing is an interesting thought. However, it would be much more convincing if HYSPLIT trajectories were included in the discussion showing this recirculation of air masses.

**Response:** Thanks for your suggestion. HYSPLIT trajectories are good indicators of recirculation of air masses.Figure blow shows that air masses flow away from Beijing

and finally blown back to Beijing at different time (02:00 on November 17, 11:00 on November 29, and 23:00 on December 12 [LST]). Note that the trajectories were conducted at a single location in Beijing. And at those moments, LTC (sulfate chemically formed in regions except Beijing from the Beijing emitted $SO_2$) accounts for large part of sulfate (figure 9a). Results are quiet consistent.

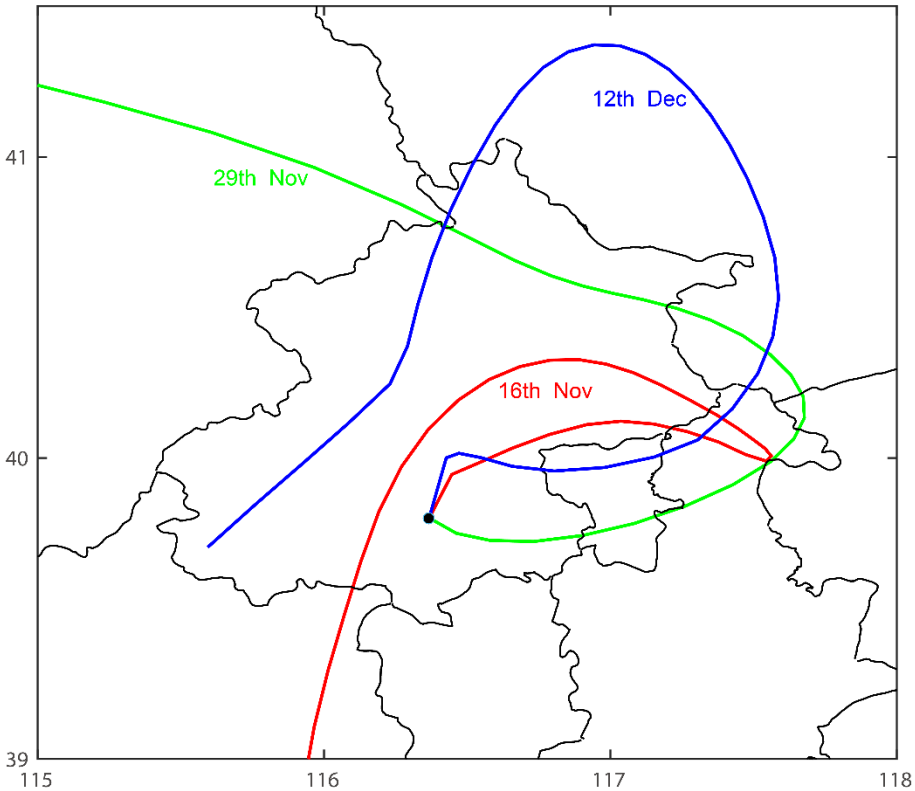


Figure 1 36 h backward trajectories at different start time (02:00 on November 17, 11:00 on November 29, and 23:00 on December 12 [LST]) at Beijing.

**Changes in the manuscript:** We will add trajectories to the manuscript as supplement. Please refer to Page 16 line 442-445.

b) Can the different source regions during the various episodes be connected to back trajectories and different emissions in the various source regions?

Response: Yes. Back trajectories during various episodes are shown below.

During Ep1, airflow passed through Hebei province to Beijing, then through Tangshan,

the Bohai sea, and finally flown back to Beijing. Western Hebei and eastern Hebei are the mainly source regions except local emission. Figure 7b showed that EHB and WHB accounted for 11% and 8% of SIA at Beijing, respectively. During Ep2, airmass flown from Inner Mongolia through Shanxi, NHB, WHB and arrived at Beijing. During Ep3, airflow travelled from Inner Mongolia through NHB, EHB, SD and finally arrived at Beijing. Figure 7b showed that SX, NHB, EHB and SD accounted for 5%, 7%, 3% and 2% of SIA at Beijing, respectively. During Ep5, airflow travelled from Inner Mongolia through SX, NHB, WHB and stayed in Baoding for some time, then finally arrived at Beijing. These are quite consistent with the result of SIA shown in Figure 7b. During Ep6, airmass mainly came from Shandong, through SHB, WHB and finally arrived at Beijing. What's more, the height of trajectory within WHB is low, so contribution of WHB should be big, which agreed with results of Figure 7b, WHB contributed 24% to SIA at Beijing during Ep6.

As back trajectory model did not consider chemical conversion of precursors, so the results are not exactly the same with those of 3-D air quality model. But in general, the on-line source-tagged module results agreed well with those from the backward trajectories.

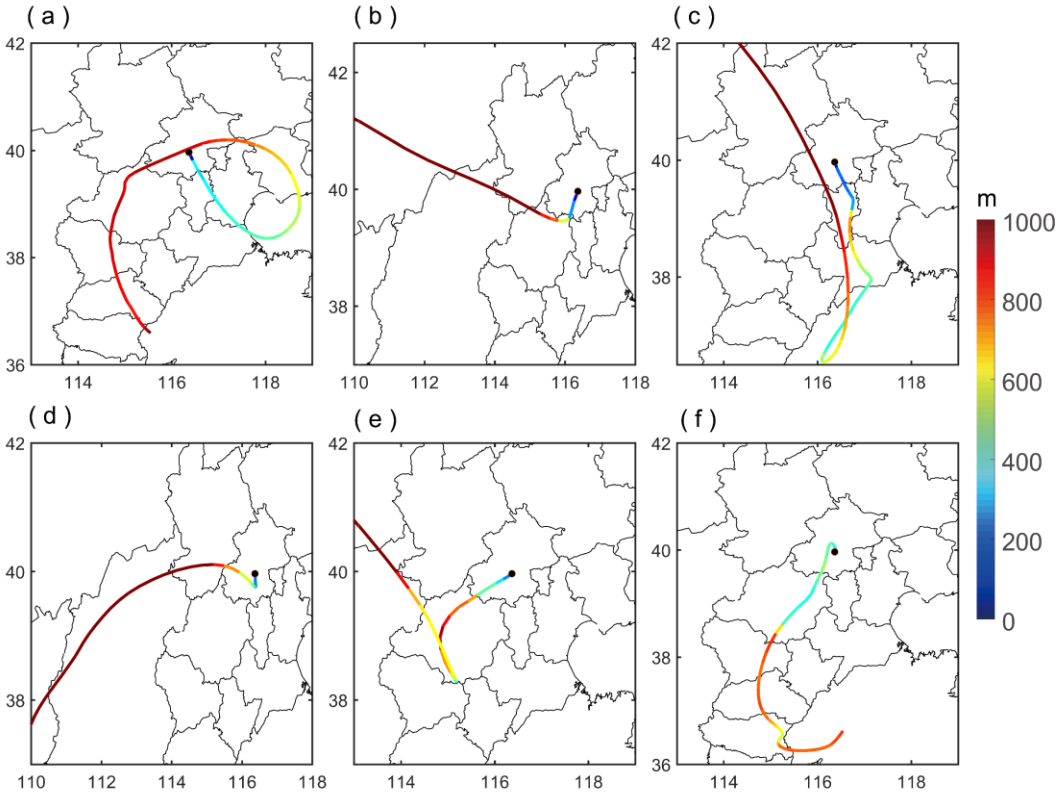


Figure 2 72 h backward trajectories during different episodes (05:00 on November 20, 18:00 on November 26, 23:00 on November 29, 20:00 on December 03, 05:00 on December 08 and 11:00 on December 12 [LST]) at Beijing at 100m. Line color represents height of trajectories. a-f refer to Ep1-6.

**Changes in the manuscript:** Back trajectories during various episodes will added to the manuscript as supplement. Please refer to Page 14 line 396-401.

**Major comments 3:** It is not clear what is exactly meant by 'aqueous' and 'heterogeneous' chemistry. Does aqueous phase chemistry only include cloud chemistry? Which oxidants are considered? Is metal-assisted oxidation included? Is heterogeneous chemistry the oxidation of S(IV) by $NO_2$ or are other processes included as well? Which parameters are included in the model parameterization? How well are they constrained?

**Response:** In this study, aqueous phase chemistry only includes cloud chemistry. Oxidants of aqueous chemistry include $O_3$, $H_2O_2$, methyl hydroperoxide and

peroxyacetic acid. Metal-assisted oxidation is also included.

Heterogeneous chemistry includes oxidation of S(IV) on aqueous layer of aerosols. Heterogeneous chemistry is parameterized according to the scheme of Li et al. (2018), using a pseudo-first-order rate constant and reaction rate is as follows

$$\kappa=\left[\frac{r}{D}+\frac{4}{C\gamma}\right]^{-1}\times A$$

$\gamma$ is the ratio of the number of collisions that result in reaction to the theoretical total number of collisions, and it depends in general on temperature and species.

A is the surface area.

$\boldsymbol{\gamma}$ is the most important parameter, and it is related to aerosol liquid water (awc), and amounts of oxidants (Li et al., 2018) . The uptake coefficient of $SO_2$ is as follows.

$$\gamma_{SO2}=\begin{cases} 1\times10^{-4} & \mathrm{awc}\ \geq\ \mathrm{C_{up}} \\ (\mathrm{awc}-\mathrm{C_{low}})\times\dfrac{10^{-4}-10^{-6}}{\mathrm{C_{up}}-\mathrm{C_{low}}} & \mathrm{C_{low}}<\ \mathrm{awc}\ <\ \mathrm{C_{up}} \\ 1\times10^{-6} & \mathrm{awc}\ \leq\ \mathrm{C_{low}} \end{cases}$$

$\gamma_{SO2}$ is the uptake coefficient of $SO_2$. Assuming that the upper limit of $\gamma_{SO2}$ does not exceed uptake coefficient on dust surface, upper limit of $\gamma_{SO2}$ is $10^{-4}$ and lower limit is $10^{-6}$. $\mathrm{C_{low}}$, the lower limit of AWC required by heterogeneous chemistry, is 10 μg $m^{-3}$. When uptake coefficient reaches peak, $\mathrm{C_{up}}$, the upper limit of AWC is 300 μg $m^{-3}$. More details can be found in Li et al., (2018).

**Changes in the manuscript:** Please refer to Page 5 line 131-133 and Page 6 line 166-168.

**Major comments 4:** Most of the figures need to be improved. Contrasts are hard to see and often they are overloaded with information in much too small font.

Figure 2: What are the horizontal green lines?

**Response:** Green lines mean 75 μg $m^{-3}$, as a criterion judging whether pollution or not.

**Changes in the manuscript:** We will add this in the caption and manuscript. Please

refer to Page 30 line 849-850.

**"Figure 2.** Comparison between the simulated and observed hourly concentrations of $PM_{2.5}$ for different sites. Black lines refer to observation and the red lines are simulation results; light blue shadows are six episodes identified; green lines mean 75 μg $m^{-3}$, as a criterion judging whether pollution or not."

Figure 4: Why is only the range up to 600 nm considered here even though the measurements and model bins extended further?

**Response:** As the upper limitation of observation is about 600nm. What's more, number concentration of $PM_{2.5}$ is almost within 600nm (Du et al., 2017;Liu et al., 2016). So only the range up to 600 nm was considered.

Figure 5: The solid circles are too small. Are they supposed to be colored as the caption suggests?

**Response:** Yes, the solid circles are colored with the same bar with the simulation. We will increase the circles for better readability.

**Changes in the manuscript:** Please refer to Page 31 line 861.

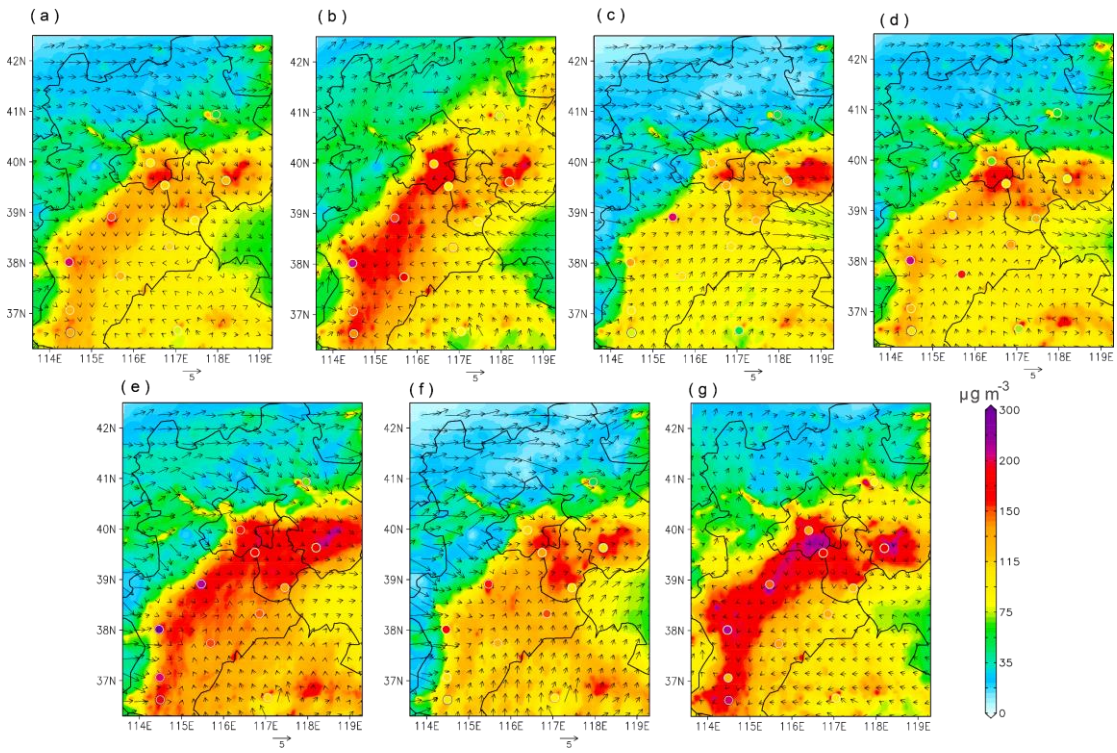


**Figure 5.** Spatial distribution of simulated average surface $PM_{2.5}$ (μg $m^{-3}$) and wind (m $s^{-1}$) over BTH area. (a) average of whole study period, (b)–(g) episode average of episode1–6 identified before. Solid circles represent observations with the same color bar with simulations.

Figure 6: The pie charts and numbers are too small. Also the legends should be increased for better readability.

**Response: Accepted. We will change it in the manuscript.**

**Changes in the manuscript:** Please refer to Page 33 line 868.

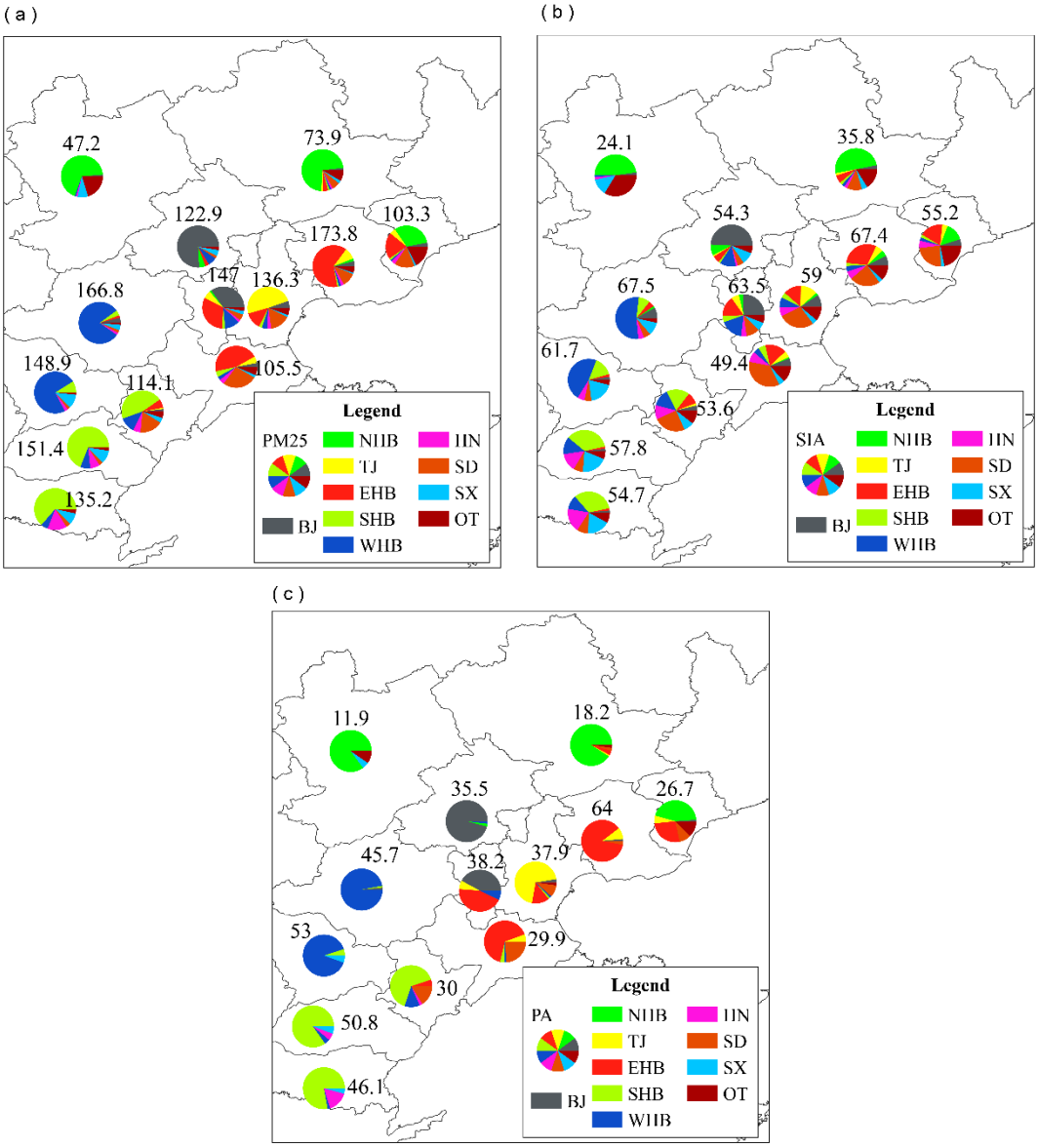


**Figure 6.** The contribution of regional transport and local emissions to the average (a) total $PM_{2.5}$, (b) secondary inorganic aerosols (SIA), (c) primary aerosols (PA, BC and primary $PM_{2.5}$) over BTH area. The numbers above the pie represent average concentrations (μg $m^{-3}$) of certain species in certain cities.

Figure 7: The black numbers on the dark grey pie charts are hard to read.

**Response:** Accepted. We will change the color in the manuscript.

**Changes in the manuscript:** Please refer to Page 35 line 874.

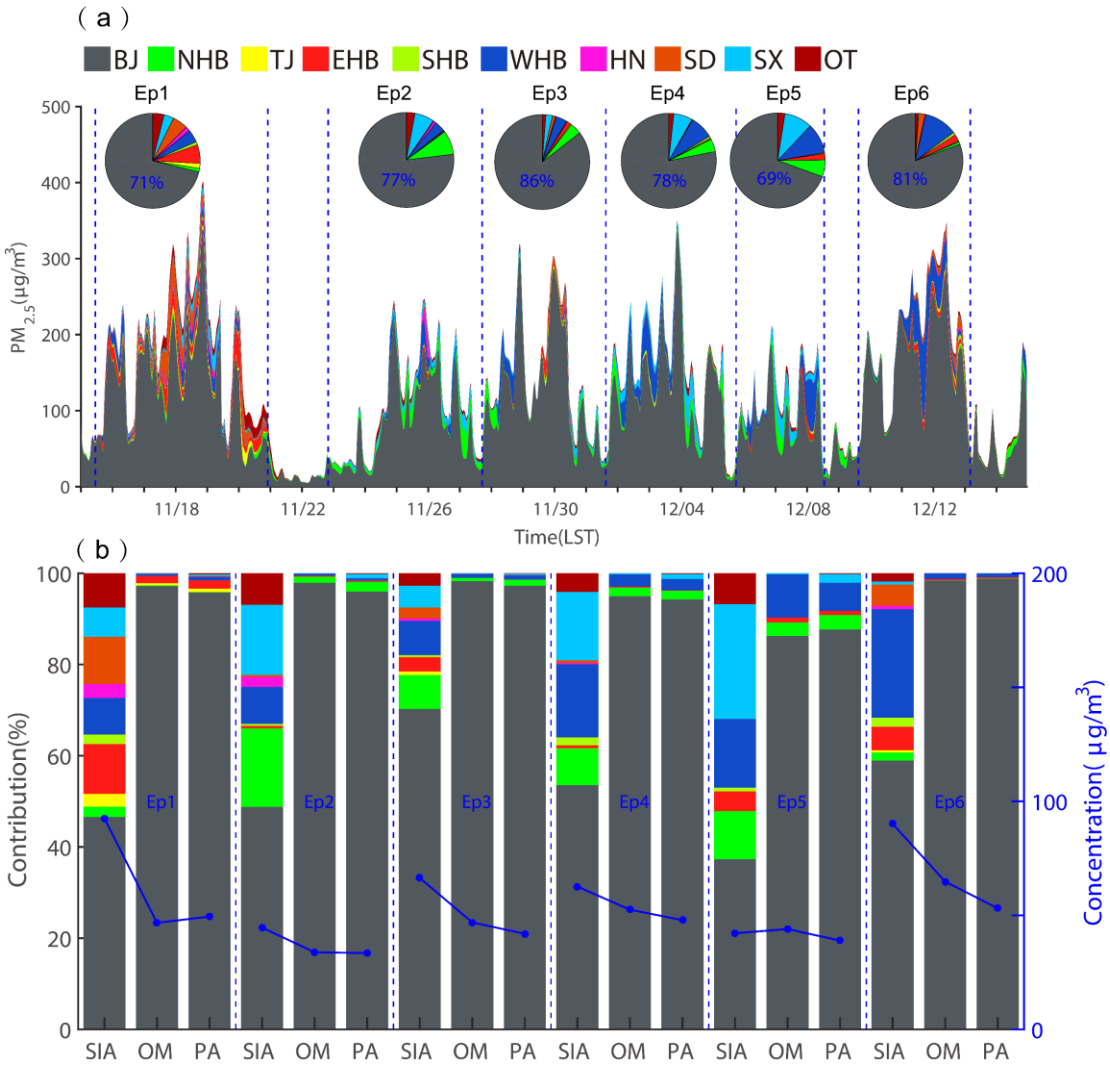


**Figure 7.** (a) Source contribution of $PM_{2.5}$ in Beijing and pies represent average status of each episode; (b) Relative contribution of different regions to SIA, OM and PA in Beijing at the surface layer during each episode (shaded). Concentrations are also shown (blue line).

Figure 9: The text says that the figure shows regional sources. However, here all sources LC, LTC, RTC and RLC are shown.

**Response:** We will change the text in the manuscript.

**Changes in the manuscript:** "(a) Sources of secondary sulfate in Beijing." Please refer to Page 37 line 886-887.

Figure 11a): I suggest removing the lines between the symbols as they are meaningless and imply a non-existing trend.

**Response:** We will revise the figure in the manuscript

**Changes in the manuscript:** Please refer to Page 38 line 898.

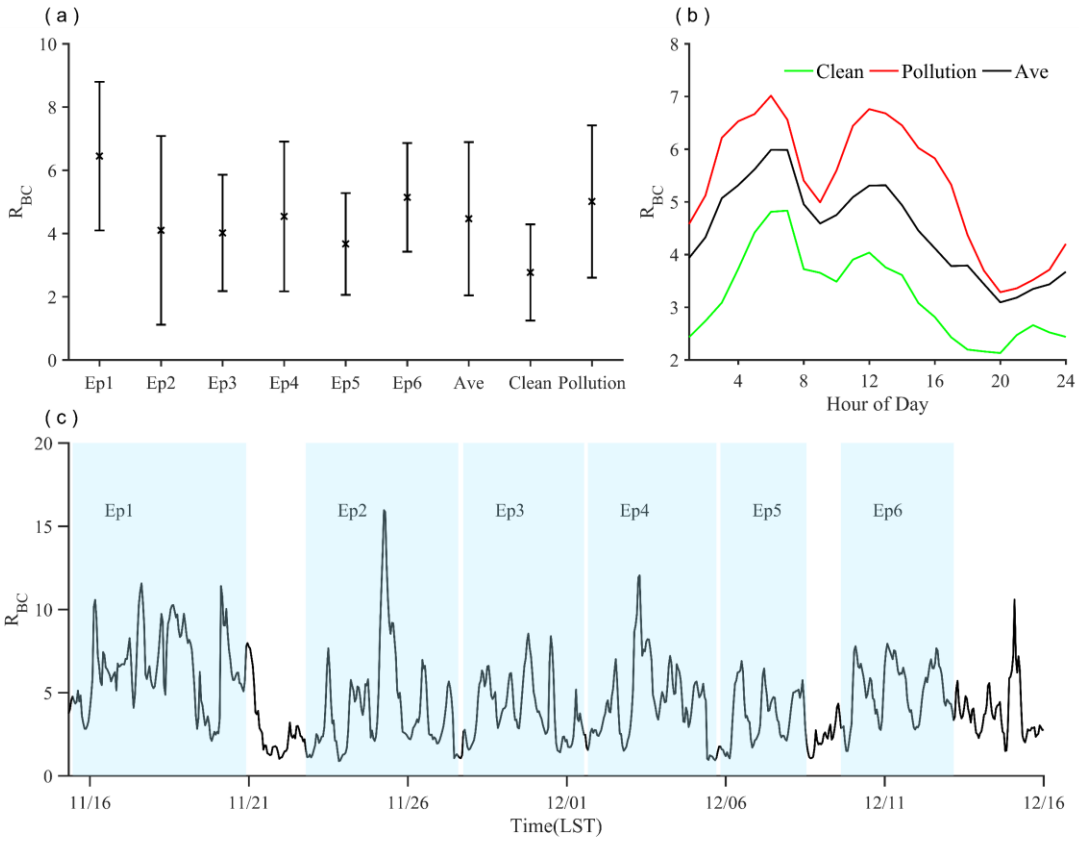


Figure 11. (a) average and standard variation of massing ratio of coating to BC ($R_{BC}$) during different episodes and pollution levels, (b) diurnal cycles of $R_{BC}$ under different pollution levels, (c) temporal variation of $R_{BC}$ during study period.

Figure 12: - This figure contains way too much information. The numbers in the pie charts cannot be read. At the very least, this figure needs to be increased in size.

However, **it might be easier to include some of the information in an additional table.**

- In the caption, it is not clear what 'black lines' are referred to here.

**Response:** Accepted. We will improve the figure and more details can be seen in Table1.

**Changes in the manuscript:** Please refer to Page 40 line 903-914

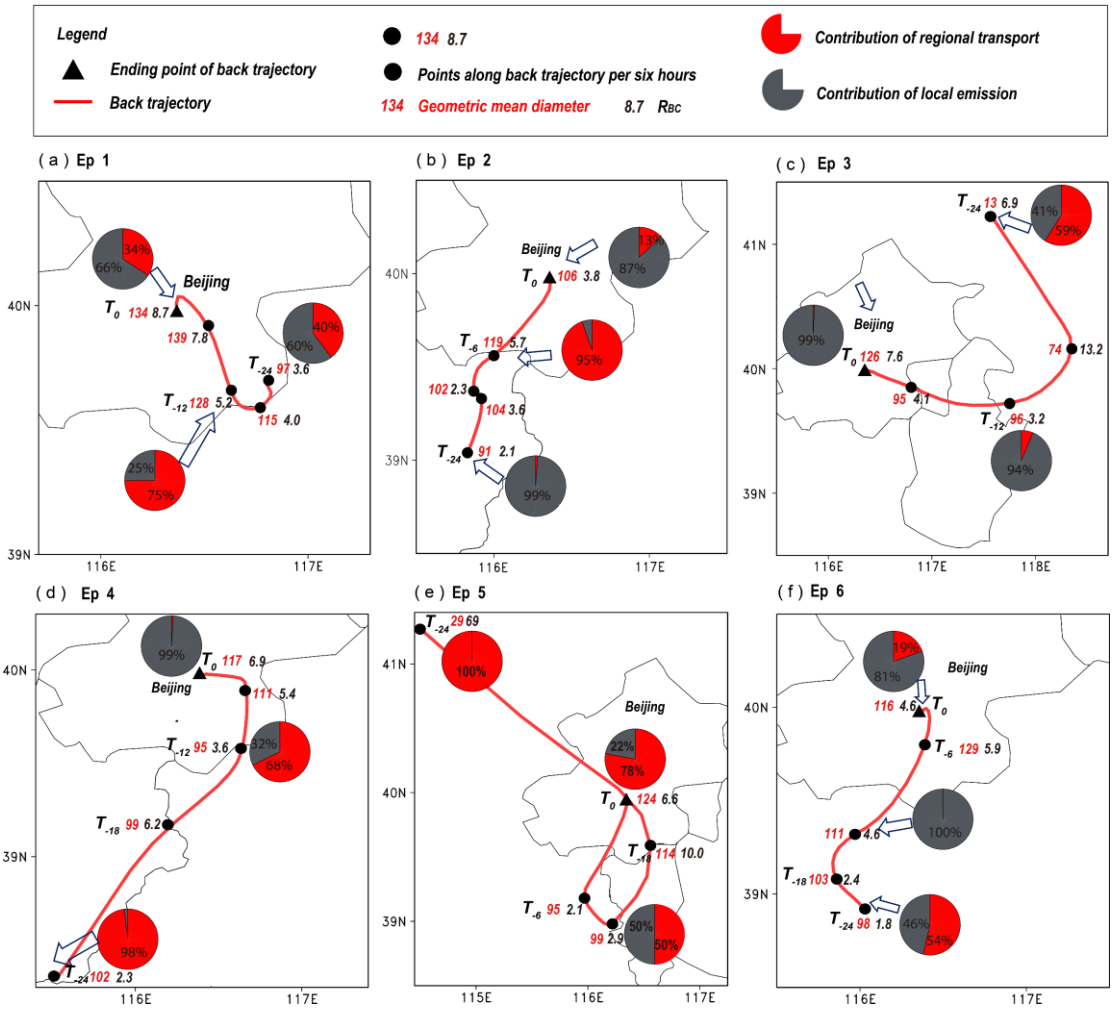


Figure 12. Variation of aerosol properties along transport. Panel a–f refers to episode 1–6. The red lines refer to 24 h backward trajectories at the altitude of 100 m. Aerosol properties include geometric mean diameter (GMD [nm], red numbers beside the solid blocks), mass ratio of coating to BC ($R_{BC}$, the black numbers beside the solid blocks, an indicator of aging degree), region source of BC (pies, the red represents regional transport and the gray is the local contribution). Shaded triangles are ending points of back trajectories, called $T_0$. Shaded circles are points along trajectories per six hours. $T_{-6}$, $T_{-12}$, $T_{-18}$, $T_{-24}$ mean 6, 12, 18, 24 hours before arriving at ending site. Ending times of backtrajectories are before pollution peaks at 21:00 on November 18, 22:00 on November 25, 16:00 on November 29, 22:00 on December 03, 0:00 on December 8 and 22:00 on December 11 (LST), respectively.

Table 1. Aerosol properties along transport, including geometric mean diameter (GMD [nm]), mass ratio of coating to BC ($R_{BC}$), number concentration (N) and contribution of region source to BC (Cr [%]). $T_0$ means ending points of back trajectories and $T_n$ means n hours before arriving at the ending point.

| Period | Property | $T_{-24}$ | $T_{-18}$ | $T_{-12}$ | $T_{-6}$ | $T_0$ |
|---|---|---|---|---|---|---|
| Ep1 | $R_{BC}$ | 3.6 | 4.0 | 5.2 | 7.8 | 8.7 |
| | GMD | 97 | 115 | 128 | 139 | 134 |
| | N | 28994 | 15494 | 15204 | 15592 | 19242 |
| | Cr | 40 | 93 | 75 | 7 | 34 |
| Ep2 | $R_{BC}$ | 2.1 | 3.6 | 2.3 | 5.7 | 3.8 |
| | GMD | 91 | 104 | 102 | 119 | 106 |
| | N | 23909 | 15189 | 17961 | 10994 | 20121 |
| | Cr | 1.2 | 0.14 | 0.01 | 95 | 13 |
| Ep3 | $R_{BC}$ | 6.9 | 13.2 | 3.2 | 4.1 | 7.6 |
| | GMD | 13 | 74 | 96 | 95 | 126 |
| | N | 22234 | 11880 | 13481 | 14241 | 12945 |
| | Cr | 59 | 81.4 | 6.2 | 8.8 | 1 |
| Ep4 | $R_{BC}$ | 2.3 | 6.2 | 3.6 | 5.4 | 6.9 |
| | GMD | 102 | 98 | 95 | 111 | 117 |
| | N | 19754 | 12805 | 21116 | 10536 | 17199 |
| | Cr | 98 | 56 | 68 | 25 | 1 |
| Ep5 | $R_{BC}$ | 69 | 10.0 | 2.9 | 2.1 | 6.6 |
| | GMD | 29 | 114 | 99 | 95 | 124 |
| | N | 8617 | 8086 | 16494 | 28211 | 13696 |
| | Cr | 100 | 100 | 50 | 4 | 78 |
| Ep6 | $R_{BC}$ | 1.8 | 2.4 | 4.6 | 5.9 | 4.6 |
| | GMD | 98 | 103 | 111 | 129 | 116 |
| | N | 31691 | 23691 | 17885 | 12897 | 21955 |
| | Cr | 54 | 0.17 | 0.01 | 65 | 19 |

**Major comments 5**: I am confused about the treatment of organics in the discussion of measured and modeled aerosol. It is well known that also organics can be directly

emitted from various sources. However, for example, in the caption of Figure 7, OM and PA are separately listed. Please explain somewhere what PA (primary aerosol) includes and how the proportions of primary vs secondary organic aerosol are tracked within the model.

**Response:**

In the Observation, Organic matters were measured by using an Aerodyne high-resolution time-of-flight aerosol mass spectrometer at Beijing (Sun et al., 2015). The OC/EC in aerosol was measured by a field semi-online OC/EC analyzer from Sunset Laboratory Inc. (USA) with a PM2.5 cyclone inlet at Tianjin and Lang Fang (Gao et al., 2016).

In the model, organics include two parts: primary organic aerosols (POA) and secondary organic aerosols (SOA). POA are from emission of OC. Six secondary organic aerosols (SOA), in which two were from anthropogenic precursors (toluene and higher aromatics) and four were from biogenic precursors (monoterpene and isoprene), were explicitly treated in NAQPMS. The formation of SOA consists of two steps: the photooxidation of volatile organic compounds (VOCs) by OH to produce semi-volatile organic compounds (SVOCs); then SVOCs can be partioned between gaseous/liquid or gaseous/solid to form secondary organic aerosols.

In the study, PA means sum of non-organic primary $PM_{2.5}$ and BC. OM includes primary organic aerosols and secondary organic aerosols.

POA is tracked by OC. SOA is tracked by its precursors.

**Changes in the manuscript:**

The measure of organics was clearly stated. Please refer to Page 9-10 line 253-254, 258-260.

PA means sum of non-organic primary $PM_{2.5}$ and BC. Please refer to Page 13 line 355.

OM includes primary organic aerosols and secondary organic aerosols. Please refer to Page 14 line 392.

**Major comments 6**: Many of the results seem trivial. They should be other presented as such or their novelty should be better highlighted if they indeed are surprising for the particular conditions in the current study.

a) l. 344 ff: It is well known that secondary aerosol exceeds primary aerosol after a short period of aging.

**Response:** Yes, after a period of aging, secondary aerosols exceed primary aerosols. Precursors of secondary aerosols can stay one day to one week in the air. We quantified the sources of SIA and found that SIA mainly came from regional transport. Therefore, region-joint control of precursors is necessary. And this is consistent with observation result that after region-joint control measures taken, derease ratio of SIA was bigger than that of PA.

**Changes in the manuscript:** Regional controls "on precursors" was added. Please refer to Page 14 line 373.

b) l. 340/341: This sentence is trivial. What other sources could SIA have if not chemical production?

Response: Accepted.

**Changes in the manuscript:** we will delete this sentence. Please refer to Page 14 line 370.

c) It is mentioned that particles are aged within _2 hours. Thus, is it surprising that in most cities a large fraction of PA originated from local emissions (l. 331)?

**Response:** Aging of BC within 2 hours means hydrophobic BC particles can be converted to be hydrophilic within 2 hours. BC, $NO_2$ and $SO_2$ are often from ths same source in anthropogenic source region. Aged means aerosols coated by secondary inorganic and organic aerosols through condensation and coagulation in the air. Therefore, BC may be aged shortly after emission in the anthropogenic source area .

Region sources of PA are managed by tagging emission regions. BC aging could not

directly change sources although their life time can be changed due to different wet deposition efficiency.

d) R(BC) for fresh particles should be _0. Thus, the sentence in l. 457 is trivial.

**Response:** Yes. This sentence will be deleted. Comparisons with other countries and other regions in China show that $R_{BC}$ of Beijing is higher than that in Fresno, located in vally region of California, of 2-3.5 (Collier et al., 2018). $R_{BC}$ of Beijing in this study is smaller than that in Tibet Plateau with average of about 7.7 (Wang et al., 2017). But $R_{BC}$ under pollution is close to SOA dominated BC-coating particles with $R_{BC}$ of 8 (Lee, 2017).

**Changes in the manuscript:** we will delete this sentence. Please refer to Page 18 line 505.

e) l. 565: 'heterogeneous chemistry played the most crucial role under high pollution levels': It is not clear how you arrive at this conclusion. It is obvious that under high pollution levels (i.e. high $SO_2$ levels) the contribution of PA might be small. However, it is not evident to me why the absolute contributions of gas and aqueous phase chemistry should not be enhanced equally.

**Response:**

UV radiative transfer (TUV) model, which calculates the effect of aerosol, cloud, and gaseous pollutant on photolysis, was included in NAQPMS (Li et al., 2011). Under pollution levels, radiation decreases and OH concentration is lower, and production of gas chemistry reduced.

In the model, aqueous phase chemistry only included in cloud chemistry.

Reaction rate of heterogeneous is positively related to **aerosol surface area and uptake coefficient**. Aerosol size increases due to hygroscopic growth under high relative humidity, which provides a good medium for heterogeneous reactions. Also, uptake coefficient is related to humidity, and higher relative humidity during high

pollution levels is favorable for gas uptake. Therefore, absolute contributions of heterogeneous increased but contribution of gas and aqueous chemistry decreased.

Therefore, heterogeneous chemistry will play a relatively crucial role under high pollution levels.

**Changes in the manuscript:** 'heterogeneous chemistry played a relatively crucial role under high pollution levels during Ep1'. Please refer to Page 22 line 619-620.

**Minor comments**

l. 158 ff: It is not clear what ith here means. Do you mean 'emission from region i'?

**Response:** Yes. We will add "region" to this line.

**Changes in the manuscript:** Please refer to Page 7 line 176,178.

l. 171: Is 'n' the number of all regions. Please specify.

**Response:** Yes, 'n' is the number of all regions. We will specify it in the manuscript.

**Changes in the manuscript:** Please refer to Page 7 line 191.

l. 279: Figure S2 only shows SO2, not NO2.

**Response:** We will change it.

**Changes in the manuscript:** Please refer to Page 11 line 308.

l. 364/365: I do not understand this sentence.

**Response:** This sentence is not closely related to stated before and it will be deleted.

**Changes in the manuscript:** This sentence will be deleted. Please refer to Page 14 line 395.

l. 368 – 374: This text sounds awkward and should be reworded. As it is written it implies that the clean or polluted conditions, respectively, determined the various

source regions. However, it would be more reasonable to say that the wind direction from the various source regions led to the transport of the respective air masses into the study region. Because of the transport distance and/or pollution level in the source region, the resulting pollution level in the study region was high or low, respectively.

**Response:** We will change it in the manuscript. Variation of wind direction with SIA level will be added to the manuscript.

When Beijing is controlled by strong northerly wind, NHB and SX are the main source regions, contributing up to 30% and 19%, resulting in clean conditions (SIA < 50 μg $m^{-3}$). When Beijing is mainly affected by southerly wind (southeast, south and southwest), WHB, EHB and SD become the main source regions, contributing 27%, 13% and 15%, respectively. Strong emissions of source regions lead to heavier pollution level in Beijing. When Beijing is dominated by weak southeast wind, contribution from far regions like HN and SD increases. Continuous transport and accumulation lead to severe pollution (SIA > 150 μg $m^{-3}$).

**Changes in the manuscript:** Please refer to Page 15 line 402-417.

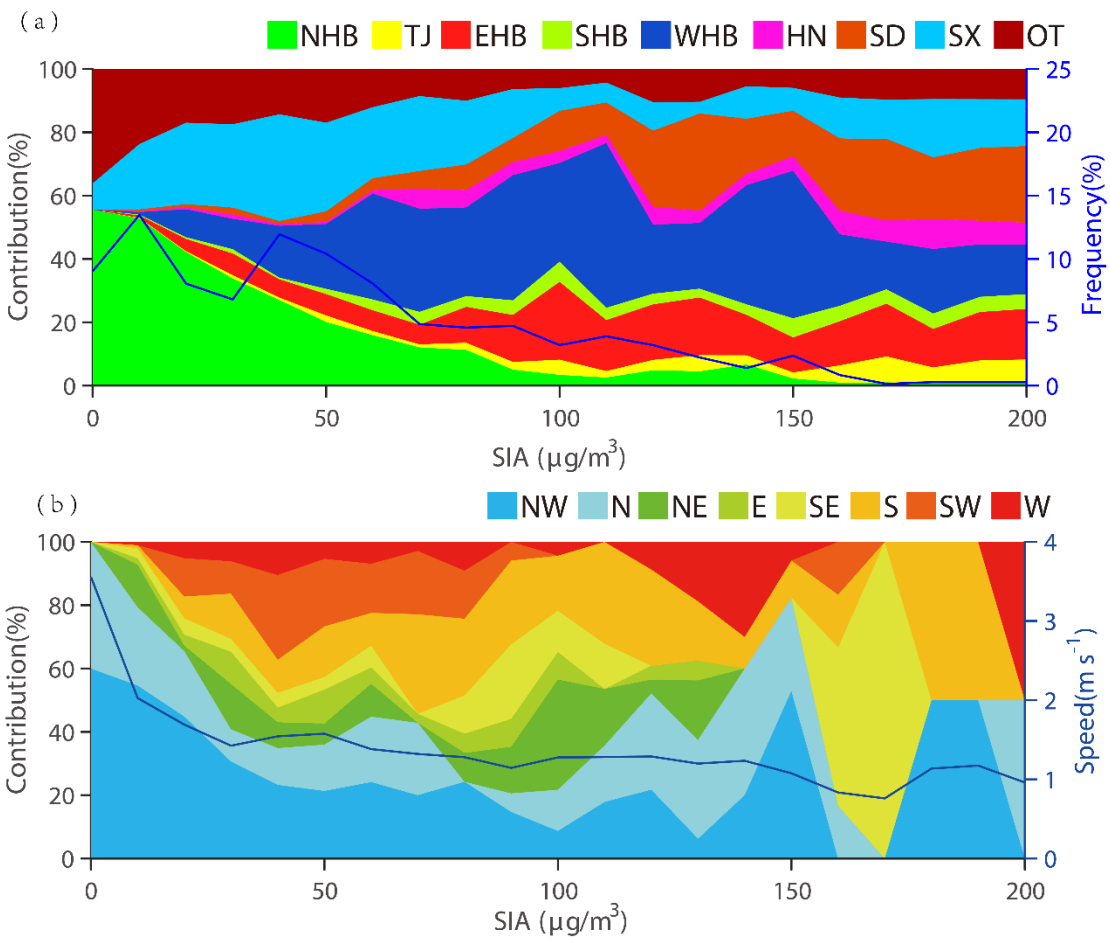


**Figure 8.** (a) Relative contribution of regionally transported SIA under different pollution levels in Beijing during whole study period; (b)Variation of wind direction under different pollution levels in Beijing during whole study period.

l. 478: ': : : this would affect radiation and climate change' should be removed.

**Response:** Accepted.

**Changes in the manuscript:** Please refer to Page 19 line 527.

l. 488: What does such a high R(BC) in a source region mean? Aerosol transported from that region will always appear aged.

**Response:** At $T_{-24}$ in Ep5, simulated $R_{BC}$ is up to 69, which is much higher than that in anthropogenic source regions. At that time, air mass is in Zhangjiakou, a clean city and almost all BC is from regional transport. GMD is 29 nm and number concentration is

8617 $cm^{-3}$, relatively small compared with other time of transport. Therefore, high $R_{BC}$ is caused by high concentration of transported coated aerosols. Correspondingly, in polluted areas, the aging degree may be relatively low due to continuous BC emissions.

Our model can quantify mass ration of coating to BC, that's $R_{BC}$. As the refree points out that aerosol aged during transport, but aging degree varies in different locations and during different episodes. And aging degree can affect extinction properties of aerosols. This index is studied seldomly by 3-D air quality models before. And the importance of studying about aging degree is confirmed by laboratory and researches (Liu et al., 2017).

l. 545: 'the major form of SO42-' should be replaced by 'the major source of SO42-'

**Response:** We will change it in the manuscript.

**Changes in the manuscript:** Please refer to Page 22 line 597.

Table S1: The caption should include more details.

**Response:** We will change it in the manuscript.

**Changes in the manuscript:**

Table S1. Statistics performances of meteorological simulations, including temperature and relative humidity at 2 m, and wind speed at 10 m. Statistical parameters include correlation coefficient (R), Normalized Mean Bias (NMB) and Root Mean Squared Error (RMSE).

**Technical comments**

l. 45: 'experiencing' should be 'experienced'

**Response:** We will change it in the manuscript.

**Changes in the manuscript:** Please refer to Page 2 line 45.

l. 71: ‘physicochemical’ misspelled

**Response:** We will change it in the manuscript.

**Changes in the manuscript:** Please refer to Page 3 line 72.

l. 204: Draxler misspelled

**Response:** We will change it in the manuscript.

**Changes in the manuscript:** Please refer to Page 8 line 224.

l. 235: were obtained

**Response:** We will change it in the manuscript.

**Changes in the manuscript:** Please refer to Page 10 line 264.

l. 296: ‘respectively’ misspelled

**Response:** We will change it in the manuscript.

**Changes in the manuscript:** Please refer to Page 12 line 325.

**References**

Collier, S., Williams, L. R., Onasch, T. B., Cappa, C. D., Zhang, X. L., Russell, L. M., Chen, C. L., Sanchez, K. J., Worsnop, D. R., and Zhang, Q.: Influence of Emissions and Aqueous Processing on Particles Containing Black Carbon in a Polluted Urban Environment: Insights From a Soot Particle-Aerosol Mass Spectrometer, Journal of Geophysical Research-Atmospheres, 123, 6648-6666, 10.1002/2017jd027851, 2018.

Du, W., Zhao, J., Wang, Y., Zhang, Y., Wang, Q., Xu, W., Chen, C., Han, T., Zhang, F., Li, Z., Fu, P., Li, J., Wang, Z., and Sun, Y.: Simultaneous measurements of particle number size distributions at ground level and 260 m on a meteorological tower in urban Beijing, China, Atmospheric Chemistry and Physics, 17, 6797-6811, 10.5194/acp-17-6797-2017, 2017.

Gao, J., Peng, X., Chen, G., Xu, J., Shi, G. L., Zhang, Y. C., and Feng, Y. C.: Insights into the

chemical characterization and sources of PM(2.5) in Beijing at a 1-h time resolution, The Science of the total environment, 542, 162-171, 10.1016/j.scitotenv.2015.10.082, 2016.

Huang, R. J., Zhang, Y., Bozzetti, C., Ho, K. F., Cao, J. J., Han, Y., Daellenbach, K. R., Slowik, J. G., Platt, S. M., Canonaco, F., Zotter, P., Wolf, R., Pieber, S. M., Bruns, E. A., Crippa, M., Ciarelli, G., Piazzalunga, A., Schwikowski, M., Abbaszade, G., Schnelle-Kreis, J., Zimmermann, R., An, Z., Szidat, S., Baltensperger, U., El Haddad, I., and Prevot, A. S.: High secondary aerosol contribution to particulate pollution during haze events in China, Nature, 514, 218-222, 10.1038/nature13774, 2014.

Lee, A. K. Y.: Formation of secondary organic aerosol coating on black carbon particles near vehicular emissions, 2017.

Li, J., Chen, X., Wang, Z., Du, H., Yang, W., & Sun, Y., et al.: Radiative and heterogeneous chemical effects of aerosols on ozone and inorganic aerosols over east Asia, Science of the Total Environment, 622-623, 1327, https://doi.org/10.1016/j.scitotenv.2017.12.041, 2018.

Li, J., Wang, Z., and Xiang, W.: Daytime Atmospheric Oxidation Capacity of Urban Beijing under Polluted Conditions during the 2008 Beijing Olympic Games and the Impact of Aerosols, Sola, 7, 73-76, 10.2151/sola.2011-019, 2011.

Liu, D. T., Whitehead, J., Alfarra, M. R., Reyes-Villegas, E., Spracklen, D. V., Reddington, C. L., Kong, S. F., Williams, P. I., Ting, Y. C., Haslett, S., Taylor, J. W., Flynn, M. J., Morgan, W. T., McFiggans, G., Coe, H., and Allan, J. D.: Black-carbon absorption enhancement in the atmosphere determined by particle mixing state, Nat Geosci, 10, 184-U132, 10.1038/Ngeo2901, 2017.

Liu, Z. R., Hu, B., Zhang, J. K., Yu, Y. C., and Wang, Y. S.: Characteristics of aerosol size distributions and chemical compositions during wintertime pollution episodes in Beijing, Atmospheric Research, 168, 1-12, 10.1016/j.atmosres.2015.08.013, 2016.

Sun, Y., Du, W., Wang, Q., Zhang, Q., Chen, C., Chen, Y., Chen, Z., Fu, P., Wang, Z., Gao, Z., and Worsnop, D. R.: Real-Time Characterization of Aerosol Particle Composition above the Urban Canopy in Beijing: Insights into the Interactions between the Atmospheric Boundary Layer and Aerosol Chemistry, Environmental science & technology, 49, 11340-11347, 10.1021/acs.est.5b02373, 2015.

Wang, J., Zhang, Q., Chen, M., Collier, S., Zhou, S., Ge, X., Xu, J., Shi, J., Xie, C., Hu, J., Ge, S., Sun, Y., and Coe, H.: First Chemical Characterization of Refractory Black Carbon Aerosols and Associated Coatings over the Tibetan Plateau (4730 m a.s.l), Environmental science & technology, 51, 14072-14082, 10.1021/acs.est.7b03973, 2017.

Zheng, G. J., Duan, F. K., Su, H., Ma, Y. L., Cheng, Y., Zheng, B., Zhang, Q., Huang, T., Kimoto, T., Chang, D., Poschl, U., Cheng, Y. F., and He, K. B.: Exploring the severe winter haze in Beijing: the impact of synoptic weather, regional transport and heterogeneous reactions, Atmospheric Chemistry and Physics, 15, 2969-2983, 10.5194/acp-15-2969-2015, 2015.

**And we carefully edited the language and expression.**

1) Change “for” with “in”. Please refer to Page 1 line 21, 22.

2) “of regional transport”was deleted. Please refer to Page 1 line 26.

3) “in Beijing” was deleted. Please refer to Page 2 line 52.

4) Change “on days of severe pollution” to “on severe pollution days”. Please refer to Page 3 line 59.

5) Change “related to” to “associated with”. Please refer to Page 3 line 61.

6) Change “support” to “explain”. Please refer to Page 3 line 63.

7) Please refer to Page 3 line 67-71.

8) Change “Recent” to “Comprehensive”. Please refer to Page 3 line 72.

9) Change ”provide more information” to “provide more insights into”. Please refer to Page 3 line 74.

10) Change “essential” to “useful”. Please refer to Page 3 line 87.

11) Delete “which mostly concentrate on mass concentrations”. Please refer to Page 4 line 89-90.

12) Reorganize the sentencess “The treatment of heterogeneous chemistry is likely another source of modeling uncertainty” . Please refer to Page 4 line 90-97.

13) Change “In the present study” to “ In this study”. Please refer to Page 4 line 106.

14) Change “ winter campain” to “research”. Please refer to Page 4 line 108.

15) Change “coupling it with” to “incorporating” and change “assess” to “explicate”. Please refer to Page 4 line 109-113.

16) Please refer to Page 5 line 118-120.

17) Change “Model structure”to “Model configuration”

18) Description of observation instruments are added. Please refer to Page 10 line 256-257, line 260-263.

# Modeling of aerosol property evolution during winter haze episodes over a megacity cluster in northern China: Roles of regional transport and heterogeneous reactions of $SO_2$

Huiyun Du[1,2], Jie Li[1,2,3*], Xueshun Chen[1], Zifa Wang[1,2,3], Yele Sun[1,2,3], Pingqing Fu[1], Jianjun Li[4], Jian Gao[5], Ying Wei[1,2]

[1] LAPC, Institute of Atmospheric Physics, Chinese Academy of Sciences, Beijing 100029, China

[2] College of Earth Sciences, University of Chinese Academy of Sciences, Beijing 100029, China

[3] Center for Excellence in Urban Atmospheric Environment, Institute of Urban Environment, Chinese Academy of Sciences, Xiamen, China

[4] China National Environmental Monitoring Center, Beijing, China

[5] Chinese Research Academy of Environmental Sciences

**Abstract.** Regional transport and heterogeneous reactions played crucial roles in haze formation over a megacity cluster centered on Beijing. In this study, the updated Nested Air Quality Prediction Model System (NAQPMS) and the HYSPLIT Lagrangian trajectory model were employed to investigate the evolution of aerosols—in terms of the number concentration, size distribution, and aging degree—in Beijing during six haze episodes between November 15 and December 15, 2016, as part of the Air Pollution and Human Health–Beijing (APHH-Beijing) winter campaign of 2016. The model exhibited reasonable performance not only ~~for~~in mass concentrations of $PM_{2.5}$ and its components in Beijing but also ~~for~~in the number concentration, size distribution, and aging degree. We ~~discovered~~ revealed that regional transport played a nonnegligible role in haze episodes, with contributions of 14%–31% to the surface $PM_{2.5}$ mass concentration. The contribution of regional transport to secondary inorganic aerosols was larger than that ~~of regional transport~~ to primary aerosols (30%–63% vs. 3%–12%). The chemical transformation of $SO_2$ in the transport pathway from source regions to Beijing was the major form of $SO_4^{2-}$ regional transport. We also found that sulfate formed outside Beijing from $SO_2$ that was emitted in Beijing; this sulfate was then blown back to Beijing and considerably influenced haze formation. In the transport

pathway, aerosols underwent aging, which altered the mass ratio of coating to black carbon ($R_{BC}$) and the size distribution of number concentrations. During the episodes, the geometric mean diameter (GMD) increased from less than 100 nm at the initial site to approximately 120 nm at the final site (Beijing), and $R_{BC}$ increased from 2–4 to 4–8. These changes would affect regional radiation and climate. In haze episodes with high humidity, the average contributions of gas and aqueous chemistry, heterogeneous chemistry, and primary ~~sulfate~~ emission to sulfate were comparable. Primary emissions had the greatest impact under light to moderate pollution levels, whereas heterogeneous chemistry had a stronger effect under high pollution levels.

**Keywords**: Regional transport; heterogeneous reactions; number size distribution; NAQPMS

# 1 Introduction

In past decades, a megacity cluster in China that is centered on Beijing and includes 28 cities (272,500 km$^2$, a population of 191.7 million people) has ~~been experiencing~~ experienced frequent severe and persistent haze episodes (Zhao et al., 2013; Sun et al., 2014; Sun et al., 2016). $PM_{2.5}$ levels exceeding 500 μg m$^{-3}$ have often been reported. The adverse effects of $PM_{2.5}$ on visibility, climate, and particularly human health have drawn widespread public attention (Hyslop, 2009; Chen et al., 2018; Yang et al., 2017a; Yang et al., 2017b; Anderson et al., 2010). Although the $PM_{2.5}$ concentration in Beijing has decreased by 35% in the recent 5 years (2013–2017) because of implementation of the Atmospheric Pollution Prevention and Control Action Plan, the $PM_{2.5}$ level ~~in Beijing~~ in 2017 still reached 58 μg m$^{-3}$, which is 1.7 times the World Health Organization-recommended safe level of 35 μg m$^{-3}$ (http://www.bjepb.gov.cn/bjhrb/index/index.html). Understanding the mechanism of haze episodes in this megacity cluster is thus an urgent task for policymakers.

Observations have revealed that haze episodes in this megacity cluster are mainly caused by the rapid formation of secondary inorganic species (SIA, including sulfate, nitrate, and ammonium) (Huang et al., 2014; Zheng et al., 2015; Han et al., 2016). The

SIA mass fraction in $PM_{2.5}$ can be up to 55% on~~ days of~~ severe pollution days, which is 2.5 times that on clear days (Ma et al., 2017). Tang et al. (2016a) proposed that local chemical transformation~~ related to~~associated with humidity dominates the rapid formation of SIA in Beijing. Yang et al. (2015) argued that local chemical conversion would not be fully able to~~ support~~explain the observed rapid formation of SIA in a short time. Using a ceilometer and in situ observation data, Zhu et al. (2016) and Ma et al. (2017) further proposed that regional transport was the major cause of the initial haze stage and that local chemistry, particularly heterogeneous chemistry, dominated the later rise in Beijing. This result is different from the findings~~ obtained using~~of modeling studies~~numerical air quality models (LOTOS-EUROS, Regional Air Quality Model System [RAQMS], and the Nested Air Quality Prediction Modeling System [NAQPMS])~~ (Timmermans et al., 2017; Li and Han, 2016; Li et al.,2017), in which regional transport was identified as the dominant factor~~dominated~~ during haze episodes in the megacity cluster. Comprehensive~~Recent~~ observations of the physicochemical properties (e.g., mixing state, number concentration, and size distribution) of aerosols can provide more insights into~~information for improving~~ the accuracy of regional transport and chemistry assessment. Black carbon (BC) is usually more thickly coated by SIA and organic aerosols in transported and aged air masses than in fresh particles, as indicated by higher fractal dimension (Wang et al., 2017b), larger coating fraction (ratio of variation in BC mass equivalent diameter to initial BC diameter, $\Delta D_{me}/D_{me,0}$) (Peng et al., 2016) and the higher mass ratio of coating to BC ($R_{BC}$) (Wang et al., 2018a). Massoli et al. (2015) and Wang et al. (2017) reported that $R_{BC}$ exceeded 10 in remote sites after BC had undergone long-term transport. This value was much higher than that in an urban area with high fresh particle emissions, where $R_{BC}$ generally was less than 1.5 (Liu et al., 2017). The geometric mean diameter (GMD) of $PM_{2.5}$ also changed significantly due to the impact of regional transport. In haze episodes in Beijing, the GMD increased to 120 nm in regionally transported air masses, which is twice that under clean conditions (Ma et al., 2017). Investigating the evolution of aerosol properties other than mass concentration during regional transport is thus ~~essential~~

useful for assessing the roles of regional and local chemistry. Such investigations are rarely conducted using the current three-dimensional chemical transport models~~, which mostly concentrate on mass concentrations~~. ~~The treatment of heterogeneous chemistry is likely another source of modeling uncertainty.~~ The current models generally account for only a part of the observed $SO_4^{2-}$ concentrations (Wang et al., 2014a). Heterogeneous chemistry is considered critical to improving model performance (Zheng et al., 2015; Cheng et al., 2016; Li et al., 2018). The treatment of heterogeneous chemistry is likely another source of modeling uncertainty. The heterogeneous reaction parameters are not related to the key parameters such as mixing state and aerosol water contents.

From November 15 to December 15, 2016, a field campaign was carried out in Beijing within the framework of the UK-China Air Pollution & Human Health (APHH) project. Details can be seen in Shi et al. (2018). ~~Nearly 30 Chinese and British institutions—including the Institute of Atmospheric Physics, Chinese Academy of Sciences, Leeds University, the University of Birmingham, the University of Reading, Tsinghua University, and Peking University—participated in this campaign.~~ Aerosol properties such as the size distribution, number concentration, and mixing states were simultaneously measured in China. APHH-Beijing aimed to explore the sources ~~of~~ and processes affecting urban atmospheric pollution in Beijing. In ~~the present~~this study, we used the NAQPMS to simulate aerosol properties in the campaign period as a part of the APHH ~~winter campaign~~research. To improve model performance, the NAQPMS was updated by ~~coupling it with~~incorporating an advanced particle microphysics (APM) module that explicitly accounts for the microphysical process (Chen et al., 2014) and a new heterogeneous chemistry scheme ~~(Chen et al., 2014;~~ (Li et al., 2018). The hybrid single-particle Lagrangian integrated trajectory model (HYSPLIT) was also employed to ~~assess~~ explicate the evolution of aerosol properties (e.g., mixing state, number concentration, and size distribution). The transport of precursors or secondary products, and heterogeneous reactions were mainly focused on sulfate, as recent studies indicated that sulfate is a key driver for severe haze events (Huang et al., 2014;Zheng et al., 2015).

Crucially, the effects of regional transport and heterogeneous chemistry of $SO_2$ on aerosol properties were quantified. To ~~the best of~~ our knowledge, this is the first study to distinguish the contributions of transport of SIA itself and its precursors to $PM_{2.5}$ in Beijing, and combine trajectories with microphysical properties evolution. We believe that this study is helpful to understanding the causes of haze in this megacity cluster.

# 2 Model description and methodology

## 2.1 Model description

The Nested Air Quality Prediction Model System (NAQPMS) developed by the Institute of Atmospheric Physics, Chinese Academy of Sciences (IAP/CAS) is a three-dimensional Eulerian terrain-following chemical transport model. WRFv3.6.1, driven by Final Analysis (FNL)data from the National Centers for Environmental Prediction (NCEP), provides the meteorology field for the NAQPMS. The NAQPMS includes emission, horizontal and vertical advection and diffusion, dry and wet deposition, and chemical (including gas, aqueous, and heterogeneous) reaction processes (Wang et al., 2001; Li et al., 2012; Li et al., 2018). In the model, aqueous chemistry happened only in cloud water. Heterogeneous chemistry reactions happen on aerosol aqueous layer and are related with aerosol liquid water. It also incorporates online source tagging, process analysis, an online WRF coupler, and other techniques (Wu et al., 2017; Wang et al., 2014b). The Carbon Bond Mechanism version-Z (CBMZ) is used for gas-phase chemistry mechanisms. The thermodynamic model ISORROPIAI1.7 is used to calculate the composition and phase state of an $NH_4^+$–$SO_4^{2-}$–$NO_3^-$–$Cl^-$–$Na^+$–$H_2O$ inorganic aerosol system (Nenes et al., 1998). Six secondary organic aerosols (SOA) are managed using a two-product module. Further details of the NAQPMS can be found in the studies of Li et al. (2013, 2014, 2017), and numerous subsequent papers have been published describing recent updates.

To accurately describe aerosol properties (e.g., number concentration, size distribution, and mixing states), an advanced multitype, multicomponent, size-resolved

microphysics (APM) module is coupled to the NAQPMS (Chen et al., 2014). APM explicitly describes microphysical aerosol processes, including nucleation, condensation, evaporation, coagulation, thermodynamic equilibrium with local humidity, hygroscopic growth, and dry and wet deposition (Yu and Luo, 2009), and it has already been applied in the global GEOS-Chem model (Ma et al., 2014). In the updated NAQPMS, 40 sectional bins covering 0.0012–12 μm were used to represent secondary particle distribution ($SO_4^{2-}$, $NO_3^-$, $NH_4^+$, and secondary organic aerosols) (Chen et al., 2014). The size distribution of BC and primary organic aerosol was represented using 28 section bins. Other primary particles such as dust and sea salt were represented using four bins. The coating of secondary species on primary particles (sea salt, BC, OC, and dust) was explicitly simulated using a scheme that dynamically calculates the aerosol aging time with an hourly resolution on the basis of aerosol microphysics. Mixing state is assumed to be semi-external. Primary particles coated with SIA or SOA are considered as core-shell mixing while nucleated secondary particle is internally mixed (Chen et al., 2014). The mass concentrations of coating species were also tracked in the model. Chen et al. (2017) employed the updated NAQPMS and revealed that the daytime aging time of BC in Beijing in winter can be less than 2 hours. This is much less time than the fixed aging time scale of 1.2 days that has been stipulated in previous studies (Liu et al. 2009) but is close to observed levels (2–4 hours) (Peng et al. 2016). Li et al. (2018) further developed a heterogeneous chemical scheme based on mixing states to reproduce the chemical transformation of gaseous precursors on an aerosol surface, which largely altered the sizes and hygroscopicity of particles. Heterogeneous chemistry includes oxidation of S(IV) on aqueous layer of aerosols and it is parameterized according to the scheme of Li et al. (2018). Comparison with long-term observations has proven that the updated NAQPMS can successfully estimate aerosol mass and the number concentration, size distribution, mixing states, and BC aging time in China (Li et al., 2017b, 2018; Chen et al., 2014, 2017).

Distinguishing the contributions of the transport of SIA itself and its precursors to

$PM_{2.5}$ is always difficult (Sun et al., 2014; Li et al., 2014, 2017; Ying et al., 2014). These contributions have generally been named regional transport in studies; this leads to ambiguity in regional transport. In this study, we divided the secondary species (e.g., SIA) in the $i^{th}$ receptor region into four parts: 1) SIA locally produced from the $i^{th}$ region locally emitted precursors (LC); 2) SIA chemically formed in other regions from the $i^{th}$ region locally emitted precursors (LTC); 3) SIA chemically formed in the transport pathway to the $i^{th}$ receptor region of precursors emitted in the $j^{th}$ source region (RTC); and 4) SIA produced in the $j^{th}$ region from precursors emitted in the $j^{th}$ source region (RLC).

An online tracer-tagging module in the NAQPMS was used to resolve the contributions from LC, LTC, RTC, and RLC. The module is capable of tracing both the emission regions of precursors and the formation regions of secondary aerosols. First, the mass contribution from the locations in which SIA was formed, called $C_2$, was tagged. The mass contribution from precursors emitted in different locations, called $C_1$, was then tagged. More technical details can be found in the studies of Li et al. (2014) and Wu et al. (2017). The following equation can be employed to calculate the degree of chemical conversion during transport (TC):

$$\mathrm{TC} = \sum_{i=1}^{n}(C_{1i} - C_{2i} \times CC_i) \quad (1)$$

Where $i$ means region, and n is the total number of regions, as n is 10 in this study. $C_{1i}$ refers to the absolute mass concentration transported to the receptor site, produced by precursors emitted in region $i$;

$C_{2i}$ refers to the absolute mass concentration formed in region $i$ and transported to receptor site;

$CC_i$ refers to the local contribution ratio of precursors in region $i$;

$C_{2i} \times CC_i$ refers to the absolute mass transported to receptor site and generated at region $i$ by chemical conversion of precursors released at region $i$. When $i = 1$, it refers to LC; when $i \neq 1$, $\sum_{i=2}^{n} C_{2i} \times CC_i$ refers to RLC;

$C_{1i} - C_{2i} \times CC_i$ is the mass concentration generated in all regions except $i$ by chemical conversion of the precursors released at region $i$ and finally transported to the receptor

site. When $i = 1$, it refers to LTC; when $i \neq 1$, $\sum_{i=2}^{n}(C_{1i} - C_{2i} \times CC_i)$ refers to RTC.

In this study, 10 regions according to administrative division are selected for source tagging (Fig. 1c), six of which—Chengde, Zhangjiakou, and Qinhuangdao (NHB); Beijing (BJ); Tianjin (LT); Hengshui, Xingtai, and Handan (SHB); Baoding and Shijiazhuang (WHB); and Tangshan, Langfang, and Cangzhou (EHB)—are a part of the Beijing–Tianjin–Hebei (BTH) area. Henan (HN), Shandong (SD), Shanxi (SX), and other regions (OT) are regions outside the BTH area.

## 2.2 Model ~~structure~~configuration

Simulation was conducted from November 10 to December 15, 2016, and the first 5 days were set aside as a spin-up period. The three nested model domains were shown in Fig. 1a. The horizontal resolutions were 27, 9, and 3 km from the coarsest to innermost domain. The first level of the NAQPMS was approximately 20 m in height, and there were approximately 17 layers under 2 km.

To quantitatively assess the contribution of primary emissions, traditional chemistry reactions (gas-phase and aqueous chemistry reactions), and heterogeneous chemistry to sulfate, three sensitivity simulations were conducted. The baseline scenario (Base) involving all heterogeneous reactions considered primary sulfate emissions and its results were used for model verification and source apportionment analysis. Control 1 (C1) involved all heterogeneous reactions but did not consider primary sulfate emissions. Compared with Base, Control 2 (C2) excluded the heterogeneous reactions of $SO_2$. Base–C2 represents the effect of heterogeneous reactions on sulfate. Base–C1 represents primary sulfate emissions.

The HYSPLIT model was used to analyze the trajectories of air masses (Drax~~i~~ler and Hess, 1998). The calculated trajectories are helpful to resolving the evolution of aerosol properties in the transport pathway by extracting the simulated results by the NAQPMS along trajectories. In this study, the same meteorology data (obtained hourly data of the third domain) used in the NAQPMS were employed to perform trajectory

analysis; this avoided the errors caused by inconsistency between the two models (the NAQPMS and HYSPLIT).

### 2.3 Emission inventory

The anthropogenic emissions were obtained from the 0.25° × 0.25° Multi–resolution Emission Inventory for China (MEIC), and the base year was 2016 for BTH (http://www.meicmodel.org/publications.html). In addition, observation data collected at sites within BTH were used to update the MEIC on the basis of their latitude and longitude information. Biomass burning emissions were taken from the Fire Inventory from NCAR (National Center for Atmospheric Research) (Wiedinmyer et al., 2011). Primary sulfate was assumed to constitute 5% of $SO_2$ emissions in the original MEIC inventory.~~,~~ ~~but through in situ measurement of source profiles,~~ Cao et al. (2014), Wang et al. (2009), Zheng et al. (2013), and Ma et al. (2015) discovered that primary sulfate comprised large amounts ~~approximately 40%, 6%, and 15%~~ of primary $PM_{2.5}$ from industrial, power, and residential emissions, but through in situ measurement of source profiles, ~~respectively,~~ in the main form of $(NH4)_2SO_4$. Thus, we ~~modified primary sulfate emissions in this study~~took 40%, 6% and 15% of primary $PM_{2.5}$ from industrial, power and residential emissions, respectively, as primary sulfate emissions in the inventory. Figure 1b displays the hourly primary $PM_{2.5}$ emission rate.

### 2.4 Observations

The surface meteorological parameters were obtained from the China Meteorological Administration, whereas the vertical profiles of meteorological parameters were obtained from the University of Wyoming (http://weather.uwyo.edu/upperair/sounding.html). Observations of $PM_{2.5}$, $SO_2$, $NO_2$, and $O_3$ concentrations were obtained from the China National Environmental Monitoring Center (http://www.cnemc.cn/). Aerosol components (including ~~BC,~~ organic matters [OM], sulfate, nitrate, and ammonium) were measured in situ at Beijing by using an Aerodyne high-resolution time-of-flight aerosol mass spectrometer. Details

of the instruments can be found in the study by Sun et al. (2015). A seven-wavelength Aethalometer (AE33, Magee Scientific Corp.) was used to measure BC at Beijing (Xie et al., 2018). The OC/EC in aerosol was measured by a field semi-online OC/EC analyzer from Sunset Laboratory Inc. (USA) with a $PM_{2.5}$ cyclone inlet at Tianjin and Lang Fang (Gao et al., 2016). Two same ambient ion monitors (AIM; Model URG 9000D, URG Corporation) were used to measure hourly concentrations of water-soluble ions in $PM_{2.5}$, including $NH_4^+$, $Na^+$, $K^+$, $Ca^{2+}$, $Mg^{2+}$, $SO_4^{2-}$, $NO_3^-$ and $Cl^-$ at TJ and LF (Gao et al., 2016). The particle number size distributions at ground level ~~was~~ were obtained using a scanning mobility particle sizer (SMPS) with a time resolution of 5 min. Details of the instruments can be found in the study by Du et al. (2017). All data in this study are presented in Beijing local time (UTC + 8 h).

# 3 Model validation

## 3.1 $PM_{2.5}$ mass and number concentrations and aging degrees

The time series of simulated and observed $PM_{2.5}$ in different cities of BTH from November 15 to December 15, 2016, are illustrated in Fig. 2. In the study period, six regional haze episodes were identified, namely, November 15–20 (Ep1), November 23–26 (Ep2), November 28–30 (Ep3), December 2–4 (Ep4), December 6–8 (Ep5), December 10–12 (Ep6). The $PM_{2.5}$ mass concentration frequently exceeded 200 μg $m^{-3}$ and the average concentration reached 120 μg $m^{-3}$ during episodes. Haze usually formed in several hours; for example, the increasing rate of $PM_{2.5}$ reached 200 μg $m^{-3}$ $h^{-1}$ and lasted approximately 12 hours in Tangshan. These observed haze patterns were generally reproduced by the NAQPMS. The correlation coefficient (R) between the observation and simulation in most cities was 0.6–0.8, and 60%–80% of simulation results were within a factor of 2 of the observation. The mean fractional bias (MFB) and mean fractional error (MFE) ranged from −0.07 to 0.7, meeting the criteria of MFB ≤ 0.6 and MFE ≤ 0.75 (Boylan et al., 2006). The simulation did however underestimate $PM_{2.5}$ in Beijing and Baoding for Ep2. This was caused by the failure of the mineral

aerosol transport simulation. Compared with other cities in the cluster, Beijing and Baoding are closer to the Gobi Desert, a major dust source in East Asia, and they are thus more easily affected by dust storm transport. Pan et al. (2018) found a pronounced peak in the size distribution at 4–5 μm for Ep2 in Beijing. The concentrations of $Ca^{2+}$ was 7 times the campaign averages (Fig. S1).

The aerosol components in Beijing, Langfang, and Baoding are compared in Fig. 3. In general, the simulation largely reproduced the variation in primary and secondary aerosols. In particular, the rapid increase in SIA during Ep1, Ep2, and Ep4 was captured by the simulation. Interestingly, the NAQPMS underestimated the sulfate concentration in Beijing during Ep2 and Ep4, but the nitrate and ammoniate concentrations during these two episodes were successfully reproduced. This was related to the transport of mineral dust (Ep2) and local emissions (Ep4). As discussed in the last paragraph, Beijing had high mineral loadings for Ep2, which provided a favorable medium for chemical transformation of anthropogenic $SO_2$ into sulfate in the form of $CaSO_4$ or $MgSO_4$ (Wang et al., 2018b;Wang et al., 2017c)~~(Zhuang et al., 1992)~~. Underestimation of the sulfate concentration for Ep4 may have been caused by local emissions in Beijing. As illustrated in Fig. 3, the simulation failed to reproduce the sharp increase in both sulfate and BC in Beijing during this episode. This is different from the case of Ep2, in which sulfate was underestimated but BC was favorably reproduced. Wang et al. (2009) and Ma et al. (2015) found that sulfate accounted for 40% and 6.6% of primary $PM_{2.5}$ emissions from industry and power plants, which also emit a large amount of BC. This sharp increase in BC was a local-scale episode. In Langfang, a site 50–60 km from Beijing, both the observed and simulated BC concentration increased slowly to 20 μg $m^{-3}$, which is much less than that in Beijing (45 μg $m^{-3}$). The monthly emissions employed in this study made it difficult to capture these short-term local-scale emission changes. The simulated $SO_2$ ~~and $NO_2$~~ concentrations are compared with the observations in Fig. S2, and the normalized mean bias (NMBs) of these concentrations were less than 40%.

The number size distribution is critical to examining aerosol evolution during haze

episodes (Ma et al., 2017). In this study, both the simulation and observation revealed a rapid increase in the GMD from 50 to approximately 120 nm during the initial stages of episodes in Beijing (Fig. 4). The observed mean number concentration of aerosols (dN/dlogDp) showed a unimodal distribution and was mainly concentrated in the Aitken mode (25–100 nm) and accumulation mode (100–1,000 nm). The highest concentration was approximately $1.8 \times 10^4$ $cm^{-3}$ at a 100-nm diameter. These patterns were favorably reproduced by the simulation. The simulated number concentrations were underestimated in 10–60 nm by 20%–30% and overestimated in 80–150 nm by 20%. This indicated that the model needs to be improved regarding its treatment of new particle formation and the volatility of primary organic aerosols.

Herein, the aging degree of BC is represented by the mass ratio of coating to BC ($R_{BC}$), which has been widely used in previous studies (Oshima et al., 2009; Collier et al., 2018). Figure 11 shows that the mean simulated $R_{BC}$ in Beijing was 4.5 and 5.0 in the entire study period and during pollution episodes, ~~receptively~~respectively, which are extremely close to the observations (~5.0 and 5.1) (Wang et al., 2018a). The high performance of the model in terms of mass and number concentrations, compositions, and the mixing state of aerosols gives us confidence for analyzing aerosol evolution during transport in the megacity cluster centered on Beijing.

### 3.2 Meteorology

The simulated wind direction and speed coincided with the observations for the haze episodes. In particular, the model captured low wind speeds, and the times at which the wind shifted direction were well reproduced (Fig. S3). Regarding relative humidity and temperature, WRF performed high values of R (0.68–0.93) and low NMBs (−0.51 to 0.44) (Table S1). In particular, the high relative humidity during Ep1 was well reproduced. Inversion layers were present during the initial stage of haze formation (Fig. S4). The height of the inversion layers varied among episodes. During Ep1 and Ep6, strongly elevated inversion layers were present between 1 and 2 km, whereas the inversion layers were close to the surface during other episodes. Temperature inversion

is favorable for pollution accumulation, and the model reproduced this feature favorably. In sum, the high performance of the meteorological simulation gave us confidence for $PM_{2.5}$ simulation.

# 4 Results and discussion

## 4.1 Source apportionment of surface $PM_{2.5}$

The simulated spatial distribution of average surface $PM_{2.5}$ levels and the wind vector during the six haze episodes are shown in Fig. 5. In general, two types of patterns were observed. The first pattern corresponded to Ep1, Ep4, and Ep6 and reflected that a highly polluted belt with >200 μg $m^{-3}$ $PM_{2.5}$ extended from the southwest to the northeast along the Taihang mountain range. In the second pattern (Ep2, Ep3, and Ep5), the $PM_{2.5}$ level of 150–200 μg $m^{-3}$ was concentrated in three northern cities (Beijing, Tianjin, and Tangshan). In the other cities, the $PM_{2.5}$ mass concentrations ranged from 75 to 115 μg $m^{-3}$, indicating a light pollution level according to the Technical Regulation on Ambient Air Quality Index (on trial).

Figure 6 shows the contributions of regional transport and local emissions to average $PM_{2.5}$, primary aerosol (PA, BC and non-organic primary $PM_{2.5}$), and SIA levels in different cities during the study period. The contribution of local emissions was more than that of regional transport to the $PM_{2.5}$ mass concentration in all cities, except Heng Shui, Cangzhou, Langfang, and Qinhuangdao; the magnitude of local emission contributions was 49%–80%. The principle reason for this was the accumulation of local PA emissions. In most cities, 64%–93% of PA originated from local emissions (Fig. 6c). In contrast to PA, the SIA contribution was dominated by regional transport of emissions in other cities (50%–87%). Even the emissions of cities outside the city cluster (e.g., Henan, Shanxi and Shandong) were transported to the megacity cluster, travelling 500–1,000 km. In Beijing, the local contribution to total $PM_{2.5}$ and PA was 74% and 94%, respectively, whereas regional transport from other cities was the major source of SIA, contributing 51%. The difference in source

apportionment between PA and SIA was related to the mechanisms of PA and SIA formation. Regarding PA, the inversion layer and weak winds during stable weather conditions prevented PA transport and resulted in local-scale accumulation of PA emissions. ~~SIA mostly originated from the chemical conversion of its gaseous precursors (e.g., $SO_2$, $NO_2$, and $NH_3$)~~. The regional transport provided sufficient time (1–3 days) and aerosol surface for this chemical transformation (Li et al., 2015; Li et al., 2017b). This also indicates that regional controls on precursors would be the most efficient way to decreasing the SIA concentration in this megacity cluster. Our results agree favorably with the observed impact of regional emission controls in Asia-Pacific Economic Cooperation China 2014. During this gathering, the SIA concentration in Beijing decreased to a greater degree than the PA concentration because of regional controls (Sun et al., 2016).

The source apportionment in haze episodes in Beijing is illustrated in Fig. 7. Regional transport contributed 14%–31% to the surface $PM_{2.5}$ mass concentration during the six episodes. The highest contribution of regional transport occurred in Ep1 and Ep5 (29% and 31% of the total $PM_{2.5}$, respectively). In Ep1 and Ep5, the contribution of the SIA originating from regional transport reached 53% and 63%, respectively. Interestingly, the regionally transported SIA had different source regions in Ep1 and Ep5. In Ep5, SX, WHB, and NHB were the dominant source regions, whereas the source regions for Ep1 were more diverse. This indicates the complexity of regional transport in this megacity cluster. Compared with the episodes in November 2015, the effects of regional transport of $PM_{2.5}$ and SIA mass concentrations were weaker in this study, which may be related to the weather system and emission controls in 2016 (Li et al., 2017b). Therefore, more studies on regional transport should be conducted to further understand regional haze formation mechanisms. In other episodes (Ep2, Ep3, Ep4, and Ep6), regional transport of surface $PM_{2.5}$, PA, OM (organic matters, primary organic aerosols [POA] and secondary organic aerosols [SOA]), and SIA mass concentrations were in the range 14%–23%, 3%–12%, 3%–14%, and 30%–51%, respectively. ~~Local emissions during the episodes were more dominant than the~~

~~monthly averages.~~ Back trajectories and emissions source regions can be connected (Fig. S5), taking Ep6 for example, airmass mainly came from Shandong, through SHB, WHB and finally arrived at Beijing. What's more, the height of trajectory within WHB is low, so contribution of WHB should be big, which agreed with results of Figure 7b, and source apportionment results showed that WHB contributed 24% to SIA at Beijing during Ep6.

Figure 8 presents the relative contribution of regionally transported SIA and variation of wind direction under different levels of pollution in Beijing. The source regions varied considerably under different pollution levels. When Beijing is controlled by strong northerly wind, NHB and SX are the main source regions, contributing up to 30% and 19%, resulting in clean conditions (SIA < 50 μg $m^{-3}$). When Beijing is mainly affected by southerly wind (southeast, south and southwest), WHB, EHB and SD become the main source regions, contributing 27%, 13% and 15%, respectively. Strong emissions of source regions lead to heavier pollution level in Beijing. When Beijing is dominated by weak southeast wind, contribution from far regions like HN and SD increases. Continuous transport and accumulation lead to severe pollution (SIA > 150 μg $m^{-3}$). ~~Under clean conditions (when SIA < 50 μg $m^{-3}$), NHB and SX were the main source regions, contributing up to 30% and 19%, respectively. With the increase of SIA concentrations, WHB, SD, and EHB became the main source regions, contributing 27%, 15%, and 13%, respectively, which is consistent with transport along the southwest and southeast corridors of BTH. Under heavy pollution, pollutants from HN and farther regions were blown to Beijing, resulting in a remarkably higher contribution of HN.~~ This indicates that wider regional emission control is necessary to reduce severe pollution.

## 4.2 Impact of regional transport of sulfate and its precursors on Beijing

Quantifying the impact of regional transport of sulfate and its precursors is a crucial task. Sun et al. (2014) considered sulfate formed outside Beijing as regionally

transported sulfate, and they estimated that its contribution reached ~~67~~75% during winter haze episodes. By tagging emissions regions of precursors in models and ignoring where secondary aerosols were formed, Li et al. (2017) and Timmermans et al. (2017) estimated the contribution of transport to be 40%–50%. These estimated contributions of regional transport are different in physical meaning, which may confuse policymakers. In this study, we divided the sulfate mass concentration in Beijing into four parts, LC, LTC, RLC, and RTC as described in Sect. 2.1. The regional transport defined by Sun et al. (2014) was LTC + RLC + RTC, whereas in the studies by Li et al. (2017) and Timmermans et al. (2017), it was RLC + RTC. In this study, we employed RLC + RTC as representing regional transport.

Figure 9a shows the contributions of LC, LTC, RLC, and RTC to the daily average sulfate concentration in Beijing during the study period. RTC and LC were the dominant sources of sulfate, contributing 71%–89% in total. The contributions of RTC ranged from 29% in Ep6 to 59% in Ep2, and contributions of LC were 30%–42%. RTC dominated the regional transport over the whole period, which indicates that chemical conversions in the transport pathway of $SO_2$ were critical to haze formation. Notably, the LTC contribution was comparable with that of LC in Ep3, Ep4, and Ep6. This suggests that the $SO_2$ emitted in Beijing was blown away and formed sulfate outside of Beijing. And recirculation of air masses can be convinced by HYSPLIT trajectories (Fig. S6). Take trajectories at 23:00 on December 12 [LST] for example, air masses were blown away Beijing by southwesterly, through Chengde, Tianjin and Langfang, and finally tarvelled back to Beijing. These formed sulfates may have been blown back to Beijing under certain weather conditions and were previously considered regional transport. The contribution of LTC also largely explains the difference in estimated regional transport contributions between Sun et al. (2014) and Li et al. (2017). In the present study, LTC + RLC + RTC accounted for 58%–70% of the sulfate concentration in the six episodes, which is relatively similar to the estimation (75%) of Sun et al. (2014), which was based on the observed hourly rate of increase of local sulfate concentration.

In the initial and subsequent pollution stages, LC, LTC, and RTC showed different patterns in Beijing. In Ep1, local contributions dominated before the sulfate concentration increased rapidly (November 15 and 16). In particular, sulfate blown back to Beijing from its local emissions (LTC) made a larger contribution (35%) than RTC (25%). In the rapid rising phase of sulfate (November 17 and 18), contribution of RTC increased from 25% to 47%. LC was also significant and increased considerably from 37% to 41%. These two parts (LC and RTC) explained the rapid formation of sulfate in Beijing. This suggests that the joint control of local and regional $SO_2$ emissions is essential for preventing the rapid formation of haze in this region, which is receiving considerable attention and eliciting widespread interest among the researchers and policymakers (Sun et al., 2014; Ma et al., 2017; Li et al., 2017b). This feature is also reflected in Fig. 9b. Under clear conditions (sulfate < 20 μg $m^{-3}$), the local contributions (LC and LTC) were positively correlated with the sulfate mass concentration. In total, they contributed 40%–60% of the sulfate mass concentration. The ratio of LC to LTC was approximately 2:1. Under moderate sulfate levels (20 μg $m^{-3}$ < sulfate < 35 μg $m^{-3}$), the local contribution was lower—particularly the LTC—leading to a ratio of LC to LTC of approximately 8. Sulfate formed in the regional transport pathway (RTC) significantly increased from 40 to 65%. Under heavy pollution levels (> 35 μg $m^{-3}$), the LC was up to at 50% due to extremely stable boundary layers. Our results are consistent with those of Ma et al. (2017), in which regional transport and local heterogeneous chemistry were qualitatively discovered to make high contributions to initial and subsequent pollution stages.

## 4.3 Evolution of aerosol properties in Beijing during haze episodes

Aerosol properties such as the particle size and aging degree can change dramatically on haze days because of fresh emissions, subsequent chemical conversions, and regional transport, which strongly affect regional radiation and climate (Cappa et al., 2012). As illustrated in Fig. 4b, the GMD of aerosols in Beijing increased

remarkably to approximately 120 nm during the six haze episodes, compared with the GMD of 50 nm under clean conditions. Two stages were identified: an initial rising stage and a sustained increase stage. In the initial stage, the GMD of aerosols increased by 50–60 nm for several hours, and the GMD then remained at 100–120 nm for several days in the subsequent elevated pollution stage. This GMD increase during the initial stage was mainly caused by the increase of accumulation-mode particles with diameters of 100–1,000 nm and Aitken-mode particles (Fig. 10). Under clean conditions (SIA < 50 μg $m^{-3}$), the average contributions of the three modes (nucleation, Aitken, and accumulation modes) to the number concentration were comparable, although the number of nucleation-mode particles decreased with SIA concentration. Under light-moderate pollution conditions (50 < SIA < 150 μg $m^{-3}$), the proportion of accumulation-mode particles significantly increased from 35% to 60%, whereas the proportion of Aitken-mode particles slowly decreased. As discussed in previous sections, regional transport played a dominant role during the initial stage. This indicates that condensation, coagulation, and chemical transformation in the transport pathway increased the number of particles with a diameter range of 100–1,000 nm. Finally, the contributions of Aitken-mode and accumulation-mode particles remained stable under the heavy-pollution conditions (SIA >150 μg $m^{-3}$).

Aging processes play a critical role in the growth of particles during haze episodes. According to observations, a significant coating of secondary components on BC was found in the study period (Wang et al., 2018a). Figure 11 presents a time series of the simulated $R_{BC}$, which is a favorable indicator of the aging degree (Oshima et al., 2009; Collier et al., 2018). Higher $R_{BC}$ indicates that BC had undergone a greater degree of aging. In this study, the simulated $R_{BC}$ was 2–10, with an average value of 4.5. ~~This value is higher than that for fresh traffic source particles (Liu et al., 2017)~~. Under pollution conditions, $R_{BC}$ was higher than that under clean conditions, with an average value of 5.0. $R_{BC}$ in Beijing even exceeded 10.0 in some extremely severe pollution events, which is close to observations of remote sites (Wang et al., 2017a; Massoli et al., 2015) and aged particles (Cappa et al., 2012). Urban aerosols usually have a lower

$R_{BC}$ because of fresh emissions and high $R_{BC}$ in this study indicates that Beijing aerosol particles were more aged during the haze episodes. On clean days, $R_{BC}$ ranged from 2 to 5, with an average of 2.8. This is similar to the $R_{BC}$ of vehicle emissions (<3) (Liu et al, 2017). Vehicle emissions contributed 70% of BC in downtown Beijing in 2016 after strict controls on coal burning had been implemented (Kebin He, personal communication).

Figure 12 shows the evolution of $R_{BC}$, GMD ~~the size distribution of number concentrations~~, and region source of BC ~~the GMD~~ along the transport pathway from the source region to Beijing during the six haze episodes. Aerosol properties including number concentration along transport per six hours are shown in Table S2. The transport pathway was calculated using the HYSPLIT model. The figure clearly shows that the aerosol properties changed considerably along the transport pathway. In Ep1, the GMD of aerosols was only 97 nm at the initial site of the 24 h back trajectories ($T_{-24}$). At a larger transport distance, the diameters of aerosol particles were markedly increased to 128 nm in the middle ($T_{-12}$) and 134 nm at the final site ($T_0$) of the back trajectory. $R_{BC}$ increased from 3.6 at $T_{-24}$ to 8.7 at Beijing ($T_0$) because of BC being coated during the transport. This indicates that BC underwent considerable aging and increased in size while moving along the transport pathway~~; this would affect radiation and climate change (Cappa et al., 2012)~~. Similar characteristics were discovered for Ep3–6. In Ep3, Ep4, Ep5, and Ep6, the GMD in Beijing ($T_0$) was 126, 117, 124, and 116 nm, respectively, compared with 96, 95, 99, and 111 nm in the middle point of transport ($T_{-12}$). $R_{BC}$ also increased to 4.6–7.6. An exception was Ep2, in which the GMD (106 nm) and $R_{BC}$ (3.8) at the final ending site (Beijing, $T_0$) were lower than those 6 h previously ($T_{-6}$). Regional transport contributed 95% of BC at $T_{-6}$, whereas local emissions accounted for 87% of BC at $T_0$. The number concentration was smaller at $T_{-6}$ than that at $T_0$. Therefore, we conclude that regional transport of aged aerosols led to a high GMD at $T_{-6}$, and that the addition of locally emitted fresh air caused a high number concentration but low GMD at $T_0$. In clean areas, such as at $T_{-24}$ in ~~Ep3 and~~ Ep5, $R_{BC}$ was higher than 10 and the GMD was considerably smaller.

## 4.4 Impact of heterogeneous chemistry on sulfate mass concentration

Current models generally account for a part of the observed $SO_4^{2-}$ concentrations in China (Wang et al., 2014a). Heterogeneous chemistry on aerosol surfaces under high relative humidity has been considered a potential missing source of sulfate formation (Cheng et al., 2016; Zheng et al., 2015; Li et al., 2017a; Tang et al., 2016b). Li et al. (2018) developed a simple parameterization of heterogeneous chemistry and discovered that $SO_2$ uptake on aerosols partly closed the gap between simulation and observation. In their study, uptake coefficients were dependent on the aerosol core and shell species, shell thickness, and amount of aerosol liquid water. Zheng et al. (2013) and Yang et al. (2014) measured local source profiles, and they reported that primary sulfate from industry and power plants accounted for a large fraction of PA. Researchers also found that household coal burning can emit certain amounts of sulfate (Zhang et al., 2018).

In this study, we examined the contributions of gas ($SO_2$ + OH) and aqueous chemistry, heterogeneous chemistry, and primary sulfate emissions to the sulfate mass concentration in Beijing (Fig. 13). In Ep1, under high relative humidity, the contribution of heterogeneous chemistry was 33%. Primary emissions exerted an effect mostly under light to moderate pollution levels (sulfate <20 μg $m^{-3}$), whereas heterogeneous chemistry played the largest role under high pollution levels (sulfate > 30 μg $m^{-3}$). The contributions of gas and aqueous chemistry were largely consistent under all pollution conditions (~30%). This indicates that high relative humidity and aerosol loading accelerated the $SO_2$ chemical transformation. Interestingly, the contribution of heterogeneous chemistry was markedly higher when the sulfate mass concentration exceeded the threshold of 20 μg $m^{-3}$. Under high relative humidity and mass concentration conditions, a higher aerosol surface area resulting from hygroscopic growth and haze particles under high RH(60–80%) with aqueous shell due to phase transition provided a favorable media for heterogeneous reactions (Tie et al., 2017; Sun

et al., 2018). –The aforementioned threshold is relatively similar to that during the haze episodes in the winter of 2013 (Li et al, 2018). For policymakers, implementing measures to prevent the sulfate concentration from exceeding this threshold is essential. Such measures would be effective for avoiding extremely high sulfate levels. In other episodes, heterogeneous chemistry was depressed because of the low relative humidity (<70%). Gas and aqueous chemistry and primary emissions contributed 35%–40% and 58%–61%, respectively. It should be noted that failure of the model to simulate mineral dust led to underestimation of the sulfate level in Ep2. The interaction between $SO_2$ and alkaline dust can contribute considerably to the sulfate concentration.

# 5 Conclusions

The contributions of regional transport to haze episodes over a megacity cluster centered on Beijing have been under debate in recent decades. Investigating the evolution of aerosol properties along the transport pathway may provide more information on how researchers can improve the accuracy of regional transport and chemistry impact assessments. To address one of the aims of the APHH 2016 winter campaign, we employed a Eulerian chemical transport model (NAQPMS) and a Lagrangian trajectory model (HYSPLIT) to assess the evolution of aerosols—in terms of the number concentration, size distribution, and aging degree—in Beijing during six haze episodes between November 15 and December 15, 2016. The transport of sulfate and its precursors was also quantitatively investigated.

The results demonstrated that regional transport contributed 14%–31% to the surface $PM_{2.5}$ mass concentration in Beijing during the six episodes, with a monthly average contribution of 26%. Regarding aerosol components, 30%–62% of the SIA in Beijing were regionally transported, whereas few PAs (<10%) were contributed from emissions in other regions. Source regions differed between episodes. During high-pollution periods, WHB, SD, and EHB were the main source regions of SIA regionally transported to Beijing, whereas NHB and SX made greater contributions under clean and light pollution conditions. This indicates the complexity of regional transport in

this megacity cluster.

The chemical transformation of $SO_2$ along the transport pathway from source regions except Beijing to Beijing (RTC) was the major ~~form~~ source of $SO_4^{2-}$ regional transport and was more critical than the transport of sulfate formed in source regions except Beijing (RTC). Compared with sulfate that was chemically transformed from Beijing-emitted $SO_2$ and then blown back to Beijing (LTC), contribution of sulfate produced in Beijing from Beijing-emitted $SO_2$ (LC) was generally greater. However, RTC markedly increased in some episodes, and this explains the rapid formation of sulfate in Beijing. This suggests that the joint control of local and regional $SO_2$ emissions is essential for reducing the rapid formation of haze in this region.

Aerosols became considerably aged during transport in haze episodes, which altered $R_{BC}$ and the size distribution of number concentrations. During haze episodes, the GMD increased from less than 100 nm at the initial site to approximately 120 nm at the final site (Beijing), and $R_{BC}$ increased from 2–4 to 4–8. The number of accumulation-mode particles with a diameter range of 100–1,000 nm increased considerably more than the number of particles of different modes. $R_{BC}$ in Beijing during the episodes was higher than that of clean regions ~~-~~(Collier et al., 2018)~~fresh particles (<1.5)~~ and $R_{BC}$ under pollution levels was close to that in remote regions (Wang et al., 2017a), which indicates that BC in Beijing was more aged and thus more likely to affect radiation and climate.

Contributions from different pathways to sulfate in Beijing were also examined. In episodes with high humidity (Ep1), the average contributions of gas and aqueous chemistry, heterogeneous chemistry, and primary sulfate were comparable. Primary emissions mostly had an effect under light to moderate pollution levels, whereas heterogeneous chemistry played ~~the most~~a a relatively crucial role under high pollution levels during Ep1. In other episodes (Ep2, Ep3, Ep4, Ep5, and Ep6), gas and aqueous chemistry and primary emissions contributed 35%–40% and 58%–61%, respectively.

**Acknowledgements:**

This work was supported by the Natural Science Foundation of China (41571130034; 91544227; 91744203; 41225019; 41705108) and the Chinese Ministry of Science and Technology (2018YFC0213205 and 2017YFC0212402).

# References

Anderson, H. R., Atkinson, R., Balbus, J., Brauer, M., Chapman, R., Chowdhury, Z.: Outdoor Air Pollution and Health in the Developing Countries of Asia: A Comprehensive Review, Special Report 18, Health Effects Institute, Boston, Massachusetts, 2010.

Boylan, J. W., & Russell, A. G.: PM and light extinction model performance metrics, goals, and criteria for three-dimensional air quality models, Atmospheric Environment, 40(26), 4946-4959, https://doi.org/10.1016/j.atmosenv.2005.09.087, 2006.

Cao J.: $PM_{2.5}$ and environment. Science Press, 2014.

Cappa, C. D., Onasch, T. B., Massoli, P., Worsnop, D. R., Bates, T. S., Cross, E. S., … Zaveri, R. A.: Radiative Absorption Enhancements Due to the Mixing State of Atmospheric Black Carbon, Science, 337(6098), 1078–1081, https://doi.org/10.1126/science.1223447, 2012.

Chen, X., Li, X., Yuan, X., Zeng, G., Liang, J., Li, X., . . . Chen, G.: Effects of human activities and climate change on the reduction of visibility in Beijing over the past 36years, Environ Int, 116, 92-100, https://doi.org/10.1016/j.envint.2018.04.009, 2018.

Chen, X., Wang, Z., Li, J., & Yu, F.: Development of a regional chemical transport model with size-resolved aerosol microphysics and its application on aerosol number concentration simulation over china, Scientific Online Letters on the Atmosphere Sola, 10, 83-87, https://doi.org/10.2151/sola.2014-017, 2014.

Chen, X., Wang, Z., Yu, F., Pan, X., Li, J., & Ge, B., et al.: Estimation of atmospheric aging time of black carbon particles in the polluted atmosphere over central-eastern china using microphysical process analysis in regional chemical transport model. Atmospheric Environment, 163, 44-56, https://doi.org/10.1016/j.atmosenv.2017.05.016, 2017.

Cheng, Y., Zheng, G., Wei, C., Mu, Q., Zheng, B., & Wang, Z., et al: Reactive nitrogen chemistry in aerosol water as a source of sulfate during haze events in china, Science Advances, 2(12), https://doi.org/10.1126/sciadv.1601530, 2016.

Collier, S., Williams, L. R., Onasch, T. B., Cappa, C. D., Zhang, X., & Russell, L. M., et al: Influence of emissions and aqueous processing on particles containing black carbon in a polluted urban environment: insights from a soot particle-aerosol mass spectrometer, Journal of Geophysical Research Atmospheres, 123(12), 6648-6666, https://doi.org/10.1002/2017jd027851, 2018.

Draxler, R. R., & Hess, G. D: An overview of the HYSPLIT 4 modeling system for trajectories, dispersion, and deposition, Australian Meteorological Magazine, 47(4), 295-308, 1998.

Du, W., Zhao, J., Wang, Y., Zhang, Y., Wang, Q., & Xu, W., et al: Simultaneous measurements of

particle number size distributions at ground level and 260 m on a meteorological tower in urban Beijing, china, Atmospheric Chemistry & Physics, 17(11), 6797-6811, https://doi.org/10.5194/acp-17-6797-2017, 2017.

Gao, J., Peng, X., Chen, G., Xu, J., Shi, G. L., Zhang, Y. C., and Feng, Y. C.: Insights into the chemical characterization and sources of $PM_{2.5}$ in Beijing at a 1-h time resolution, The Science of the total environment, 542, 162-171, 10.1016/j.scitotenv.2015.10.082, 2016.

Han, B., Zhang, R., Yang, W., Bai, Z., Ma, Z., & Zhang, W: Heavy haze episodes in Beijing during January 2013: inorganic ion chemistry and source analysis using highly time-resolved measurements from an urban site, Science of the Total Environment, 544, 319-329, https://doi.org/10.1016/j.scitotenv.2015.10.053, 2016.

Huang, R. J., Zhang, Y., Bozzetti, C., Ho, K. F., Cao, J. J., Han, Y., . . . Prevot, A. S: High secondary aerosol contribution to particulate pollution during haze events in China, Nature, 514(7521), 218-222, https://doi.org/10.1038/nature13774, 2014.

Hyslop, N. P.: Impaired visibility: the air pollution people see, Atmospheric Environment, 43(1), 182-195, https://doi.org/10.1016/j.atmosenv.2008.09.067, 2009.

Lee, A. K. Y., Chen, C. L., Liu, J., Price, D. J., Betha, R., Russell, L. M., Zhang, X., and Cappa, C. D.: Formation of secondary organic aerosol coating on black carbon particles near vehicular emissions, Atmos. Chem. Phys., 17(24), 15055-15067, https://doi.org/10.5194/acp-17-15055-2017, 2017.

Li, G., Bei, N., Cao, J., Huang, R., Wu, J., & Feng, T., et al.: A possible pathway for rapid growth of sulfate during haze days in china, Atmospheric Chemistry & Physics, 17(5), 3301-3316, https://doi.org/10.5194/acp-17-3301-2017, 2017a.

Li, J., Chen, X., Wang, Z., Du, H., Yang, W., & Sun, Y., et al.: Radiative and heterogeneous chemical effects of aerosols on ozone and inorganic aerosols over east Asia, Science of the Total Environment, 622-623, 1327, https://doi.org/10.1016/j.scitotenv.2017.12.041, 2018.

Li, J., Du, H., Wang, Z., Sun, Y., Yang, W., & Li, J., et al.: Rapid formation of a severe regional winter haze episode over a mega-city cluster on the North China Plain, Environmental Pollution, 223, 605-615, https://doi.org/10.1016/j.envpol.2017.01.063, 2017b.

Li, J., Han, Z.: A modeling study of severe winter haze events in Beijing and its neighboring regions, Atmospheric Research, 170, 87-97, https://doi.org/10.1016/j.atmosres.2015.11.009, 2016.

Li, J., Wang, Z., Huang, H., Min, H. U., Meng, F., & Sun, Y., et al.: Assessing the effects of trans-boundary aerosol transport between various city clusters on regional haze episodes in spring over east china, Tellus, 65(1), 60-73, https://doi.org/10.3402/tellusb.v65i0.20052, 2013.

Li, J., Yang, W., Wang, Z., Chen, H., Hu, B., & Li, J., et al.: A modeling study of source–receptor relationships in atmospheric particulate matter over northeast Asia. Atmospheric Environment, 91(7), 40-51, https://doi.org/10.1016/j.atmosenv.2014.03.027, 2014.

Li, J., Wang, Z.F., Zhuang, G., Luo, G., Sun, Y., Wang, Q.: Mixing of Asian mineral dust with anthropogenic pollutants over East Asia: a model cast study of a super-dust storm in March

2010. Atmos. Chem. Phys. 12 (16), 7591-7607. https://dx.doi.org/10.5194/acp-12-7591-2012, 2012.

Li, P., Yan, R., Yu, S., Wang, S., Liu, W., & Bao, H.: Reinstate regional transport of $PM_{2.5}$ as a major cause of severe haze in Beijing, Proc Natl Acad Sci U S A, 112(21), E2739-2740, https://doi.org/10.1073/pnas.1502596112, 2015.

Liu, D., Whitehead, J., Alfarra, M. R., Reyes-villegas, E., Spracklen, D. V., & Reddington, C. L., et al.: Black-carbon absorption enhancement in the atmosphere determined by particle mixing state, Nature Geoscience, 10(3), 184-188, https://doi.org/10.1038/ngeo2901, 2017.

Liu, X., Zhang, Y., Jung, J., Gu, J., Li, Y., & Guo, S., et al.: Research on the hygroscopic properties of aerosols by measurement and modeling during CAREBeijing-2006, Journal of Geophysical Research Atmospheres, 114(16), 4723-4734, https://doi.org/10.1029/2008jd010805,2009.

Ma, Q., Wu, Y., Zhang, D., Wang, X., Xia, Y., Liu, X., . . . Zhang, R.: Roles of regional transport and heterogeneous reactions in the $PM_{2.5}$ increase during winter haze episodes in Beijing, Sci Total Environ, 599-600, 246-253, https://doi.org/10.1016/j.scitotenv.2017.04.193, 2017.

Ma, X., & Yu, F.: Seasonal variability of aerosol vertical profiles over east us and west Europe: GEOS-Chem/APM simulation and comparison with CALIPSO observations, Atmospheric Research, 140-141(31), 28-37, https://doi.org/10.1016/j.atmosres.2014.01.001, 2014.

Ma, Z., Liang YP, Zhang J.: $PM_{2.5}$ profiles of typical sources in Beijing, Acta Science Circumstantiae, 35(12), 4043-4052, https://doi.org/10.13671/j.hjkxxb.2015.0584, 2015.

Massoli, P., Onasch, T. B., Cappa, C. D., Nuamaan, I., Hakala, J., & Hayden, K., et al.: Characterization of black carbon containing particles from soot particle aerosol mass spectrometer measurements on the R/V Atlantis during CalNex 2010, Journal of Geophysical Research Atmospheres, 120(6), 2575-2593, https://doi.org/10.1002/2014jd022834, 2015.

Nenes, A., Pandis, S.N., Pilinis, C.: ISORROPIA: A new thermodynamic equilibrium model for multiphase multicomponent inorganic aerosols, Aquat. Geochem. 4(1), 123-152. https://dx.doi.org/10.1023/A:1009604003981, 1998.

Oshima, N., Koike, M., Zhang, Y., Kondo, Y., Moteki, N., & Takegawa, N., et al.: Aging of black carbon in outflow from anthropogenic sources using a mixing state resolved model: model development and evaluation, Journal of Geophysical Research Atmospheres, 114(D6), https://doi.org/10.1029/2008jd010680, 2009.

Pan, X., Ge, B., Wang Z., Tian, Y., et al.: Synergistic effect of water-soluble species and relative humidity on morphological changes of aerosol particles in Beijing mega-city during severe pollution episodes, Atmos. Chem. Phys. Discuss, 1-24, https://doi.org/10.5194/acp-2018-623, 2018.

Peng J, Hu M, Guo S, et al.: Markedly enhanced absorption and direct radiative forcing of black carbon under polluted urban environments, Proc Natl Acad Sci USA, 113(16), 4266-4271, https://doi.org/10.1073/pnas.1602310113, 2016.

Shi, Z., Vu, T., and Kotthaus, S.: Introduction to Special Issue-In-depth study of air pollution sources

and processes within Beijing and its surrounding region(APHH-Beijing), Atmos. Chem. Phys. Discuss., 2018.,

Sun, Y., Chen, C., Zhang, Y., Xu, W., Zhou, L., Cheng, X., . . . Wang, Z.: Rapid formation and evolution of an extreme haze episode in Northern China during winter 2015, Sci Rep, 6(1), 27151. https://doi.org/10.1038/srep27151, 2016.

Sun, Y., Du, W., Wang, Q., Zhang, Q., Chen, C., & Chen, Y., et al. Real-time characterization of aerosol particle composition above the urban canopy in Beijing: insights into the interactions between the atmospheric boundary layer and aerosol chemistry, Environmental Science & Technology, 49(19), 11340-11347, https://doi.org/10.1021/acs.est.5b02373, 2015.

Sun, Y., Jiang, Q., Wang, Z., Fu, P., Li, J., Yang, T., & Yin, Y.: Investigation of the sources and evolution processes of severe haze pollution in Beijing in January 2013, Journal of Geophysical Research: Atmospheres, 119(7), 4380-4398, https://doi.org/10.1002/2014jd021641, 2014.

Tang, G., Zhang, J., Zhu, X., Song, T., Münkel, C., Hu, B., et al.: Mixing layer height and its implications for air pollution over Beijing, China, Atmos. Chem. Phys., 16(4), 2459-2475, https://doi.org/10.5194/acp-16-2459-2016, 2016a.

Tang, M. J., Larish, W. A., Fang, Y., Gankanda, A., and Grassian, V. H.: Heterogeneous Reactions of Acetic Acid with Oxide Minerals: Effects of Mineralogy and Relative Humidity, J. Phys. Chem. A, 120(28), 5609-5616, https://doi.org/10.1021/acs.jpca.6b05395, 2016b.

Tie, X., Huang, R. J., Cao, J., Zhang, Q., Cheng, Y., Su, H., . . . O'Dowd, C. D.: Severe Pollution in China Amplified by Atmospheric Moisture, Sci Rep, 7(1), https://doi.org/10.1038/s41598-017-15909-1, 2017.

Timmermans, R., Kranenburg, R., Manders, A., Hendriks, C., Segers, A., & Dammers, E., et al.: Source apportionment of $PM_{2.5}$ across china using LOTOS-EUROS, Atmospheric Environment, 164, 370-386, https://doi.org/10.1016/j.atmosenv.2017.06.003, 2017.

Wang, J., Liu, D., Ge, X., Wu, Y., Shen, F., Chen, M., . . . Sun, Y.: Characterization of black carbon-containing fine particles in Beijing during wintertime, Atmospheric Chemistry and Physics Discussions, 1-25, https://doi.org/10.5194/acp-2018-800, 2018a.

Wang, J., Zhang, Q., Chen, M. D., Collier, S., Zhou, S., & Ge, X., et al.: First chemical characterization of refractory black carbon aerosols and associated coatings over the Tibetan plateau (4730 m a.s.l), Environmental Science & Technology, 51(24), 14072-14082, https://doi.org/10.1021/acs.est.7b03973, 2017a.

Wang, S., Zhao, X., Li, X., Wei, W., Hao, J.: Study on fine particle emission characteristics of industrial coal-fired chain furnace. Environmental Science (Chines), 30 (4), 963-968, https://doi.org/10.3321/j.issn:0250-3301.2009.04.004, 2009.

Wang, Y. Y., Liu, F. S., He, C. L., Bi, L., Cheng, T. H., Wang, Z. L., Zhang, H., Zhang, X. Y., Shi, Z. B., and Li, W. J.: Fractal Dimensions and Mixing Structures of Soot Particles during Atmospheric Processing, Environ Sci Tech Let, 4, 487-493, 10.1021/acs.estlett.7b00418, 2017b.

Wang, Y., Zhang, Q., Jiang, J., Zhou, W., Wang, B. Y., He, K. B., . . . Xie, Y. Y.: Enhanced sulfate formation during china's severe winter haze episode in January 2013 missing from current models, Journal of Geophysical Research Atmospheres, 119(17), 10425-10440, https://doi.org/doi: 10.1002/2013jd021426, 2014a.

Wang, Z., Maeda, T., Hayashi, M., Hsiao, L.F., Liu, K.Y.: A nested air quality prediction modeling system for urban and regional scales, application for high-ozone episode in Taiwan, Water, Air, Soil Pollut, 130, 391-396, https://dx.doi.org/10.1023/A:1013833217916. 2001.

Wang, Z., Jie, L., Wang, Z., Yang, W. Y., Tang, X., & Ge, B. Z., et al.: Modeling study of regional severe hazes over mid-eastern China in January 2013 and its implications on pollution prevention and control, Science China Earth Sciences, 57(1), 3-13, https://dx.doi.org/10.1007/s11430-013-4793-0, 2014b.

Wang, Z., Pan, X., Uno, I., Li, J., Wang, Z., Chen, X., Fu, P., Yang, T., Kobayashi, H., Shimizu, A., Sugimoto, N., and Yamamoto, S.: Significant impacts of heterogeneous reactions on the chemical composition and mixing state of dust particles: A case study during dust events over northern China, Atmospheric Environment, 159, 83-91, 10.1016/j.atmosenv.2017.03.044, 2017c.

Wang, Z., Pan, X., Uno, I., Chen, X., Yamamoto, S., Zheng, H., Li, J., and Wang, Z.: Importance of mineral dust and anthropogenic pollutants mixing during a long-lasting high PM event over East Asia, Environmental pollution, 234, 368-378, 10.1016/j.envpol.2017.11.068, 2018b.

Wiedinmyer, C., Akagi, S. K., Yokelson, R. J., & Emmons, L. K.: The fire inventory from NCAR (FINN) – a high resolution global model to estimate the emissions from open burning, Geoscientific Model Development, 4(3), 625-641, https://doi.org/10.5194/gmd-4-625-2011, 2011.

Wu, J. B., Wang, Z., Wang, Q., Li, J., Xu, J., & Chen, H., et al.: Development of an on-line source-tagged model for sulfate, nitrate and ammonium: A modeling study for highly polluted periods in Shanghai, China. Environmental Pollution, 221, 168-179, https://doi.org/10.1016/j.envpol.2016.11.061, 2017.

Xie, C., Xu, W., Wang, J., Wang, Q., Liu, D., Tang, G., Chen, P., Du, W., Zhao, J., Zhang, Y., Zhou, W., Han, T., Bian, Q., Li, J., Fu, P., Wang, Z., Ge, X., Allan, J., Coe, H., and Sun, Y.: Vertical characterization of aerosol optical properties and brown carbon in winter in urban Beijing, China, Atmospheric Chemistry and Physics Discussions, 1-28, 10.5194/acp-2018-788, 2018

Yang, H. H.: Filterable and condensable fine particulate emissions from stationary sources, Aerosol & Air Quality Research, 14(7), 2010-2016, https://doi.org/10.4209/aaqr.2014.08.0078, 2014.

Yang, Y., Liu, X., Qu, Y., Wang, J., An, J., & Zhang, Y., et al.: Formation mechanism of continuous extreme haze episodes in the megacity Beijing, China, in January 2013. Atmospheric Research, 155, 192-203, https://doi.org/10.1016/j.atmosres.2014.11.023, 2015.

Yang, Y., Wang, H., Smith, S. J., Easter, R., Ma, P. L., Qian, Y., . . . Rasch, P. J.: Global source attribution of sulfate concentration and direct and indirect radiative forcing, Atmospheric Chemistry and Physics, 17(14), 8903-8922, https://doi.org/10.5194/acp-17-8903-2017, 2017a.

Yang, Y., Wang, H., Smith, S. J., Ma, P.-L., & Rasch, P. J.: Source attribution of black carbon and its direct radiative forcing in China, Atmospheric Chemistry and Physics, 17(6), 4319-4336, https://doi.org/10.5194/acp-17-4319-2017, 2017b.

Ying, Q. Wu, L. Zhang, H.: Local and inter-regional contributions to $PM_{2.5}$ nitrate and sulfate in China, Atmos. Environ., 94, 582-592, https://doi.org/10.1016/j.atmosenv.2014.05.078, 2014.

Yu, F., & Luo, G.: Simulation of particle size distribution with a global aerosol model: contribution of nucleation to aerosol and CCN number concentrations, Atmospheric Chemistry & Physics, 9(20), 7691-7710, https://doi.org/10.5194/acp-9-7691-2009, 2009.

Zhang, Y., Yuan, Q., Huang, D., and Kong, S.: Direct Observations of Fine Primary Particles From Residential Coal Burning: Insights Into Their Morphology, Composition, and Hygroscopicity, Journal of Geophysical Research, 123, 12964–12979, 2018.

Zhao, X. J., Zhao, P. S., Xu, J., Meng, W., Pu, W. W., Dong, F., . . . Shi, Q. F.: Analysis of a winter regional haze event and its formation mechanism in the North China Plain, Atmospheric Chemistry and Physics, 13(11), 5685-5696, https://doi.org/10.5194/acp-13-5685-2013, 2013.

Zheng, B., Zhang, Q., Zhang, Y., He, K. B., Wang, K., Zheng, G. J., . . . Kimoto, T.: Heterogeneous chemistry: a mechanism missing in current models to explain secondary inorganic aerosol formation during the January 2013 haze episode in North China, Atmospheric Chemistry and Physics, 15(4), 2031-2049, https://doi.org/10.5194/acp-15-2031-2015, 2015.

Zheng M., Zhang Y., Yan C., et al.: Establishment of $PM_{2.5}$ industrial source profile in Shanghai, China Environmental Science, 33(8), 1354-1359, https://doi.org/10.3969/j.issn.1000-6923.2013.08.002, 2013.

Zhu, X., Tang, G., Hu, B., Wang, L., Xin, J., & Zhang, J., et al.: Regional pollution and its formation mechanism over north China plain: a case study with ceilometer observations and model simulations, Journal of Geophysical Research Atmospheres, 121(24), 14574-14588, https://doi.org/10.1002/2016jd025730, 2016.

~~Zhuang, G. Yi, Z. Duce, R.A. Brown, P.R.: Link between iron and sulphur cycles suggested by detection of Fe(n) in remote marine aerosols, Nature, 355(6360), 537-539, https://doi.org/10.1038/355537a0, 1992.~~

**Figures**

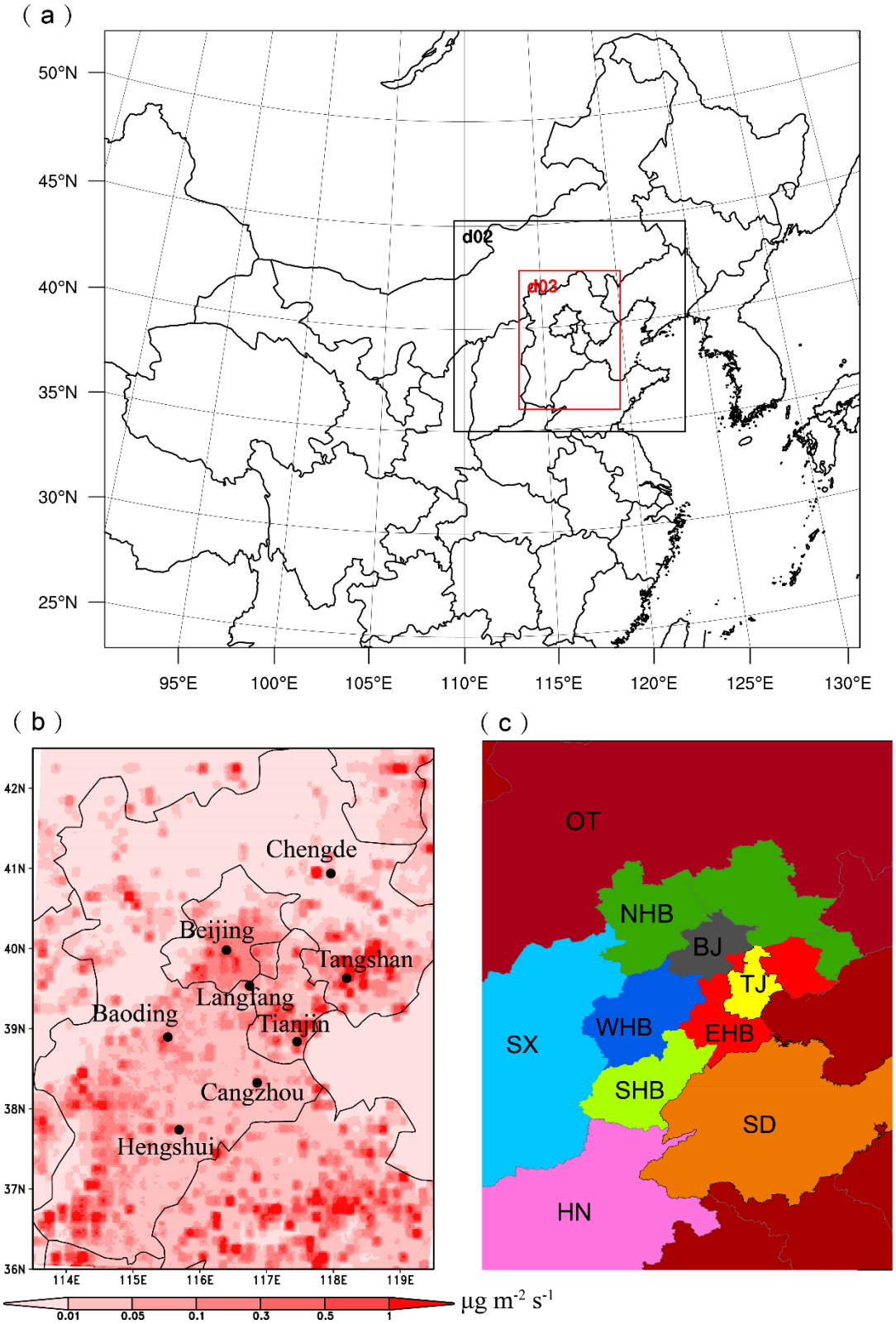


**Figure 1.** (a) Simulation domains. (b) Primary $PM_{2.5}$ emission rates of the innermost domain and locations of observation sites (black dots). (c) tracer tagging regions which are described in Table 1.

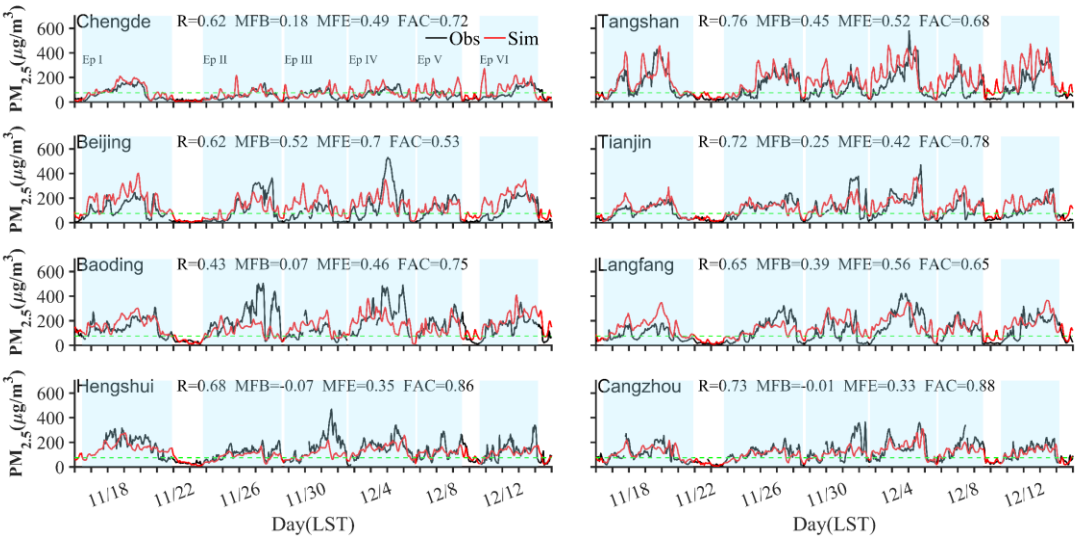


**Figure 2.** Comparison between the simulated and observed hourly concentrations of $PM_{2.5}$ for different sites. Black lines refer to observation and the red lines are simulation results; light blue shadows are six episodes identified~~.~~ ; green lines mean 75 μg $m^{-3}$, as a criterion judging whether pollution or not.

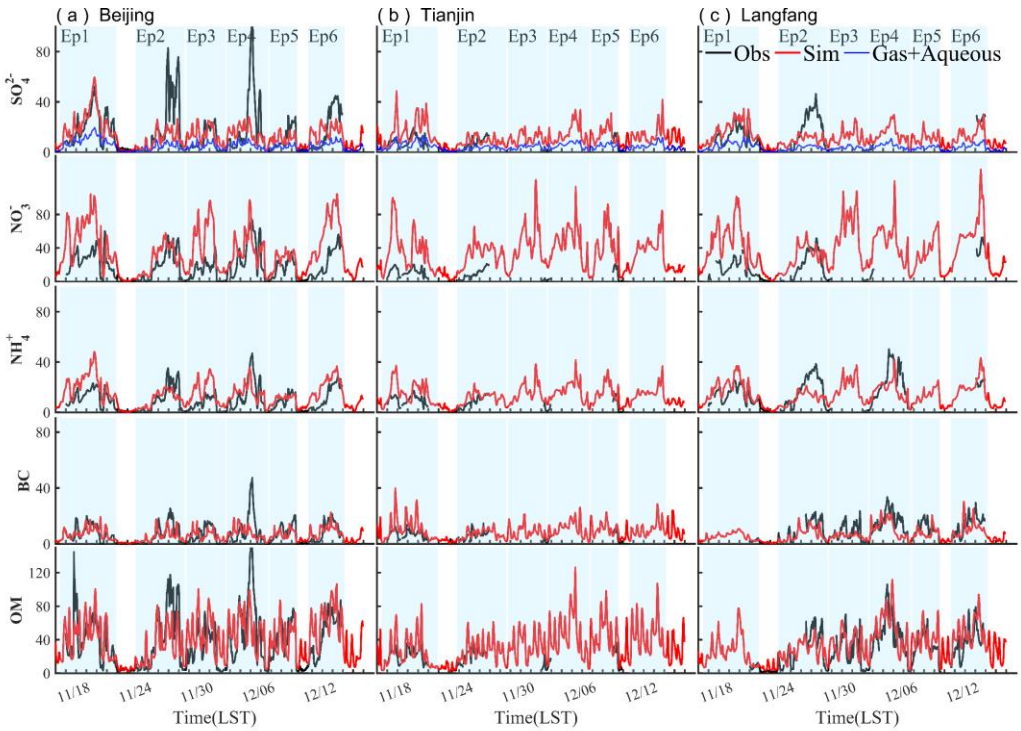


**Figure 3.** Comparison between the simulated (red) and observed (solid black) hourly components including sulfate, nitrate, ammonia, black carbon and organic aerosols at (a) Beijing, (b) Tianjin and (c) Langfang. Blue lines refer to sulfate produced by gas

and aqueous chemistry reactions.

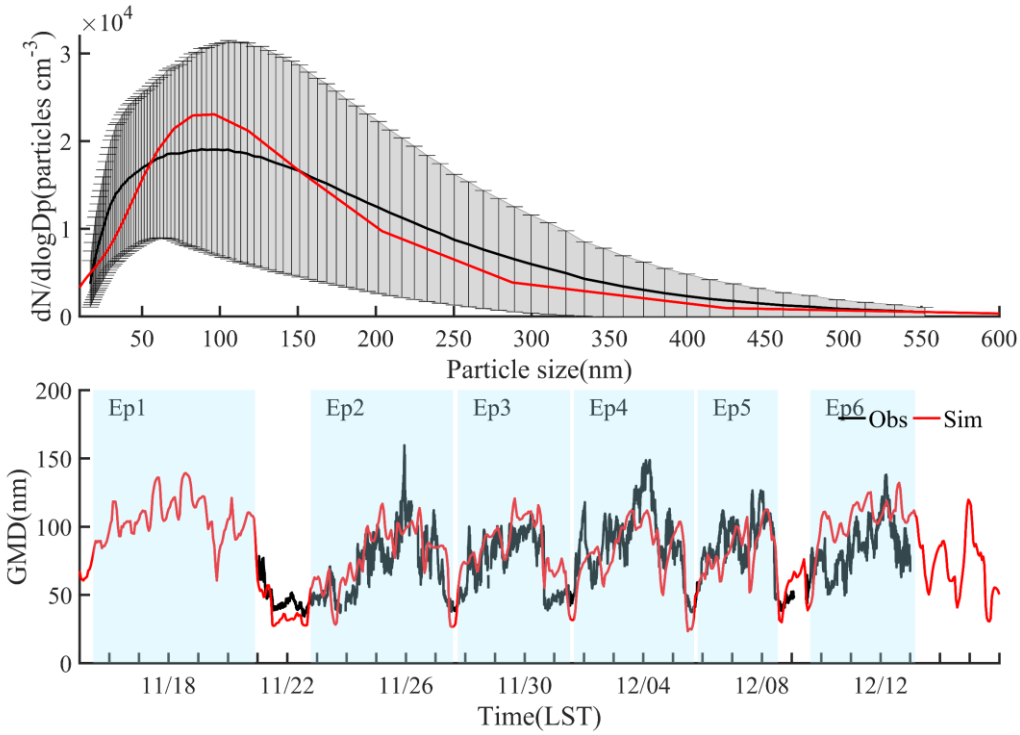


**Figure 4.** (a) Particle size distribution in Beijing at ground level. (b) Comparison of geometric mean diameter (GMD) for particles during range of 16–600nm between observation and simulation in Beijing. Black solid line and red solid line represent observation and simulation respectively.

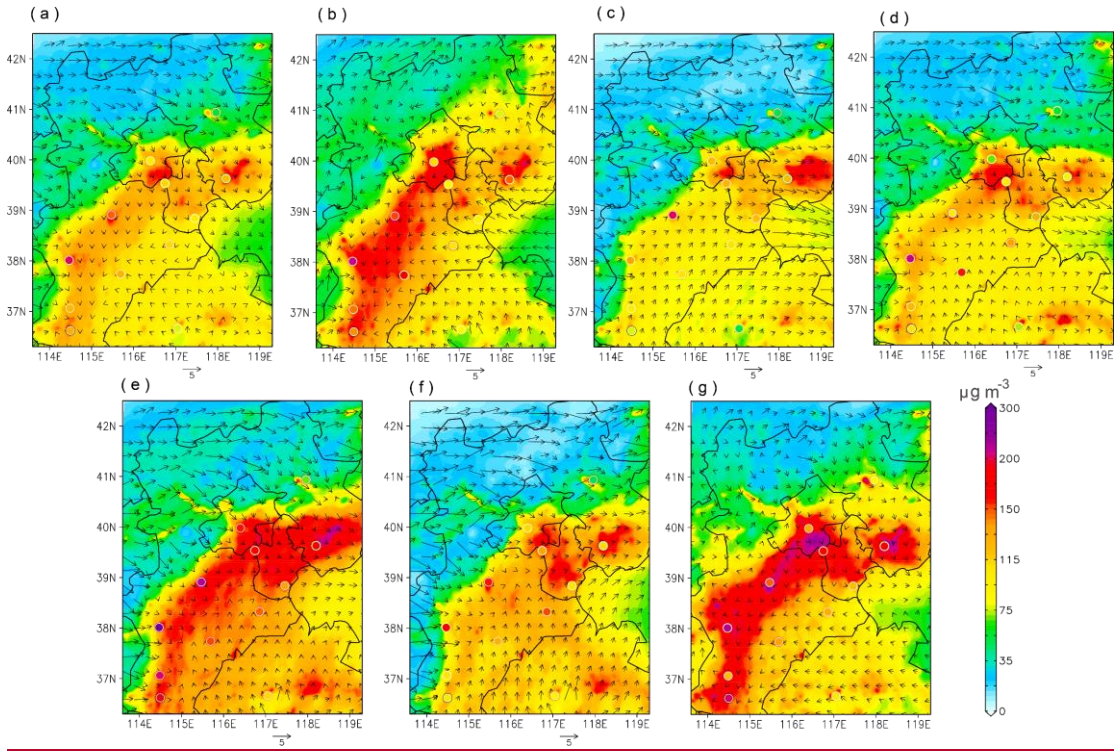

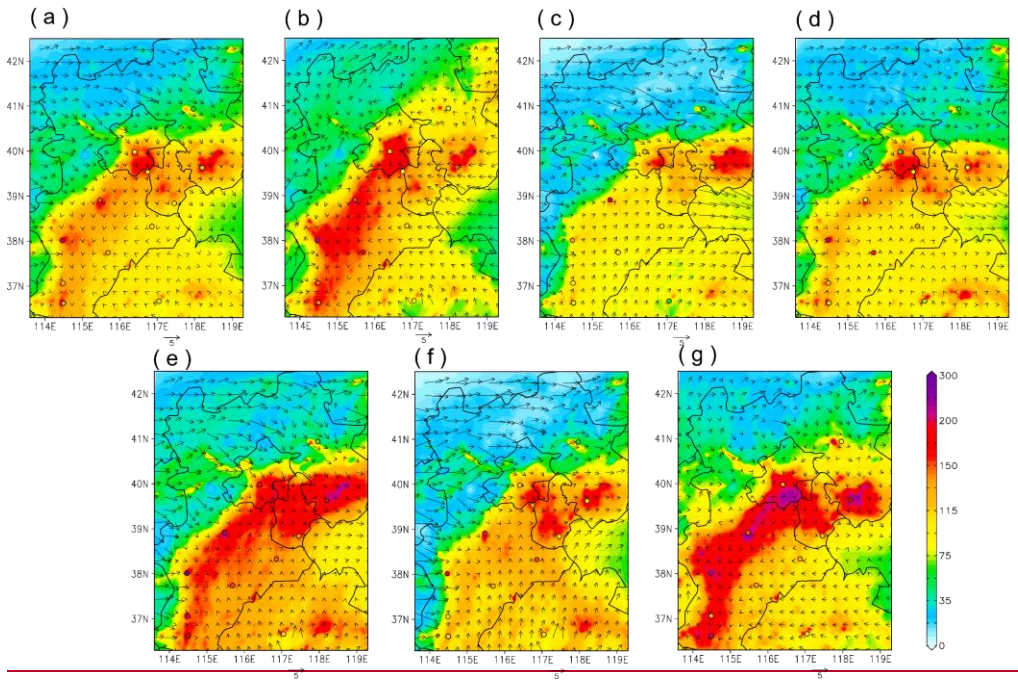


**Figure 5.** Spatial distribution of simulated average surface $PM_{2.5}$ (μg $m^{-3}$) and wind (m $s^{-1}$) over BTH area. (a) average of whole study period, (b)–(g) episode average of episode1–6 identified before. Solid circles represent observations with the same color bar with simulations.

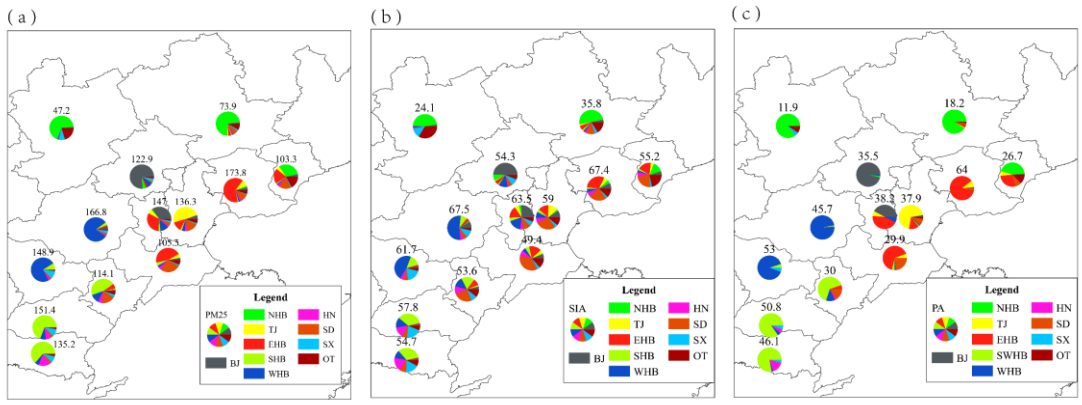

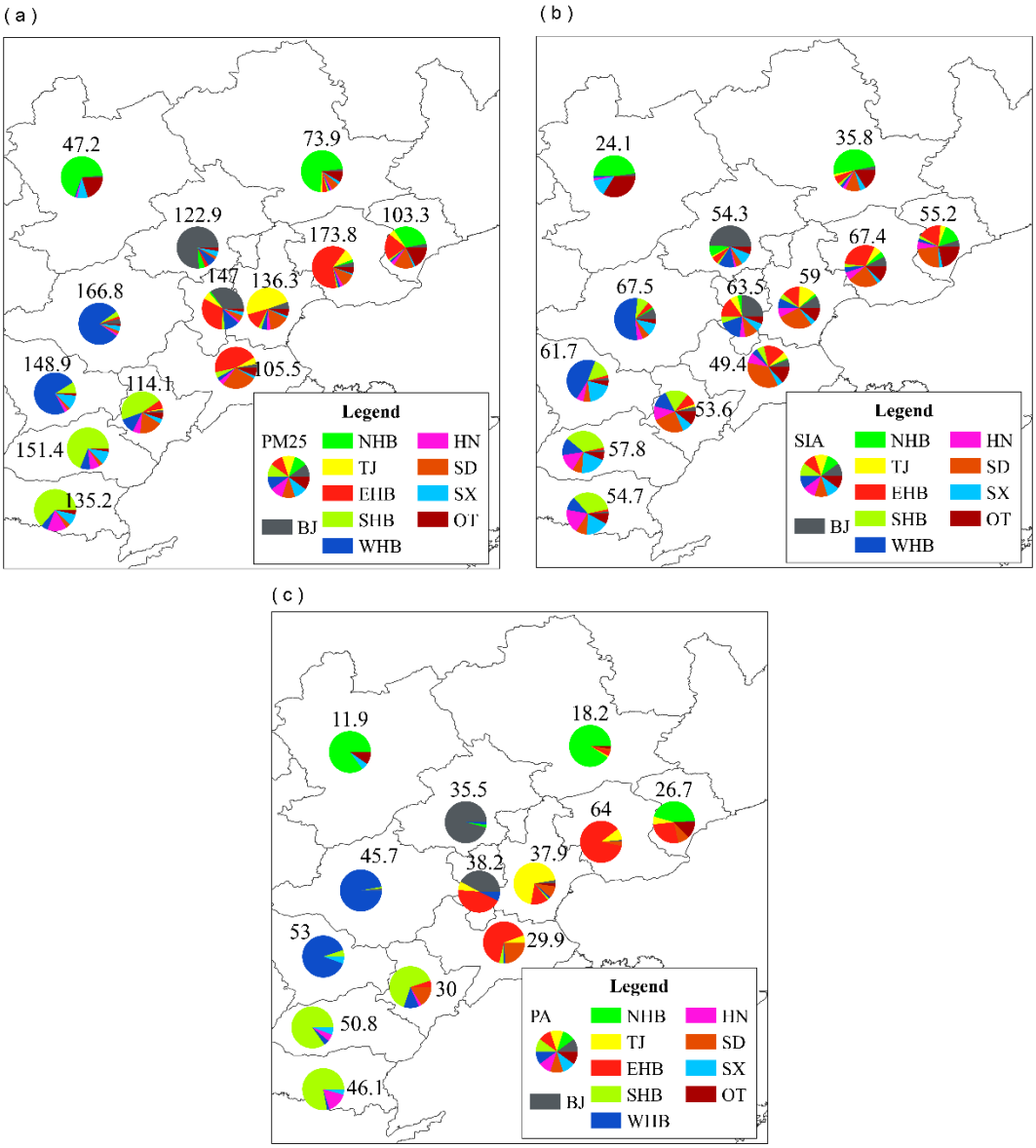


**Figure 6.** The contribution of regional transport and local emissions to the average (a) total $PM_{2.5}$, (b) secondary inorganic aerosols (SIA), (c) primary aerosols (PA, BC and primary $PM_{2.5}$) over BTH area. The numbers above the pie represent average concentrations (μg $m^{-3}$) of certain species in certain cities.

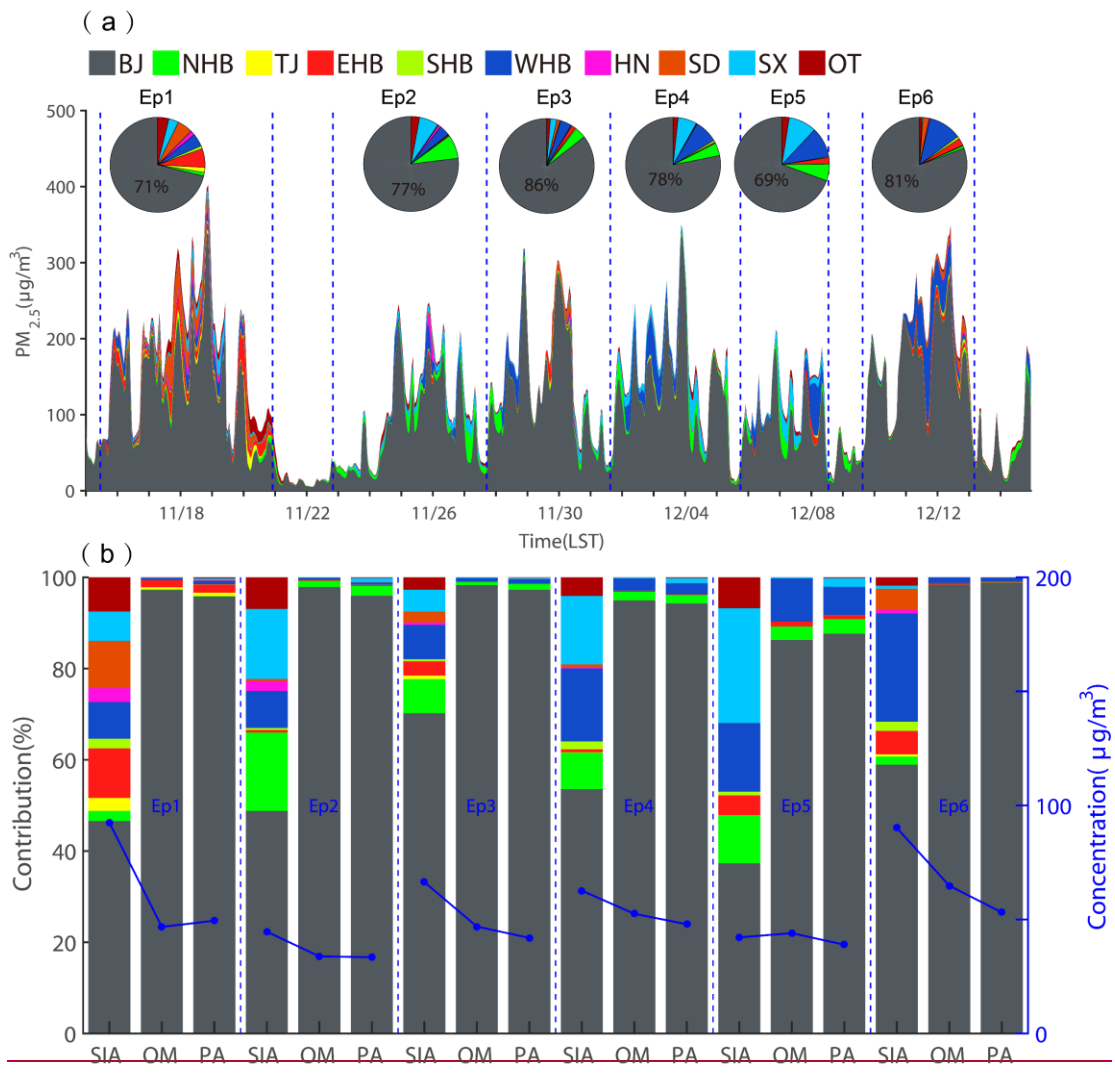
( a )
BJ NHB TJ EHB SHB WHB HN SD SX OT
Ep1
Ep2
Ep3
Ep4
Ep5
Ep6
71%
77%
86%
78%
69%
81%
PM2.5(μg/m3)
11/18
11/22
11/26
11/30
12/04
12/08
12/12
Time(LST)
( b )
Contribution(%)
Concentration( μg/m3)
SIA OM PA

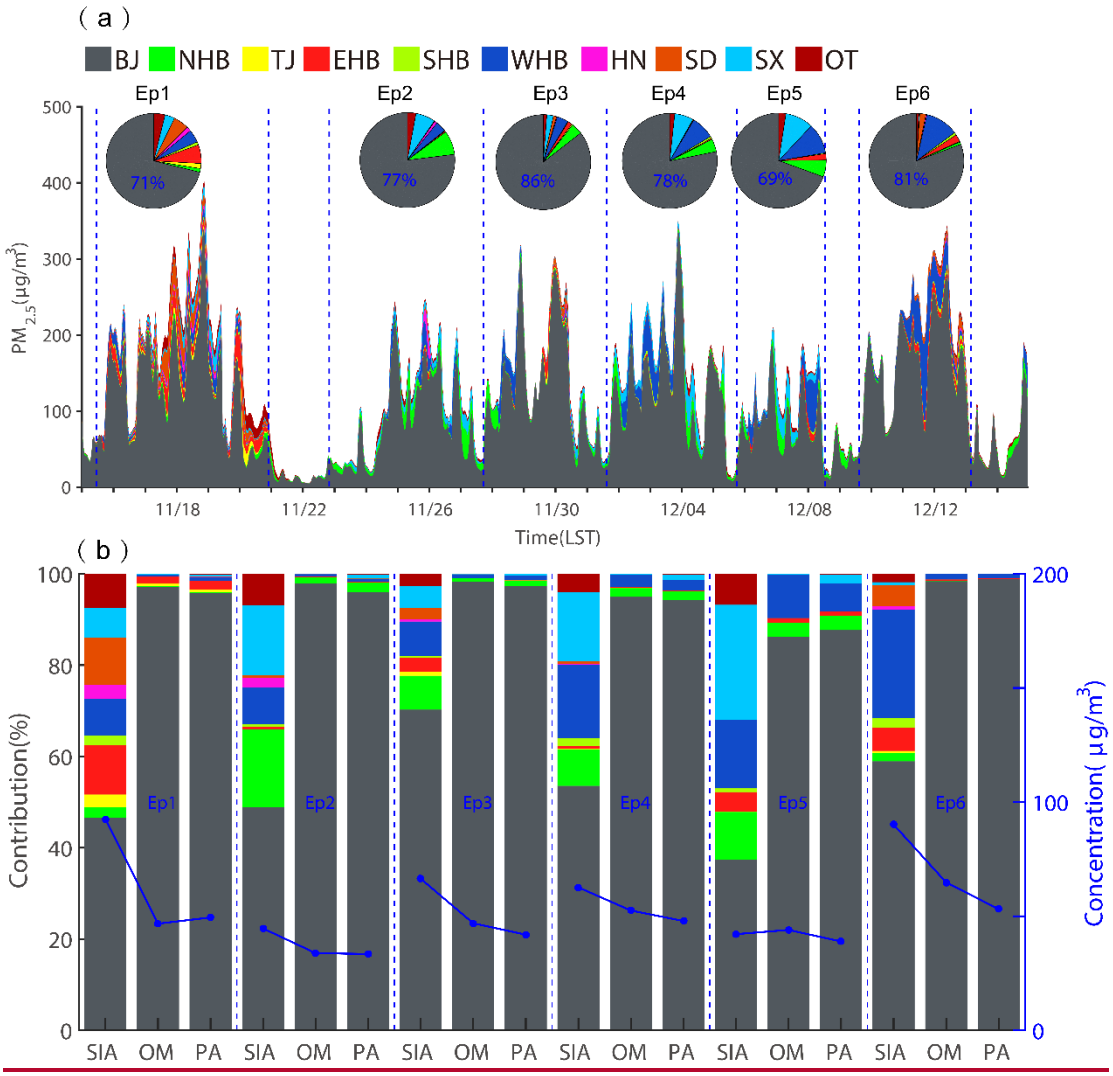


**Figure 7.** (a) Source contribution of $PM_{2.5}$ in Beijing and pies represent average status of each episode; (b) Relative contribution of different regions to SIA, OM and PA in Beijing at the surface layer during each episode (shaded). Concentrations are also shown (blue line).

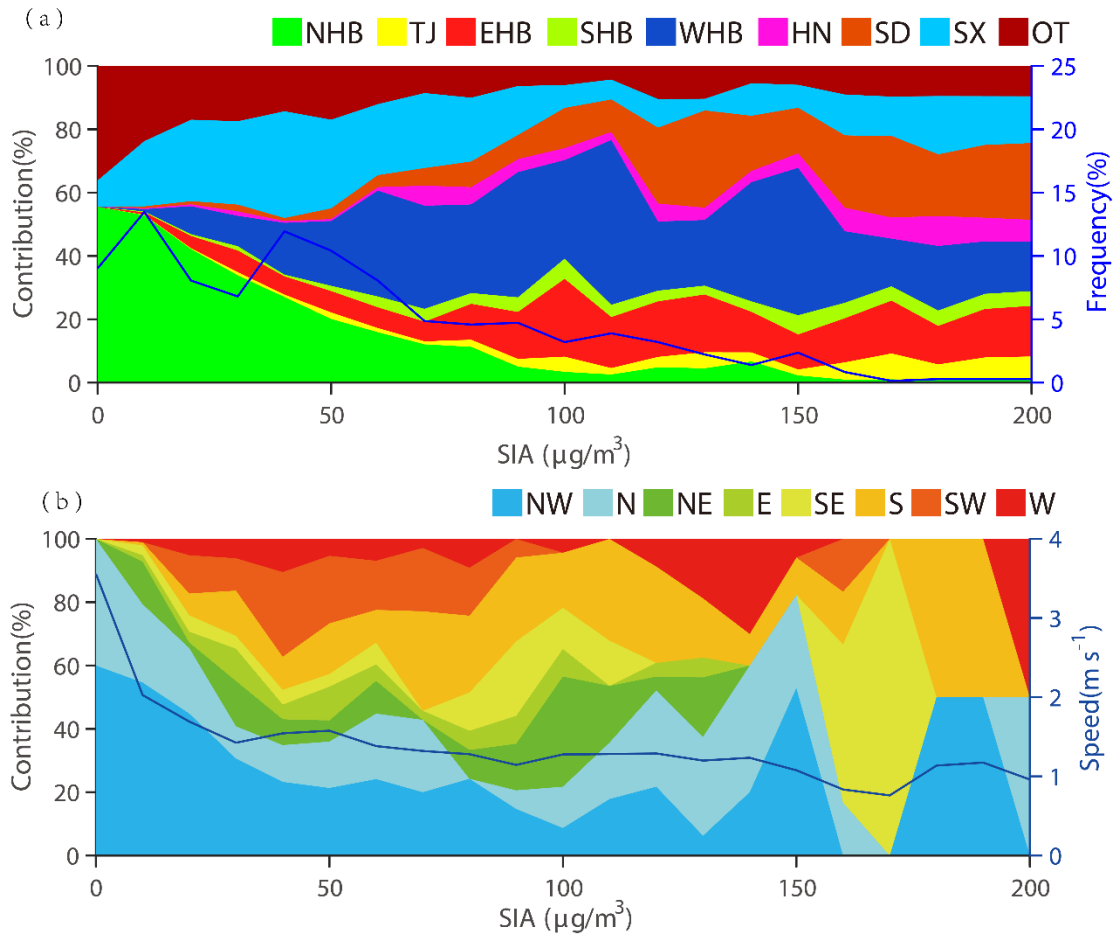


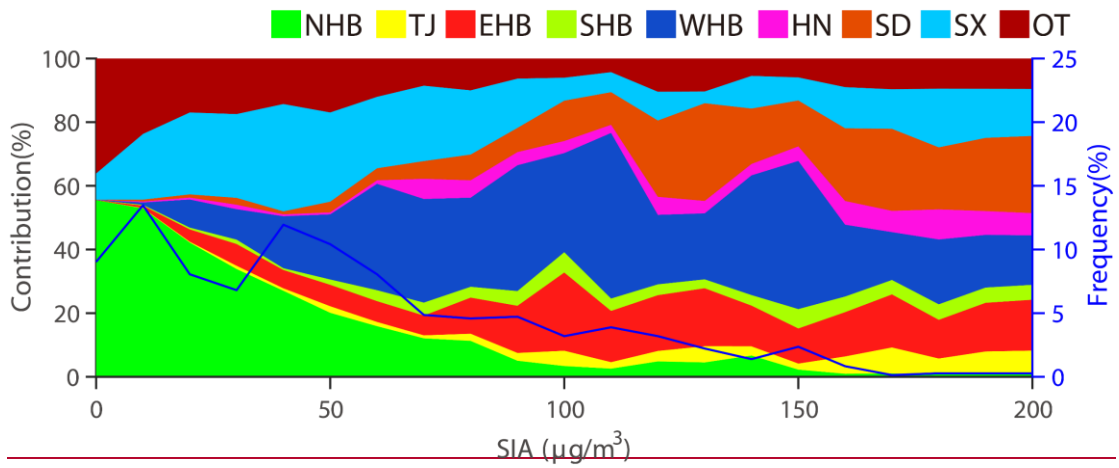


**Figure 8.** (a) Relative contribution of regionally transported SIA under different levels of pollution in Beijing during whole study period; (b)Variation of wind direction under different pollution levels in Beijing during whole study period.

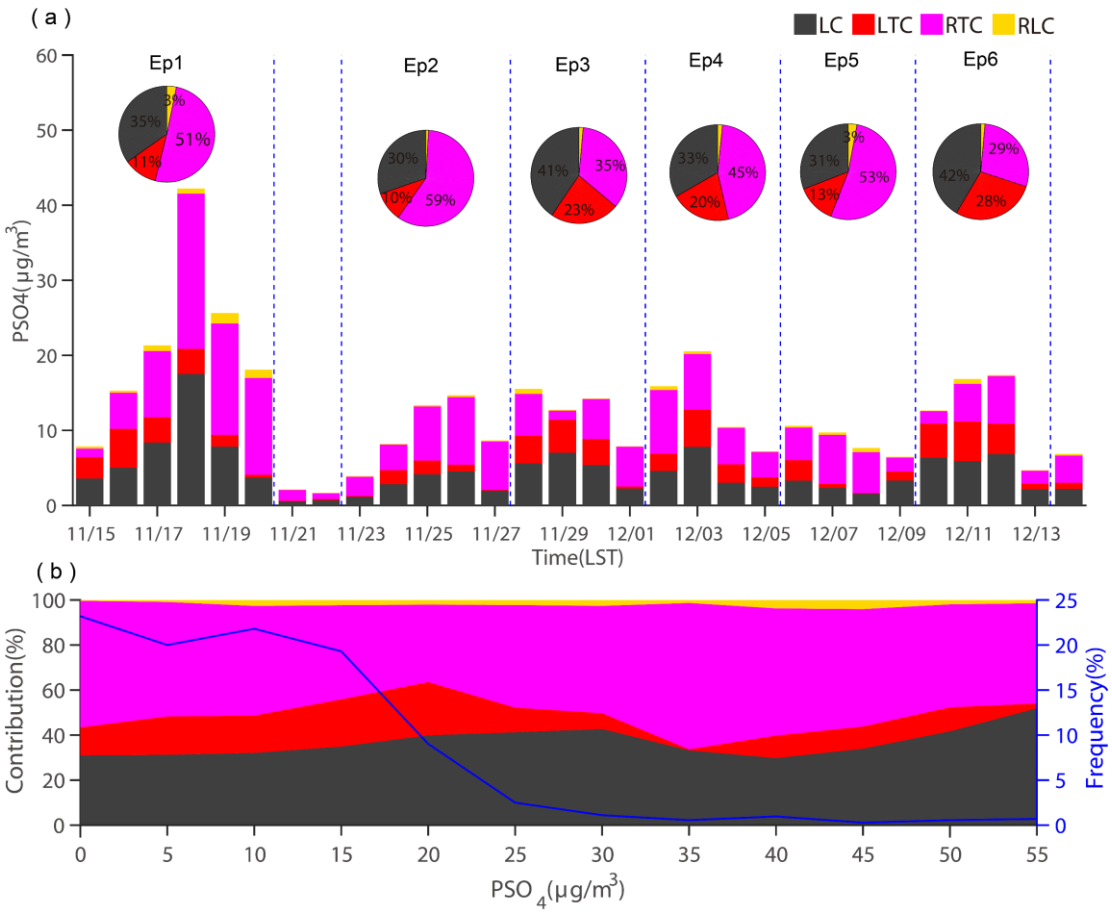


**Figure 9.** (a) ~~Regional s~~Sources of ~~chemical conversion of~~ secondary sulfate in Beijing. (b) Variation of ~~region~~ sources of ~~chemical conversion of~~ secondary sulfate with hourly surface sulfate concentration level in Beijing for the whole study period. LC means sulfate locally produced from Beijing emitted $SO_2$; LTC refers to sulfate chemically formed in regions except Beijing from the Beijing emitted $SO_2$; RTC is sulfate chemically formed in the transport pathway to Beijing from $SO_2$ emitted in source regions except Beijing; RLC is sulfate produced in regions except Beijing from locally emitted $SO_2$ and transported to Beijing.

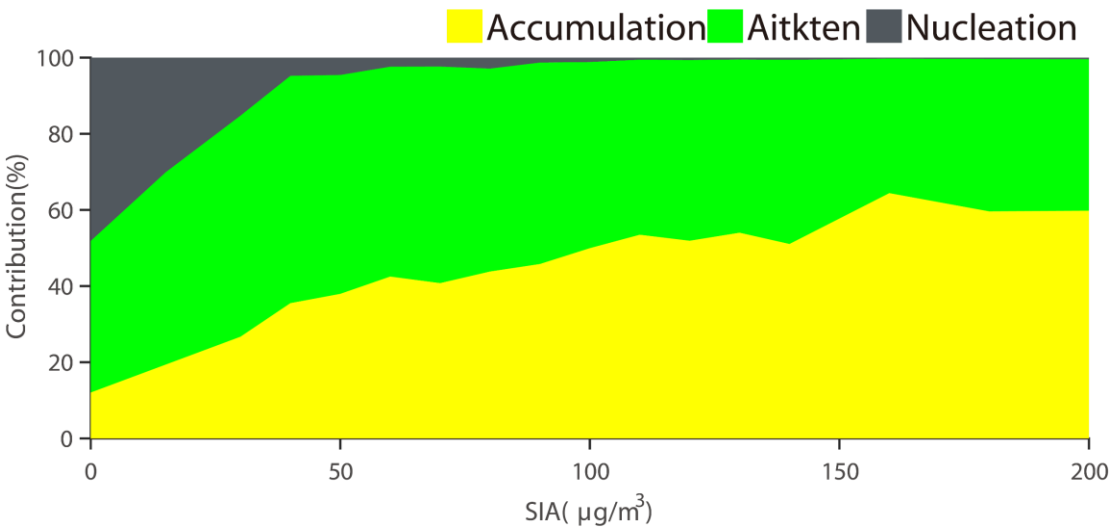


**Figure 10.** Variation of number concentration fraction of particles with SIA in Beijing during whole study period.

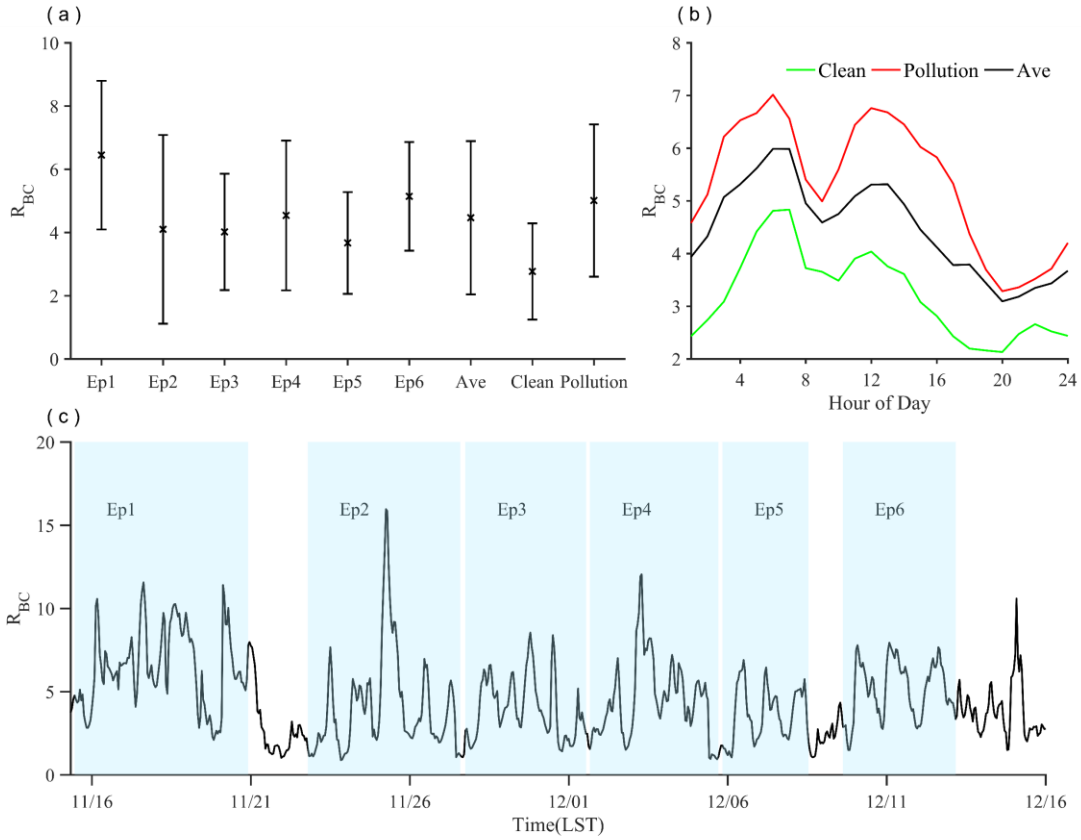

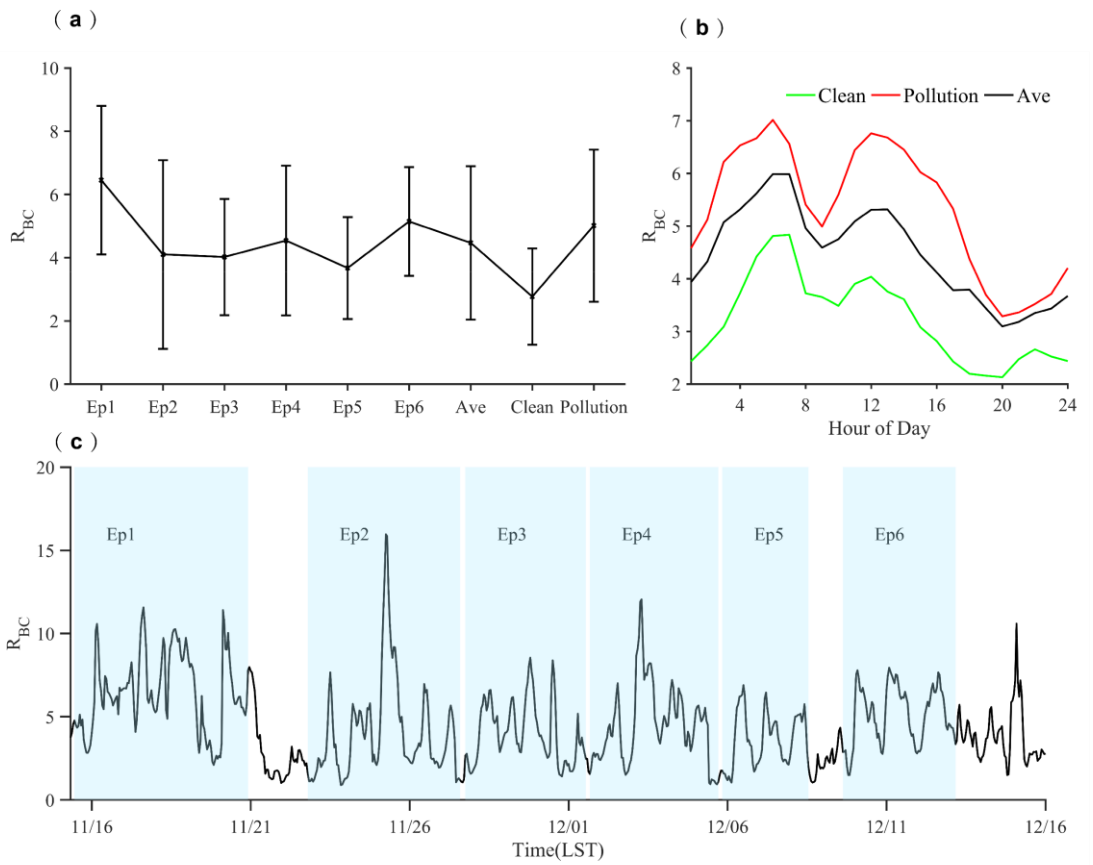


**Figure 11.** (a) average and standard variation of massing ratio of coating to BC ($R_{BC}$) during different episodes and pollution levels, (b) diurnal cycles of $R_{BC}$ under different pollution levels, (c) temporal variation of $R_{BC}$ during study period.

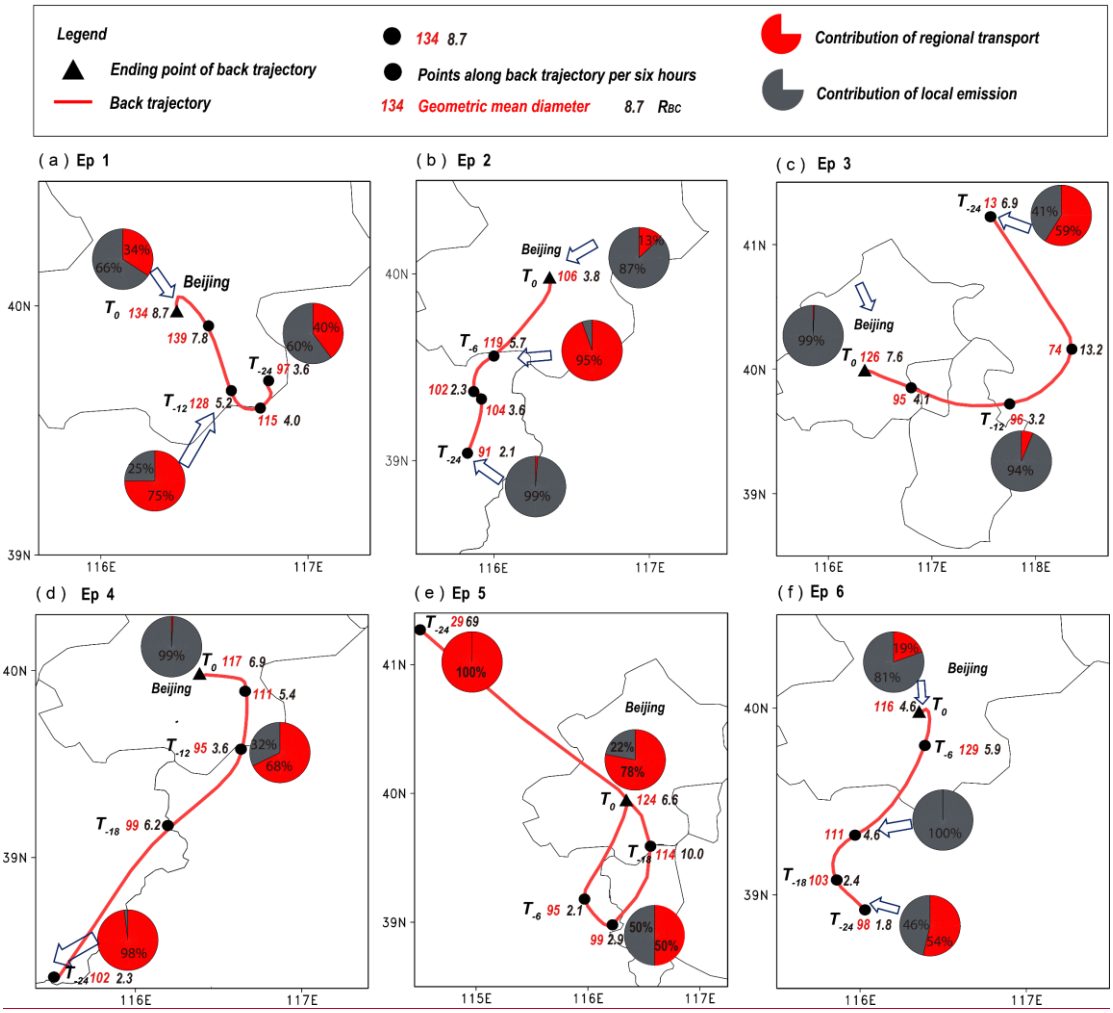


Figure 12. Variation of aerosol properties along transport. Panel a–f refers to episode 1–6. The red lines refer to 24 h backward trajectories at the altitude of 100 m. Aerosol properties include geometric mean diameter (GMD [nm], red numbers beside the solid blocks), mass ratio of coating to BC ($R_{BC}$, the black numbers beside the solid blocks, an indicator of aging degree), region source of BC (pies, the red represents regional transport and the gray is the local contribution). Shaded triangles are ending points of back trajectories, called $T_0$. Shaded circles are points along trajectories per six hours. $T_{-6}$, $T_{-12}$, $T_{-18}$, $T_{-24}$ mean 6, 12, 18, 24 hours before arriving at ending site. Ending times of backtrajectories are before pollution peaks at 21:00 on November 18, 22:00 on November 25, 16:00 on November 29, 22:00 on December 03, 0:00 on December 8 and 22:00 on December 11 (LST), respectively.

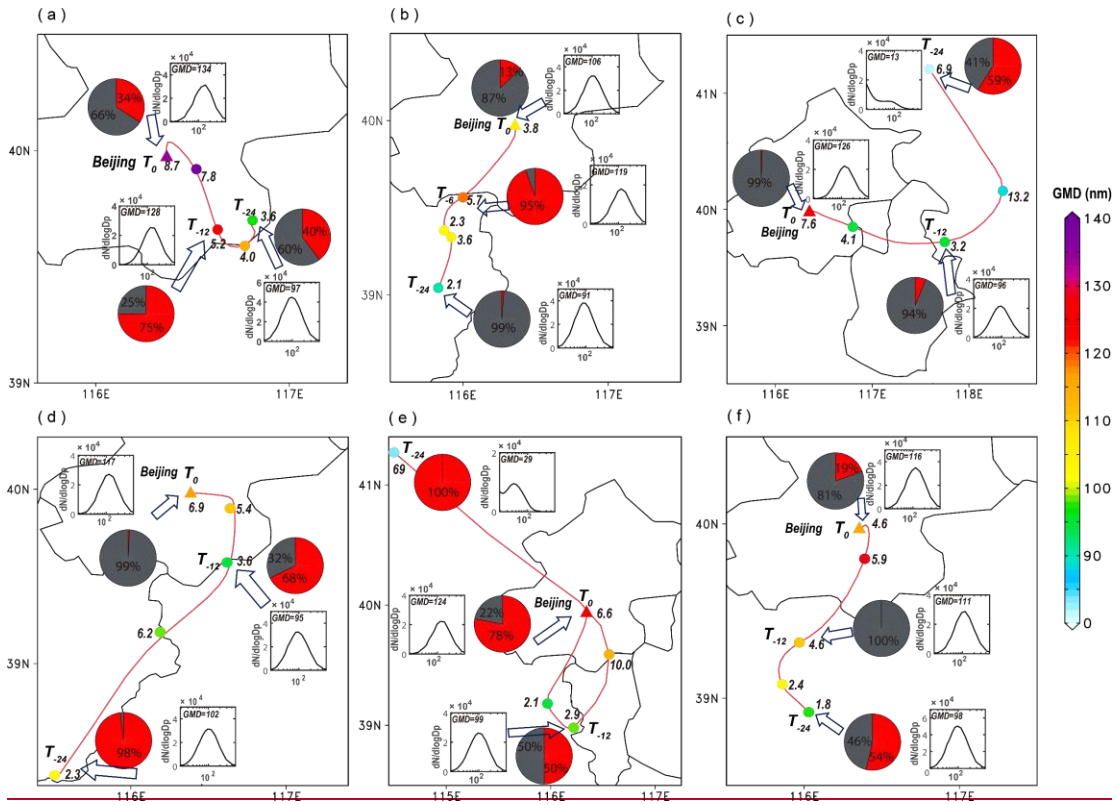


**Figure 12.** 24 h back trajectories for air mass at the altitude of 100 m and aerosol properties along each trajectory. Panel a–f refers to episode 1–6 at 21:00 on November 18, 22:00 on November 25, 16:00 on November 29, 22:00 on December 03, 0:00 on December 8, 22:00 on December 11 (LST). Triangles show ending site at Beijing, called $T_0$. $T_{-6}$, $T_{-12}$, $T_{-18}$, $T_{-24}$ mean 6, 12, 18, 24 hours before arriving at ending site. The red lines refer to backward trajectories and the solid shaded circles represent the geometric mean particle size (GMD, nm) labeled in color bar on the right. The number beside the solid circle is the mass ratio of coating to BC, called $R_{BC}$ for short. The pie chart shows the region source of BC. The gray represents the local contribution, and the red represents the contribution of regional transport. The blacklines refer to the distribution of number concentration.

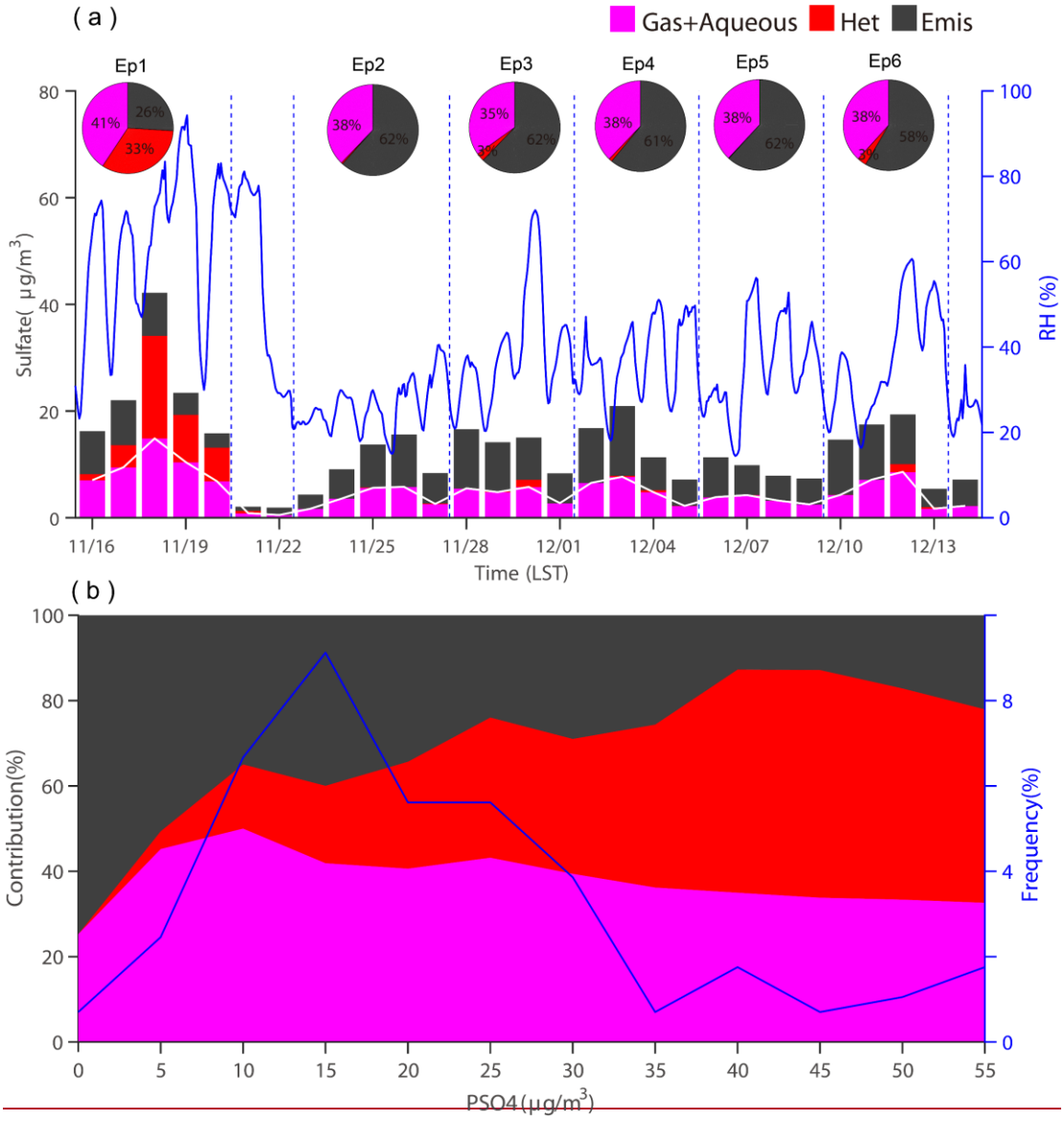
( a )
Gas+Aqueous
Het
Emis
Ep1
Ep2
Ep3
Ep4
Ep5
Ep6
41%
26%
33%
38%
62%
35%
3%
62%
38%
61%
38%
62%
38%
58%
3%
Sulfate( μg/m3)
RH (%)
11/16
11/19
11/22
11/25
11/28
12/01
12/04
12/07
12/10
12/13
Time (LST)
( b )
Contribution(%)
Frequency(%)
PSO4(μg/m3)

927

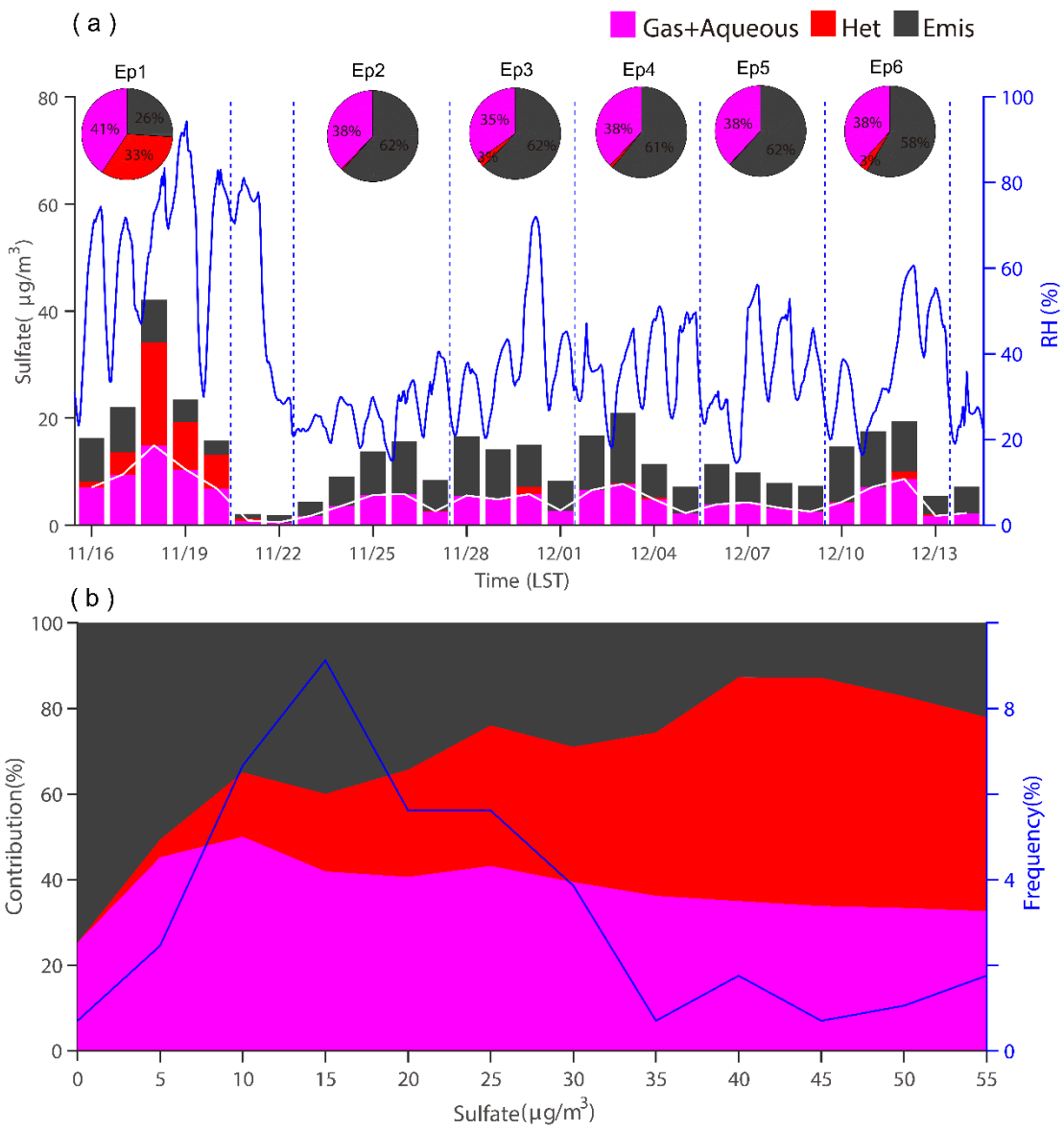


**Figure 13.** Contribution of different ways of sulfate formation in Beijing. (a) Daily average. Blue line shows relative humidity at Beijing. Pies show average contribution of different ways during each episode. (b) Relationship between sulphate concentration and different pathways of sulphate formation during Ep1.

## Tables

**Table 1.** Source-tagging regions and primary $PM_{2.5}$ emissions during 15 November–15 December, 2016 in this study. [a]

| Regions | Descriptions | Area $10^3$ km$^2$ | Population $10^6$ | GDP [b] ($10^{12}$ CNY) | Emission [c] ($10^9$g) |
|---|---|---|---|---|---|
| BJ | Beijing | 16.4 | 21.7 | 2.5 | 3.6 |
| TJ | Tianjin | 11.9 | 15.6 | 1.8 | 3.9 |

| | | | | | | |
|---|---|---|---|---|---|---|
| | NHB | Chengde, Zhangjiakou and Qinhuangdao | 84.1 | 11.6 | 0.4 | 3.6 |
| BTH | WHB | Baoding and Shijiazhuang | 38.0 | 21.2 | 0.9 | 8.1 |
| | EHB | Tangshan, Langfang and Cangzhou | 33.9 | 20.3 | 1.1 | 10.1 |
| | SHB | Hengshui, Xingtai and Handan | 33.3 | 22.9 | 0.7 | 6.8 |
| HN | | Henan | 167.0 | 95.3 | 4.0 | 26.6 |
| SD | | Shandong | 155.8 | 99.5 | 6.8 | 38.5 |
| SX | | Shanxi | 156.7 | 36.8 | 1.3 | 25.9 |
| OT | | Other regions | | | | |

[a] Regions are shown in Fig. 1c.

[b] GDP unit in 2016 is Chinese Yuan (CNY) (http://www.tjcn.org/tjgb/).

[c] $PM_{2.5}$ emissions data are obtained from the 2016 Multi–resolution Emission Inventory for China (MEIC) with 0.25° × 0.25° resolution.

# Supplementss

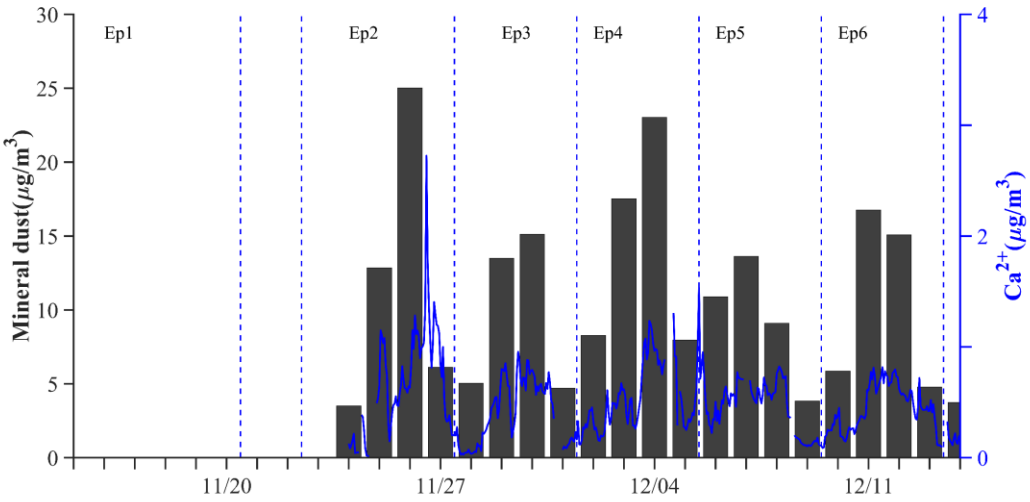


**Figure S1.** Concentration of mineral dust and $Ca^{2+}$ in $PM_{2.5}$ during the study period. And $\text{Mineral} = 2.2 \times [\text{Al}] + 2.49 \times [\text{Si}] + 1.63 \times [\text{Ca}] + 2.42 \times [\text{Fe}] + 1.94 \times [\text{Ti}]$.

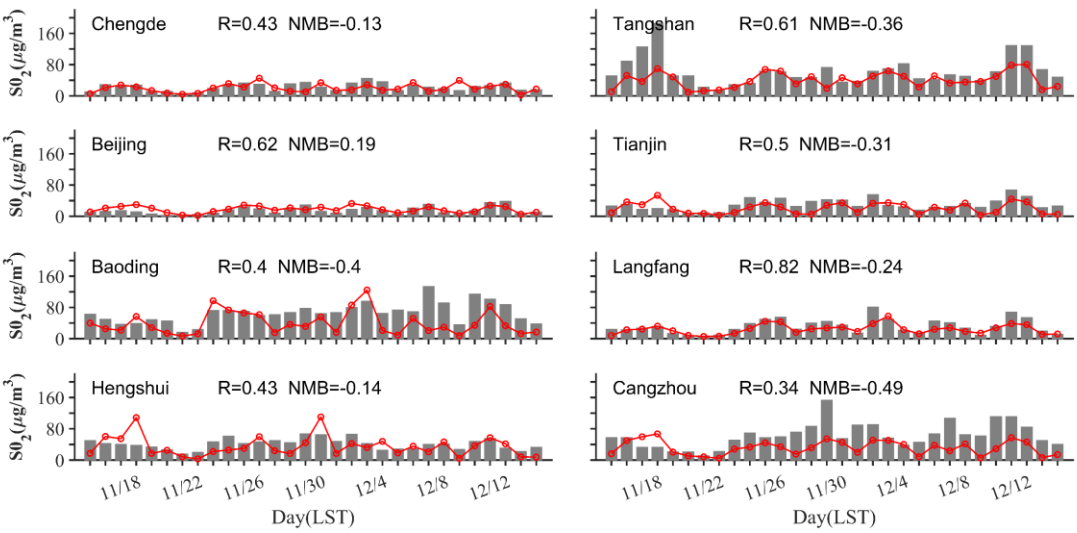


**Figure S2.** Comparison between the simulated (red) and observed (gray bars) daily concentrations of $SO_2$.

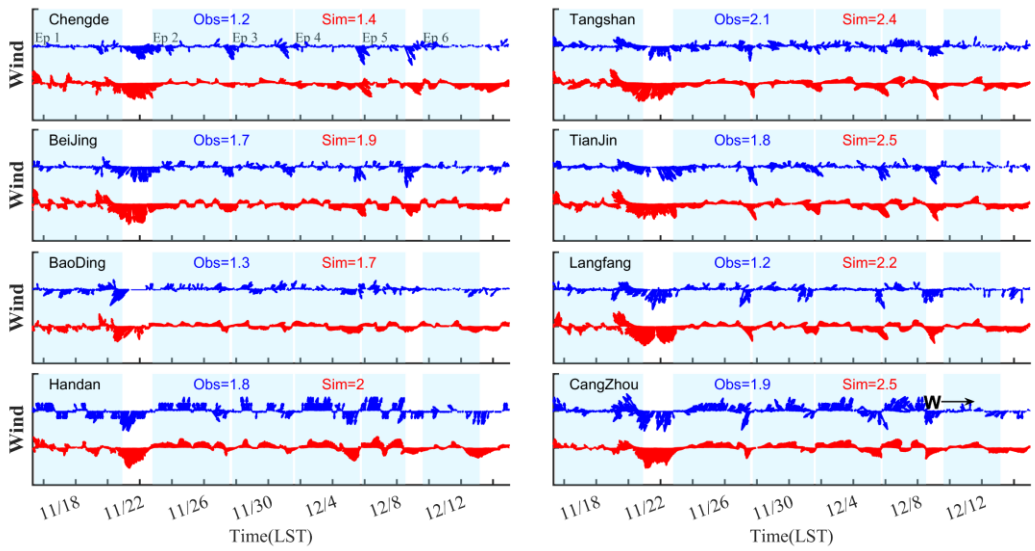


**Figure S3.** Comparison between simulated (red) and observed (blue) wind vector and wind speeds (data) at cities of BTH.

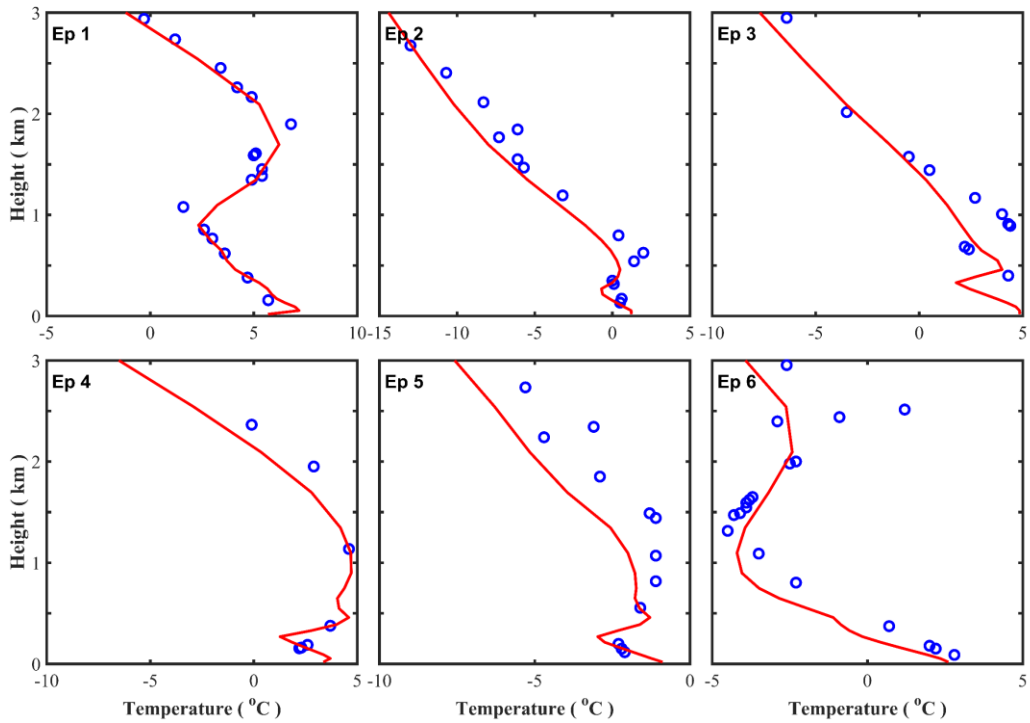


**Figure S4.** Comparison between simulated (red solid line) and observed (blue dot) temperature profiles during episodes in Beijing.

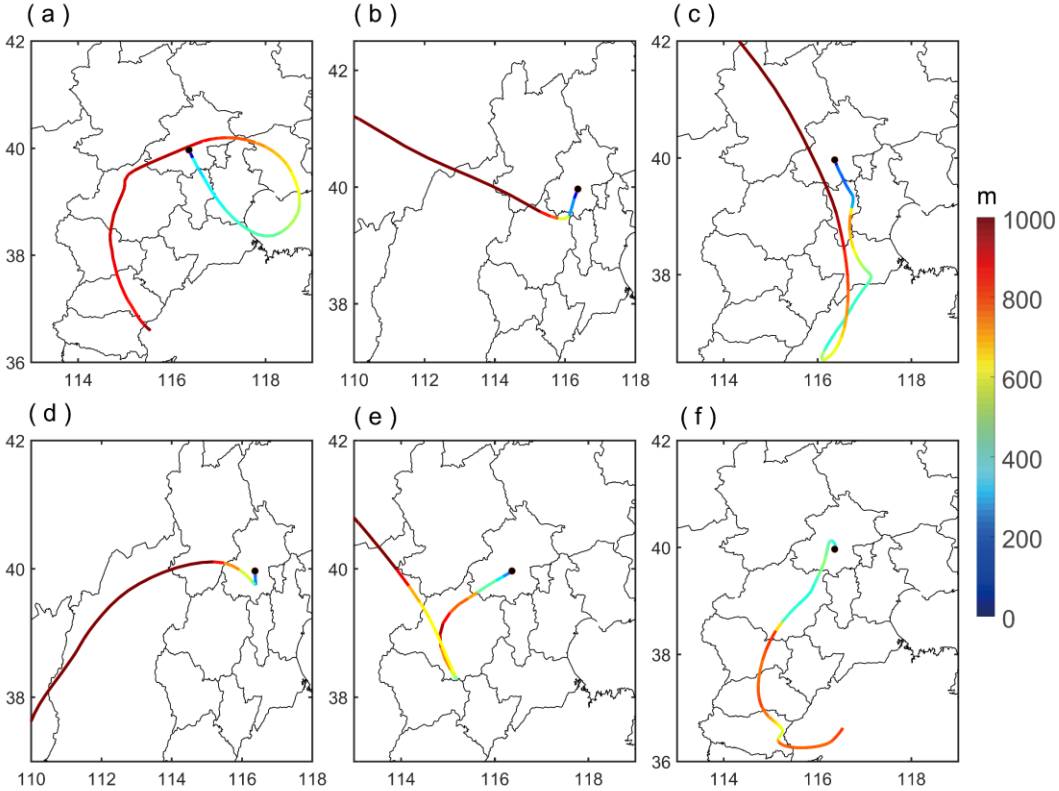


Figure 2 72 h backward trajectories during different episodes (05:00 on November 20, 18:00 on November 26, 23:00 on November 29, 20:00 on December 03, 05:00 on December 08 and 11:00 on December 12 [LST]) at Beijing at 100m. Line color represents height of trajectories. a-f refer to Ep1-6.

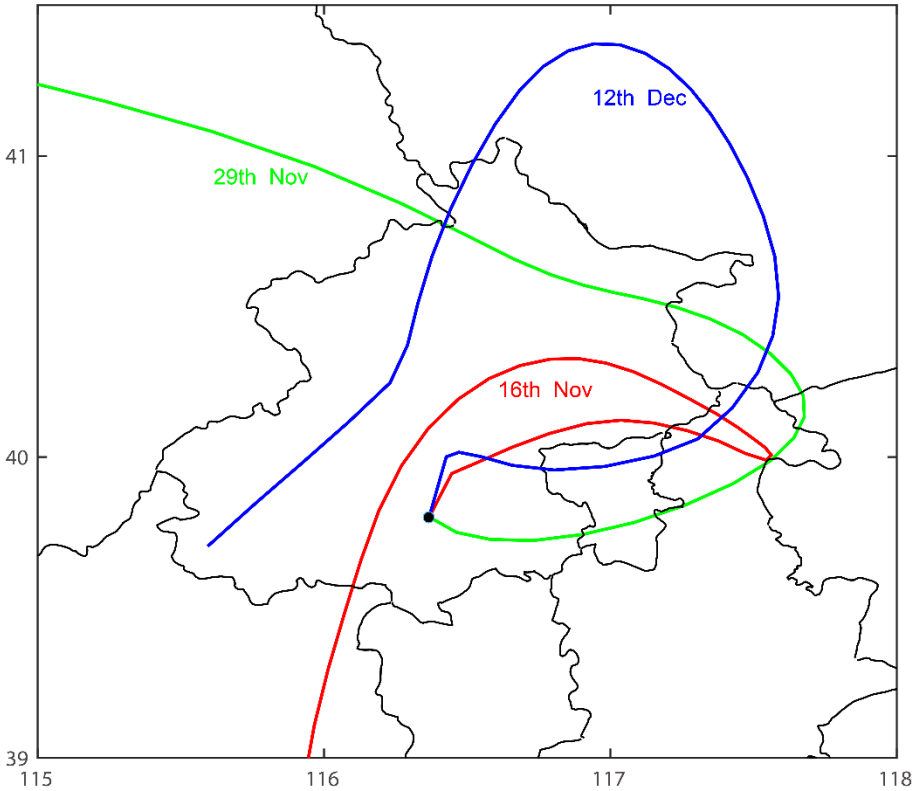


Figure S6 36 h backward trajectories at different start time (02:00 on November 17, 11:00 on November 29, and 23:00 on December 12 [LST]) at Beijing.

**Table S1.** Statistics performances of meteorological simulations, including temperature and relative humidity at 2 m, and wind speed at 10 m. Statistical parameters include correlation coefficient (R), Normalized Mean Bias (NMB) and Root Mean Squared Error (RMSE).~~Statistics performances of meteorological simulations~~

| | | Obs | Sim | NMB | R | RMSE |
|---|---|---|---|---|---|---|
| **T2(K)** | Beijing | 2.42 | 3.31 | 0.37 | 0.88 | 2.11 |
| | Tianjin | 4.05 | 3.73 | -0.08 | 0.93 | 1.48 |
| | Langfang | 2.13 | 3.06 | 0.44 | 0.89 | 2.13 |
| | Chengde | -3.39 | -1.66 | -0.51 | 0.89 | 3.31 |
| **RH2(%)** | Beijing | 53.93 | 39.53 | -0.27 | 0.69 | 21.87 |
| | Tianjin | 56.95 | 47.58 | -0.16 | 0.73 | 18.09 |

| | | | | | | |
|---|---|---|---|---|---|---|
| | Langfang | 60.39 | 46.54 | -0.23 | 0.71 | 21.54 |
| | Chengde | 61.56 | 55.96 | -0.09 | 0.47 | 20.26 |
| **WS10(m/s)** | Beijing | 1.68 | 1.93 | 0.15 | 0.65 | 1.30 |
| | Tianjin | 1.76 | 2.46 | 0.39 | 0.70 | 1.50 |
| | Langfang | 1.23 | 2.15 | 0.74 | 0.57 | 1.56 |
| | Chengde | 1.16 | 1.41 | 0.21 | 0.63 | 1.22 |

**Table S2.** Aerosol properties along transport, including geometric mean diameter (GMD [nm]), mass ratio of coating to BC ($R_{BC}$), number concentration (N) and contribution of region source to BC (Cr [%]). $T_0$ means ending points of back trajectories and $T_n$ means n hours before arriving at the ending point.

| Period | Property | $T_{-24}$ | $T_{-18}$ | $T_{-12}$ | $T_{-6}$ | $T_0$ |
|---|---|---|---|---|---|---|
| **Ep1** | $R_{BC}$ | 3.6 | 4.0 | 5.2 | 7.8 | 8.7 |
| | GMD | 97 | 115 | 128 | 139 | 134 |
| | N | 28994 | 15494 | 15204 | 15592 | 19242 |
| | Cr | 40 | 93 | 75 | 7 | 34 |
| **Ep2** | $R_{BC}$ | 2.1 | 3.6 | 2.3 | 5.7 | 3.8 |
| | GMD | 91 | 104 | 102 | 119 | 106 |
| | N | 23909 | 15189 | 17961 | 10994 | 20121 |
| | Cr | 1.2 | 0.14 | 0.01 | 95 | 13 |
| **Ep3** | $R_{BC}$ | 6.9 | 13.2 | 3.2 | 4.1 | 7.6 |
| | GMD | 13 | 74 | 96 | 95 | 126 |
| | N | 22234 | 11880 | 13481 | 14241 | 12945 |
| | Cr | 59 | 81.4 | 6.2 | 8.8 | 1 |
| **Ep4** | $R_{BC}$ | 2.3 | 6.2 | 3.6 | 5.4 | 6.9 |
| | GMD | 102 | 98 | 95 | 111 | 117 |
| | N | 19754 | 12805 | 21116 | 10536 | 17199 |
| | Cr | 98 | 56 | 68 | 25 | 1 |
| **Ep5** | $R_{BC}$ | 69 | 10.0 | 2.9 | 2.1 | 6.6 |
| | GMD | 29 | 114 | 99 | 95 | 124 |
| | N | 8617 | 8086 | 16494 | 28211 | 13696 |
| | Cr | 100 | 100 | 50 | 4 | 78 |
| **Ep6** | $R_{BC}$ | 1.8 | 2.4 | 4.6 | 5.9 | 4.6 |
| | GMD | 98 | 103 | 111 | 129 | 116 |
| | N | 31691 | 23691 | 17885 | 12897 | 21955 |

| | | | | | | |
|---|---|---|---|---|---|---|
| 33 | Cr | 54 | 0.17 | 0.01 | 65 | 19 |